Bosonic and Fermionic Greybody Factors of Four-dimensional Black Holes in Various Theories

Sara Kanzi

Submitted to the
Institute of Graduate Studies and Research
in partial fulfillment of the requirements for the degree of

Doctor of Philosophy
in
Physics

Eastern Mediterranean University
September 2021
Gazimağusa, North Cyprus

Approval of the Institute of Graduate Studies and Research

Prof. Dr. Ali Hakan Ulusoy
Director

I certify that this thesis satisfies all the requirements as a thesis for the degree of Doctor of Philosophy in Physics.

Prof. Dr. İzzet Sakallı
Chair, Department of Physics

We certify that we have read this thesis and that in our opinion it is fully adequate in scope and quality as a thesis for the degree of Doctor of Philosophy in Physics.

Prof. Dr. S. Habib Mazharimousavi
Co-Supervisor

Prof. Dr. İzzet Sakallı
Supervisor

Examining Committee

1. Prof. Dr. Muzaffer Adak
2. Prof. Dr. Mustafa Gazi
3. Prof. Dr. Özay Gürtuğ
4. Prof. Dr. Mustafa Halilsoy
5. Prof. Dr. İzzet Sakallı

ABSTRACT

This PhD thesis examines the bosonic and fermionic greybody factors of four-dimensional black holes (BHs) in various theories.

A high-energy collision creates a BH that evaporates through Hawking radiation (HR). One of the most important quantum quantities of a BH is the BH gravitational factor (GF), is the HR fraction that can reach the known spatial infinity. GFs have the potential to carry a significant amount of information that could drive the theory of quantum gravity. When HR is scattered from the gravitational potential, part of it returns to BH, while the other part is transmitted to spatial infinity. In this context, the GF is also known as the transmission probability. A very high GF value indicates a high probability of HR to reach spatial infinity.

By calculating the GF radiation in various ways, we shall first derive the Schrödinger equation because it represents a kind of wave equation that applies to matter waves. For this purpose, we use the Klein-Gordon equation for scalar perturbation (bosonic particles) and the Dirac equation for fermionic perturbation (fermionic particles), which are discussed in Chapters 4 and 5, respectively. In fact, the GFs will be determined by the associated effective potential of the wave equation. In short, the detailed analysis of the GF via different methods are given in this thesis.

In the framework of general relativity (GR), the radiation of gravitational waves has an important phase defined by the appropriate oscillation frequencies of BH. These frequencies are called quasinormal modes (QNMs), which depend on the BH parameters. The propagation of QNMs is different from the classical normal modes.

That is, while the real parts of the characteristic complex frequencies obtained represent the frequency of oscillation, the imaginary parts represent the damping ratio. We shall employ a semi-analytical technique, the sixth order WKB approach, to calculate the QNMs of the BHs that we consider in this thesis.

Keywords: Greybody Factors, Klein-Gordon Equation, Dirac Equation, Scalar Perturbation, Fermionic Perturbation, Effective Potential, Black Holes, Bumblebee Gravity Model, Kerr Spacetime.

ÖZ

Bu doktora tezi, çeşitli teorilerdeki dört boyutlu kara deliklerin (BHs) bozonik ve fermiyonik gricisim faktörlerini incelemektedir.

Yüksek enerjili bir çarpışma, Hawking radyasyonu (HR) yoluyla buharlaşan bir BH oluşturur. Bir karadeliğin en önemli kuantum niceliklerinden birisi olan BH gricisim faktörü (GF) bilinen uzaysal sonsuzluğa ulaşabilen HR kesridir. GF'ler, kuantum yerçekimi teorisini sürdürebilecek önemli miktarda bilgi taşıma potansiyeline sahiptir. HR yerçekimi potansiyelinden saçıldığında, bunun bir bölümü BH'ye geri dönerken, diğer bölümü uzaysal sonsuzluğa iletilir. Bu bağlamda, gricisim faktörü (GF) aktarım olasılığı olarak da bilinir. Çok yüksek bir GF değeri, HR'nin sonsuzluğa ulaşma olasılığının yüksek olduğunu gösterir.

GF radyasyonunu çeşitli şekillerde hesaplayarak, ilk olarak Schrödinger denklemini türeteceğiz çünkü madde dalgalarına uygulanan bir tür dalga denklemini temsil ediyor. Bu amaçla, sırasıyla Bölüm 4 ve 5'te tartışılan skaler pertürbasyon (bosonik parçacıklar) için Klein-Gordon denklemini ve fermiyonik pertürbasyon için (fermiyonik parçacıklar) Dirac denklemini kullanıyoruz. Aslında, GF'ler, dalga denkleminin ilişkili etkin potansiyeli tarafından belirlenecektir. Kısacası, bu tezde GF'nin farklı yöntemlerle detaylı analizi verilmektedir.

Genel görelilik (GR) çerçevesinde, yerçekimi dalgalarının radyasyonu, BH'nin uygun salınım frekansları tarafından tanımlanan önemli bir faza sahiptir. Bu frekanslar BH parametrelerine bağlı olan kuazinormal modlar (QNM'ler) olarak adlandırılır. QNM'lerin yayılması klasik normal modlardan farklıdır. Yani, elde edilen karakteristik

kompleks frekansların gerçek kısımları salınımın frekansını temsil ederken, sanal kısımları ise sönüm oranını göstermektedir. Bu tezde dikkate aldığımız BH'lerin QNM'lerini hesaplamak için yarı analitik bir teknik olan altıncı dereceden WKB yaklaşımı kullanacağız.

Anahtar Kelimeler: Gricisim Faktörleri, Klein-Gordon Denklemi, Dirac Denklemi, Skaler Pertürbasyon, Fermiyonik Pertürbasyon, Efektif Potansiyel, Karadelikler, Yaban Arıs Yerçekimi Modeli, Kerr Uzay-zamanı.

TO MY FAMILY FOR

THEIR UNSPARING SUPPORTS

ACKNOWLEDGMENT

I would like to acknowledge and give my warmest thanks to my dear supervisor, Prof. Dr. İzzet Sakallı for his supports. His guidance and advice carried me through all the steps of my Ph.D. program, moreover, for giving a long period of time to depend this dissertation. I would also like to give special thanks to my Co-supervisor Prof. Dr. S. Habib Mazharimousavi for his effort in the completion and success of this study.

My deepest gratitude and appreciation for the help and support are extended to my dear professors, Prof. Dr. Mustafa Halilsoy, Assist. Prof. Dr. Mustafa Rıza, Prof. Dr. Özay Gürtuğ, and Prof. Dr. Omar Mustafa. My special thanks to our dear secretary, Mrs. Çilem Aydınlık and our lab technician, Mr. Reşat Akoğlu for their kindness helps.

I would also like to express my gratitude to my dear boyfriend, Kayvan Khatibi, also my friends and classmates Danial Forghani, Huriye Gursel, Gülnihal Tokgöz, and Zeinab Alghadhi for their moral support, understanding and encouragement.

My appreciation would not be complete without giving credit to my dear parents Maryam and Mohammad, and my brother Saman.

To all who are not mentioned but in one way or another helped in completion of this study, thank you very much.

TABLE OF CONTENTS

LIST OF TABLES

LIST OF FIGURES

LIST OF ABBREVIATIONS

BBH	Bardeen Black Hole
BGM	Bumblebee Gravity Model
BH	Black Hole
CDEs	Chandrasekar Dirac Equations
GFs	Greybody Factors
GR	General Relativity
GUP	Generalized Uncertainty Principle
HR	Hawking Radiation
LIV	Lorentz Invariance Violation
LSV	Lorentz Symmetry Violence
NP	Newman Penrose
QGT	Quantum Gravity Theory
QNMs	Quasinormal Modes
SBHBGM	Schwarzschild Black Hole in Bumblebee Gravity Model
SM	Standard Model
VEV	Vacuum Expectation Value

Chapter 1

INTRODUCTION

For almost a century, the theory of GR has been known to describe the force of gravity in perfect harmony with observations. However, the unanswered questions like the interface between cosmology/gravity and particle physics such as the hierarchy problem, the cosmological constant problem, and the source of the late-time acceleration of Universe have boosted the researchers to seek for alternatives to GR theory. Moreover, it has been understood that GR cannot define Universe neither in ultraviolet nor in infrared region. In other words, according to the observations of large scale phenomena, the gravity necessitates a vast effort and understanding.

In spite of their overwhelming successes in describing nature, GR (i.e., detection of the gravitational waves [1,2] and observation of the shadow of the M87 supermassive (BH) [3]) and Standard Model (SM) (i.e., detection of the Higgs boson [4]) of particle physics are incomplete theories. While Einstein's theory of GR successfully describes gravity at a classical level, SM explains particles and the other three fundamental forces (electromagnetic, and the strong and weak nuclear forces) at a quantum level. The unification of GR and SM is a fundamental quest, and this success will necessarily lead us to a deeper understanding of nature. In the search for this unification, some quantum gravity theories (QGTs) have been proposed, but direct tests of their features are beyond the energy scale of the currently available experiments.

Because, they will be observed on the Planck scale which is around 10^{19}(GeV). However, it is possible that some signals of the QGT appear at sufficiently low energy scales and their effects can be observed in experiments on existing energy scales. In a simple way, the modern theoretical physics can be represented by two major theories: GR which deals with the world at very large (in fact at any) scales and quantum field theory with the world at very small scales.

In preparation of QGT, physicists have to seek out systems under extreme conditions, in which quantum and gravitational effects are on the same base. As we just elucidated above, BHs satisfy this condition perfectly. This extraordinary attribute makes BHs a unique testing focus for ideas and proposals coming from any theory of quantum gravity.

The BHs in the framework of quantum field theory behave as a thermal system which obey the laws of thermodynamics, furthermore, it emits radiation with a characteristic black body spectrum, known as Hawking radiation (HR) [5]. Therefore, HR, as one of the most conspicuous effects which leap up from the combination of GR and quantum theory, has gained widespread interest [6-15]. However, as the radiations that generate from the BHs travel away, they will get modified by the non-trivial space-time geometry. Therefore, a spectrum measured by an observer located at infinity will differs from the original one, and is frequency and geometry dependent which filter the initial HR is known as GF [16,17]. In a general method, GF can be studied in a semi-classical approximation [18], by making use of Schrödinger-form equations to evaluate the scattering of a field by the BH background. Within this method, we are also able to compute the transmission and reflection properties of the BH, which enable us to find the corresponding GF.

To compute the transmission probability and thus the GF, such as the WKB approximation, matching method [19-25], and rigorous bound method [26,56]. Studies about GFs have been increasingly gaining attention in the literature due to its observational evidence potential (see for example [27–37] and references therein).

In the substructure of QG, there are various theories derived from gravity and quantum physics, which are modified due to incorporate the effects of gravity in quantum physics. One of the promising theories is Generalized Uncertainty Principle (GUP) [38] Combining with the theory of Heisenberg's uncertainty principle (HUP) [39], represents that for certain pairs of variables, like the position and momentum, one cannot have an exact measurement of both the variables simultaneously. GUP which is a modification of the HUP, which should be properly modified at the QG scale, in order to accommodate the existence of Planck length [38].

Among the approaches in the QG, the most successful one is the Lorentz invariance, which is regarded to combination of gravity and the standard model (SM) [95], and is also known as a fundamental principle in the construction of the SM is Lorentz invariance. Therefore, the theory of Lorentz symmetry breaking (LSB) has been under intense research since the proposed SM Extension (SME) [96-98]. This effective field theory that includes the SM, GR, and every possible operator that breaks the Lorentz symmetry, which the coupling constants related to LSB terms are dominant at the scales of Planckian energy. With the SME, further investigations of the LSB can be made in the context of high energy particle physics, nuclear physics, gravitational physics, and astrophysics.

The outline of the thesis is as follows: In chapter 2, we study HR extensively and laws of BHs thermodynamics. Chapter 3, is allocated to elucidation of the BGM properties. In chapter 4, we address the quantum gravity correction with the GUP modification for non-rotating BGM and polytropic BHs in Kerr spacetime. For both BHs we study the GUP modified HR. In the chapters 5 and 6, we construct the one-dimensional wave function of Schrödinger equation with the effective potentials. To this end, we consider the scalar and fermionic perturbations for spin zero and spin-1/2 particles, respectively. Namely, we use Klein-Gordon equation for bosons and Dirac equation for fermions. Chapter 7 is devoted to the greybody radiation: we explain the methods to be used with the considered line-elements in rotating and non-rotating spacetime and interpret their behavior under the specific parameters based on their graphs. We also study the QNMs of the Kerr like BH in the BGM in chapter 8 to this end purpose, we use the 6^{th} order of WKB method and the results for both bosonic and fermionic particles are tabulated in tables 8.1 and 8.2, respectively. Chapter 9 is devoted to summary and conclusions.

Throughout the manuscript, we work in geometrized units where $G = c = \hbar = 1$.

Chapter 2

HAWKING RADIATION

The HR is a fundamental theory which describes the radiation and thus the evaporation for the BHs [46-54,61]. Hence, the temperature of this radiation is called as Hawking temperature which is inversely proportional to the mass of the Schwarzschild family (in general for type-D [55]) of BHs. Such radiation would be significant only for very small BHs. Moreover, the flux is also inversely proportional to the mass squared for the type-D BHs. Ultimately, the heavier BHs live longer by a factor of their mass cubed and the lowest-mass BHs are the brightest sources of the HR. Additionally, the most powerful HR appears in regions where are near to the geometry of event horizon area. Therefore, they will be visible only if they pass through such regions [62]. Hawking's ground-breaking studies [117,118] can be considered as the onset of QGT [119,120]. Since then there have been numerous research papers on the subject of HR in the literature (see, for instance, [121-127]). Several methods have been developed to calculate the HR of BHs [128-132].

For a BH as a thermal system the laws of thermodynamics can be determined as [40-45, 63]:

Zeroth law represents that the surface gravity κ is a constant on the horizon of a stationary BH.

First law is given by

$$\delta M = \frac{T_H}{8\pi}\delta A + \Omega\delta J + \Phi\delta Q, \tag{2.1}$$

Where $T_H = \frac{\kappa}{2\pi}$ appears for Hawking temperature, M is the mass, A is the area, J is the angular momentum and Q denotes the charge of the BH, Ω is the angular velocity and Φ represents the electrostatic potential.

Second law states that the horizon area of the BH must be increasing in time

$$\delta A \geq 0. \tag{2.2}$$

and based on the **Third law,** it is not possible to achieve $\kappa = 0$ along a physical process.

These theorems are perfectly match with the laws of classical thermodynamics. Meanwhile, based on the Bekenstein theory, there exist a number of resemblances between the physics of BHs and thermodynamics [64]. One of this similarity represents that the radiation from BHs is as if the radiation in black bodies. Thus, it should be stationary which was proven by Hawking in (1974) [65]. Today, there are many notable theoretical studies on the HR and BHs thermodynamics, and this subject keeps its importance without losing its currency.

In order to have a wider perspective, we should contemplate the regarded observations and simulations. However, some gravitational phenomena are difficult or even impossible to observe in real spacetime. HR in astrophysics is excessively small to be detected or recorded directly by any possible experiment, telescope or satellite hitherto. So a quantum effect attributed to gravity would be difficult to measure. In 1981, William Unruh [71] figured out some interesting coincidences between the equations for the dispersion of sonic waves in a moving fluid and those for light waves

around the Hawking BH geometry [66]. Lots of new researches are motivated by this investigation, in order to study phenomena regarded to gravity in other physical systems, creating a new branch called analogue gravity. Moreover, the conspicuous improvements to the experimental apparatus, allow us to study the Hawking spectrum experimentally. Henceforth, one possible way, due to Unruh theory, is to create an analogue BH, where light can be replaced by sound and the metric of the analogue spacetime can be defined by speed of sound and local flow velocity [67].

Subsequently, the Hawking temperature characterized [66,68], which imply a great agreement assignable to predictions [69]. In the classical framework, stimulated HR in water waves was observed, by employing the analogy between the dispersions of the fields around BHs and surface waves on moving water (Mathematically, the moving fluid sets a spacetime such as the geometry of event horizons [71]) [72].

HR in the analogue BH has recently been confirmed by an experiment [70]. In this remarkable research, the spontaneous HR, at different times, was measured after the horizon formation and it has been confirmed that the emission of HR from an acoustic (analogue) BH is stationary. For an analogue BH, the Hawking temperature is given by [70]

$$T_H = \frac{\hbar}{2\pi k_B}\left(\frac{dv}{dx} + \frac{dc}{dx}\right)_{horizon}, \tag{2.3}$$

where v is the flow velocity, c indicates the speed of sound, and k_B is Boltzmann's constant. Here, $v(x)$ and $c(x)$ are the functions having metric features and their derivatives at the horizon are the surface gravity analogue which is in excellent complement with theory ($T = \frac{\hbar \mathrm{K}}{2\pi k_B c}$, where K is the surface gravity).

These particular studies are a selection of a large amount phenomena that one can study from the analogue gravity perspective [73, 74], with the purpose of providing a physical and real laboratory model for the theory of curved spacetime.

Certainly, analogy is not an absolutely perfect model, and there is no claim that the considered analogue models are completely match with the GR but it accurately reflects a sufficient number of important features of GR.

In summary, one of the most important problems in physics waiting to be solved is the combination of quantum field theory (QFT) and GR, which are the two theories that do not work great with each other. We have in fact not yet been able to deduce/induce a theory that combines these two and is falsifiable, so we just do not know what happens when someone can fully combine the effects of QFT and GR. HR however, although unproven, gives us a glimpse into how such a unified theory could look like. Therefore, studies on HR will advance both theoretical and experimental physics. Namely, HR has always been up to date.

Chapter 3

BUMBLEBEE GRAVITY MODEL (BGM)

The simplest models that contain a vector field which dynamically breaks the Lorentz symmetry are called bumblebee models [99–102]. These models, although owning a simpler form, have interesting features such as rotations, boosts, and CPT violations. In a bumblebee gravity model (BGM), potential V is included in the action S_{BM}, which evokes a vacuum expectation value (VEV) for the vector field. The potential V is formed as a function of a scalar combination $\aleph$ of the vector B_μ and the metric $g_{\mu\upsilon}$ (plus the other matter fields, if there are any). The potential has a minimum at $\frac{dV}{d\aleph} = 0$. At the V_{min}, the bumblebee field B_μ incorporates a vacuum value shown by $< B_\mu >= b_\mu$, which is the so-called vacuum vector. In fact, the vacuum vector is nothing but a background vector that gives rise to local (spontaneous) LSB [103] The scalar of the BGM, in general, reads as $\aleph = \left(B^\mu B_\mu \pm b^2\right)$ in which b is a constant having dimensions of mass (M). Thus, the V_{min} satisfies the condition of $\frac{dV}{d\aleph} = 0$ for $\aleph = 0$. Here, b_μ is spontaneously induced as a time like vector abiding by $b_\mu b^\mu = -b^2$. For instance, the aether models [104,105] are based on a vector field, which is in the Lagrangian density of the system with a non-vanishing VEV. The vector field dynamically selects a preferred frame at each point in the considered space-time and spontaneously breaks the Lorentz invariance. This is a mechanism reminiscent of the breaking of local gauge symmetry described by the Higgs mechanism. In general, the subclass of aether models obeys the following action [106]:

$$S_{BM} = \int d^4x \left[\frac{1}{16\pi G}\left(R + \not{c}B^{\mu}B_{\upsilon}R_{\mu\upsilon}\right) - \frac{1}{4}B^{\mu\upsilon}B_{\mu\upsilon} - V\aleph\right], \tag{3.1}$$

where parameter $\not{c}$, having dimension M^{-2} denotes the coupling between the Ricci tensor $\left(R_{\mu\upsilon}\right)$ and B^{μ}. $B_{\mu\upsilon}$ is the bumblebee field strength:

$$B_{\mu\nu} = \nabla_{\mu}B_{\upsilon} - \nabla_{\upsilon}B_{\mu}. \tag{3.2}$$

As mentioned above, V is the potential of the bumblebee field that drives the breaking of the Lorentz symmetry of the Lagrangian by collapsing onto a non-zero minimum at $\aleph = 0$ or $B_{\mu}B^{\mu} = \mp b^2$. In fact, B_{μ} is one of the Lorentz breaking coefficients and it shows a preferred direction in which the equivalence-principle is locally broken for a certain Lorentz frame. Observations of Lorentz violation can emerge if the particles or fields interact with the bumblebee field [106]. It is worth noting that when a smooth quadratic potential is chosen as

$$V = A\aleph^2, \tag{3.3}$$

where A is a dimensionless constant, one gets the Nambu-Goldstone excitations (massless bosons) besides the massive excitations. Besides, the linear Lagrange-multiplier potential is given by $V = \lambda\aleph$. These potentials present also the breaking of the $U(1)$ gauge invariance and other implications to the behavior of the matter sector, the photon, and the graviton. For a topical review (from experimental proposals to the test results of the BGMs, the reader is referred to [101] and references therein.) Furthermore, the studies using the bumblebee models have gained momentum for the last two decades. The vacuum solutions for the bumblebee field for purely radial, temporal-radial, and temporal-axial Lorentz symmetry breaking were obtained in [107]. New spherically static BH [108] and traversable wormhole [109] solutions in the BGM have been recently discovered. Bluhm [110] discussed the Higgs mechanism in the BGM. The electrodynamics of the bumblebee fields was studied by [111] in

which the bumblebee field was considered as a photon field. Propagation velocity of the photon field, along with its possible effects on the accelerator physics and cosmic ray observations, was also investigated. BGMs are also used to limit the likelihood of Lorentz violation in astrophysical objects such as the Sun [112].

For other studies demonstrating the physical effects (QNMs, thermodynamics, etc.) of the bumblebee field, the reader may refer to [111, 113-116] and references therein. The Lagrangian density of the BGM yields the following extended vacuum Einstein equations

$$G_{\mu\upsilon} = R_{\mu\upsilon} - \frac{1}{2} R g_{\mu\upsilon} = \Re T^{B}_{\mu\upsilon}, \tag{3.4}$$

where $G_{\mu\upsilon}$ and $T^{B}_{\mu\upsilon}$ are the Einstein and bumblebee energy-momentum tensors, respectively. $\Re = 8\pi G_N$ is the gravitational coupling and $T^{B}_{\mu\upsilon}$ is given by

$$T^{B}_{\mu\upsilon} = -B_{\mu\alpha}B^{\alpha}_{\upsilon} - \frac{1}{4} B_{\alpha\beta}B^{\alpha\beta} g_{\mu\nu} - V g_{\mu\upsilon} + 2V' B_{\mu}B_{\upsilon} + \frac{\xi}{\Re}\Big[\frac{1}{2} B^{\alpha}B^{\beta} R_{\alpha\beta} g_{\mu\upsilon} -$$

$$B_{\mu}B^{\alpha}R_{\alpha\upsilon} - B_{\upsilon}B^{\alpha}R_{\alpha\mu} + \frac{1}{2}\nabla_{\alpha}\nabla_{\mu}(B^{\alpha}B_{\upsilon}) + \frac{1}{2}\nabla_{\alpha}\nabla_{\upsilon}\big(B^{\alpha}B_{\mu}\big) - \frac{1}{2}\nabla^{2}\big(B_{\mu}B_{\upsilon}\big) -$$

$$\frac{1}{2} g_{\mu\upsilon}\nabla_{\alpha}\nabla_{\beta}\big(B^{\alpha}B^{\beta}\big)\Big], \tag{3.5}$$

where ξ is the real coupling constant (having dimension M^{-1}) that controls the non-minimal gravity-bumblebee interaction. From now on, the prime symbol shall denote the differentiation with respect to its argument. Meanwhile, there are other generic bumblebee models having nonzero torsion in the literature. In Eq. (3.5), the potential $V \equiv V(\aleph)$ provides a non-vanishing VEV for B_{μ}. As it was stated above (see also [133,134]), the VEV of the bumblebee field is determined when $V = V' = 0$. Taking the covariant divergence of the bumblebee Einstein equations (3.4) and using the contracted Bianchi identities, one gets

$$\nabla^{\mu} T^{\beta}_{\mu\upsilon} = 0, \tag{3.6}$$

which gives the covariant conservation law for the bumblebee total energy-momentum tensor $T_{\mu\upsilon}$. Thus, Eq. (3.4) reduces to

$$R_{\mu\upsilon} = \Re T^{B}_{\mu\upsilon} + \frac{\xi}{4} g_{\mu\upsilon} \nabla^2 (B_{\alpha} B^{\alpha}) + \frac{\xi}{2} g_{\mu\upsilon} \nabla_{\alpha} \nabla_{\beta} \left(B^{\alpha} B^{\beta} \right). \tag{3.7}$$

One can immediately see that when the bumblebee field B_{μ} vanishes, we recover the ordinary Einstein equations. Recently, the vacuum solution in the BGM induced by the LSB has been derived by Casana et al. [108]. The solution is obtained when the bumblebee field B_{μ} remains frozen in its VEV b_{μ} [107,109]. Namely, we have

$$B_{\mu} = b_{\mu} \implies b_{\mu\upsilon} = \partial_{\mu} b_{\upsilon} - \partial_{\upsilon} b_{\mu}. \tag{3.8}$$

Thus, the extended Einstein equations are found to be

$$R_{\mu\upsilon} + \kappa b_{\mu\alpha} b^{\alpha}{}_{\nu} + \frac{\kappa}{4} b_{\alpha\beta} b^{\alpha\beta} g_{\mu\upsilon} + \xi b_{\mu} b^{\alpha} R_{\alpha\upsilon} + \xi b_{\upsilon} b^{\alpha} R_{\alpha\mu} - \frac{\xi}{2} b^{\alpha} b^{\beta} R_{\alpha\beta} g_{\mu\upsilon} -$$

$$\frac{\xi}{2} \nabla_{\alpha} \nabla_{\mu} (b^{\alpha} b_{\upsilon}) - \frac{\xi}{2} \nabla_{\alpha} \nabla_{\upsilon} \left(b^{\alpha} b_{\mu} \right) + \frac{\xi}{2} \nabla^2 \left(b_{\mu} b_{\upsilon} \right) = 0. \tag{3.9}$$

Assuming a space like background for b_{μ} as

$$b_{\mu} = [0, b_r, 0, 0], \tag{3.10}$$

and using the condition $b^{\mu} b_{\mu} = b^2 = constant$, LSB parameter (L) is defined as $L = \xi b^2 \geq 0$. A spherically symmetric static vacuum solution to Eq. (3.9) is obtained as follows

$$ds^2 = -\left(1 - \frac{2M}{r}\right) dt^2 + (1 + L) \left(1 - \frac{2M}{r}\right)^{-1} dr^2 + r^2 (d\theta^2 + sin^2 \theta d\varphi^2), \tag{3.11}$$

which we call it SBHBGM solution. This BH solution represents a purely radial Lorentz violation outside a spherical body characterizing a modified BH solution. In the limit $\rightarrow 0$ $(b^2 \rightarrow 0)$, one can immediately see that the usual Schwarzschild metric is recovered. For the metric (3.11), the Kretschmann scalar becomes

$$\mathcal{K} = \frac{4(12M^2 + 4LMr + L^2r^2)}{r^6(1+L)^2}, \tag{3.12}$$

which is different than the Kretschmann scalar of the Schwarzschild BH. It means that none of the coordinate transformations link the metric (3.11) to the usual Schwarzschild BH. When $r = 2M$, Eq. (3.11) becomes finite: the coordinate singularity can be removed by applying a proper coordinate transformation. However, in the case of $r = 0$, physical singularity cannot be removed. So, we see that the behaviors of the physical ($r = 0$) and coordinate ($r = r_h = 2M$: event horizon) singularities do not change in the BGM. The Hawking temperature of the metric (3.11) can be computed from Eq. (3.3), in which the surface gravity is given by [119]

$$\kappa = \nabla_\mu \chi^\mu \nabla_\upsilon \chi^\upsilon, \tag{3.13}$$

where χ^μ is the time-like Killing vector field. Thus, the Hawking temperature of the SBHBGM (3.11) reads

$$T_H = \frac{1}{4\pi\sqrt{-g_{tt}g_{rr}}}\left(\frac{dg_{tt}}{dr}\right)_{r=r_h} = \frac{1}{2\pi\sqrt{1+L}}\left(\frac{M}{r^2}\right)_{r=r_h} = \frac{1}{8\pi M\sqrt{1+L}}. \tag{3.14}$$

One can easily see from Eq. (3.14) that the non-zero LSB parameter has the effect of reducing the Hawking temperature of a Schwarzschild BH.

Moreover, the Kerr-like rotating black hole metric in the BGM was recently found by [60] as follows

$$ds^2 = -\left(1 - \frac{2Mr}{\rho^2}\right)dt^2 - \frac{4Mra\sqrt{1+L}sin^2\theta}{\rho^2}dtd\varphi + \frac{\rho^2}{\Delta}dr^2 + \rho^2 d\theta^2 + \frac{Asin^2\theta}{\rho^2}d\varphi^2, \tag{3.15}$$

where

$$\Delta = \frac{r^2 - 2Mr}{1+L} + a^2, \rho^2 = r^2 + (1+L)a^2cos^2\theta, \tag{3.16}$$

$$A = [r^2 + (1+L)a^2]^2 - \Delta(1+L)^2 a^2 sin^2\theta. \tag{3.17}$$

One can immediately see that as $L \to 0$ in the metric (3.15), the spacetime reduces to the metric of well-known Kerr BH. Besides, when the rotation parameter $a \longrightarrow 0$ it represents the Schwarzschild-like solution having the LSB Eq. (3.11). In short, metric (3.15) is nothing but a solution of LIV BH with a rotation parameter, which is equal to the angular momentum per unit mass: $a = \frac{J}{M}$. Its singularities appear at $\rho^2 = 0$ and $\Delta = 0$. For $\rho^2 = 0$, we have a ring-shape physical singularity at the equatorial plane of the center of rotating BH having radius a. The roots of Eq. (3.16) reveal the locations of the event horizon and ergosphere:

$$r_\pm = M \pm \sqrt{M^2 - a^2(1+L)},\ r_\pm^{ergo} = M \pm \sqrt{M^2 - a^2(1+L)cos^2\theta}, \tag{3.18}$$

in which $\pm$ signs indicate the outer and inner horizon/ergosphere, respectively. For having a BH solution, it is conditional on

$$a \leq \frac{M}{\sqrt{1+L}}. \tag{3.19}$$

Now, we can write the metric tensor of the Kerr-like space-time as

$$g_{\mu\upsilon} = \begin{pmatrix} -\left(1 - \frac{2Mr}{\rho^2}\right) & 0 & 0 & \frac{-2Mra\sqrt{1+L}sin^2\theta}{\rho^2} \\ 0 & \frac{\rho^2}{\Delta} & 0 & 0 \\ 0 & 0 & \rho^2 & 0 \\ \frac{-2Mra\sqrt{1+L}sin^2\theta}{\rho^2} & 0 & 0 & \frac{Asin^2\theta}{\rho^2} \end{pmatrix}, \tag{3.20}$$

from which one can compute the determinant of the metric tensor as follows

$$g \equiv det(g_{\mu\upsilon}) = -\rho^4(1+L)sin^2\theta. \tag{3.21}$$

Thus, the contravariant form of $g_{\mu\upsilon}$ can be easily obtained as

$$g^{\mu\upsilon}=\begin{pmatrix} -\frac{A}{\rho^2\Delta(1+L)} & 0 & 0 & \frac{-2Mra}{\rho^2\Delta\sqrt{1+L}} \\ 0 & \frac{\Delta}{\rho^2} & 0 & 0 \\ 0 & 0 & \rho^{-2} & 0 \\ \frac{-2Mra}{\rho^2\Delta\sqrt{1+L}} & 0 & 0 & \frac{\rho^2-2Mr}{\rho^2\Delta(1+L)sin^2\theta} \end{pmatrix}. \tag{3.22}$$

One can also get the Hawking temperature of this Kerr-like BH which is derived from its surface gravity (K) as follows

$$T_H=\frac{\mathrm{K}}{2\pi}, \qquad \kappa=-\frac{1}{2}\lim_{r\to r_+}\sqrt{\frac{-1}{Y}}\frac{dY}{dr}, \;\; Y\equiv g_{tt}-\frac{g_{t\varphi}^2}{g_{\varphi\varphi}}. \tag{3.23}$$

By using the relevant metric components given in Eq. (3.20) and substituting them into Eq. (3.24), the Hawking temperature is found to be

$$T_H^{KBGM}=\frac{\sqrt{M^2-a^2(1+L)}}{4\pi M\sqrt{1+L}\left(M+\sqrt{M^2-a^2(1+L)}\right)}. \tag{3.24}$$

If we eliminate the rotation parameter Eq. (3.24) the temperature of SBHBGM in Eq. (3.14) recovered.

Chapter 4

GUP MODIFIED HAWKING RADIATION

In the all approaches for the quantum gravity such as string theory [75,76], BH physics [77,78], there exist a common measurable parameter like minimum length which is at the order of the Planck length $l_p = \sqrt{\frac{G\hbar}{C^3}} \cong 10^{-23} cm$, in which G is the gravitational constant [79-81]. The manifestations of this minimal length appear in several theories of quantum gravity phenomenology, such as the deformed special relativity (DSR) [82], modified dispersion relation (MDR) [83], and GUP [84]. Moreover, it employs in the further fields like, cosmology [85], superconductivity, and quantum Hall effect [86].

In this thesis, we shall work on the gravity correction of the Heisenberg uncertainty principle ($\Delta x \sim \frac{\hbar}{\Delta P}$) at energies close to the Planck scale which called GUP which represented as

$$\Delta x_i \Delta p_i \geq \frac{\hbar}{2}[1 + \beta((\Delta p)^2 + < p >^2) + 2\beta(\Delta p_i^2 + < p_i >^2)], \qquad (4.1)$$

where $i = 1,2,3$ and

$$p^2 = \sum_{j=1}^{3} P_j P_j\,, \;\; \beta = \frac{\beta_0}{(M_{Pl}c)^2} = \frac{l_{Pl}^2}{2\hbar^2}, \qquad (4.2)$$

and M_{Pl} is the Plank mass also Plank energy is $M_{Pl}c^2 \approx 1.2 \times 10^{19}\ GeV$.

Involving of the different fields into Cosmology, High Energy Physics, and BHs, with GUP have attracted lots of attention among them, study thermodynamics of the BHs

under GUP modification is an interesting active research area [87-90]. As the effect of GUP on the BHs, one can mention to the self-complete characteristic of gravity, which likely cover any curvature singularity behind of the event horizon as a matter compression at the Plank scale [91]. Moreover, the effects of the GUP on HR have also been considered [92] in our earlier findings [93,94]. In particular, we have studied the modification of the Hawking temperature of BHs in the BGM due to the GUP.

4.1 GUP Modified Hawking Radiation in Bumblebee Gravity Model

In this subsection, we aim to defined the Hawking temperature of bumblebee BH under the modification of GUP. Thus, we shall attempt to reveal the effects of both LSB and GUP on the HR.

Here, we mainly focus on the quantum gravity effects on the HR of SBHBGM in the tunneling paradigm. Although a number of QGTs have been proposed, however, physics literature does not as yet have a complete and consistent QGT. In the absence of a complete quantum description of the HR, we use effective models to describe the quantum gravitational behavior of the BH evaporation. In particular, string theory, loop quantum gravity, and quantum geometry predict the minimal observable length on the Planck scale [57,58], which leads to the GUP theory:

$$\Delta x \Delta p \geq \frac{\hbar}{2}[1 + \beta(\Delta p)^2], \tag{4.3}$$

where $\beta = \frac{\alpha_0}{M_p^2}$ in which $M_p = \sqrt{\frac{\hbar c}{G}}$ denotes the Planck mass and α_0 is the dimensionless parameter, which encodes the quantum gravity effects on the particle dynamics. The upper bound for α_0 was obtained as $\alpha_0 < 10^{21}$ [135].

Since the GUP and LSB effects are high energy modifications of the QGT, it is interesting to investigate their combined effects. To this end, we study the GUP-assisted HR of bosons (spin-0) and fermions' (spin$-1/2$) quantum tunneling [136,137] from the SBHBGM.

4.1.1 GUP-assisted HR of SBHBGM: bosons' tunneling

The generic Klein-Gordon equation within the framework of GUP is given by

$$-(i\hbar)^2\partial^t\partial_t\psi = \left[(i\hbar)^2\partial^\mu\partial_\mu + m^2\right]\left\{1 - 2\beta\left[(i\hbar)^2\partial^\mu\partial_\mu + m^2\right]\right\}\psi, \qquad (4.4)$$

where β and m are the GUP parameter mass of the scalar particle, respectively. Introducing the following ansatz for the wave function ψ

$$\psi = exp\left[\frac{i}{\hbar}I(t,r,\theta,\varphi)\right], \qquad (4.5)$$

where $I(t,r,\theta,\varphi)$ is the classically forbidden action for quantum tunneling. Substituting Eq. (4.5), together with the metric functions of line-element (3.11), into Eq. (4.4), we get

$$(f)^{-1}(\partial_t I)^2 = \left[\frac{f}{1+L}(\partial_r I)^2 + \frac{1}{r_h^2}(\partial_\theta I)^2 + \frac{1}{r_h^2 sin^2\theta}\left(\partial_\varphi I\right)^2 + m^2\right] \times\left\{1 - 2\beta\left[\frac{f}{1+L}(\partial_r I)^2 + \frac{1}{r^2}(\partial_\theta I)^2 + \frac{1}{r^2 sin^2\theta}\left(\partial_\varphi I\right)^2 + m^2\right]\right\}, \qquad (4.6)$$

where $f = 1 - \frac{2M}{r}$.

It is easy to see that SBHBGM (3.11) admits two Killing vectors $< \partial_t, \partial_\varphi >$. The existence of these symmetries implies that we can assume a following separable solution for the action

$$I = -\omega t + R(r) + S(\theta) + J\varphi, \tag{4.7}$$

where ω and J denote the energy and angular momentum of the radiated particle, respectively. Substituting Eq. (4.7) in Eq. (4.6), we obtain

$$\frac{\omega^2}{f} = \left[\frac{f}{1+L}(\partial_r R)^2 + \frac{1}{r^2}\left((\partial_\theta S)^2 + \frac{J^2}{sin^2\theta}\right) + m^2\right] \times \left\{1 - 2\beta\left[\frac{f}{1+L}(\partial_r R)^2 + \frac{1}{r^2}\left((\partial_\theta S)^2 + \frac{J^2}{sin^2\theta}\right) + m^2\right]\right\}. \tag{4.8}$$

We focus only on the radial trajectories in which only the $(r-t)$ sector is considered. Thus, one can set

$$\frac{1}{r^2}\left((\partial_\theta S)^2 + \frac{J^2}{sin^2\theta}\right) = e, \tag{4.9}$$

where e is a constant. So, Eq. (4.8) becomes

$$\left[\frac{f}{1+L}(\partial_r R)^2 + e + m^2\right]\left\{1 - 2\beta\left[\frac{f}{1+L}(\partial_r R)^2 + e + m^2\right]\right\} = \frac{\omega^2}{f}, \tag{4.10}$$

which can be rewritten as a bi-quadratic equation as follows

$$a(\partial_r R)^4 + b(\partial_r R)^2 + c = 0, \tag{4.11}$$

where

$$a = -2\beta\frac{f^2}{(1+L)^2}, \tag{4.12}$$

$$b = \frac{f}{1+L}[1 - 4\beta(m^2 + e)], \tag{4.13}$$

and

$$c = e - 2\beta e^2 - 4\beta e m^2 + m^2 - \frac{\omega^2}{f} - 2\beta m^4. \tag{4.14}$$

Eq. (4.11) has four roots if $b^2 - 4ac > 0$. We deduced from our analytical computations that only two roots $(R_{\pm})$ have physical meaning at the event horizon of the SBHBGM. These roots are

$$R_{\pm} = \pm \int dr \sqrt{(1+L)\frac{\omega^2 - m^2 f + 2\beta m^4 f}{f^2}}(1+2\beta m^2)$$

$$= i\pi\omega M\sqrt{1+L}(1+2\beta m^2). \qquad (4.15)$$

It is worth noting that a $+/-$ sign represents an outgoing/ingoing wave. On the other hand, the integrand of the integral (4.15) has a pole at $r = r_h$. Evaluating the integral by using the Cauchy's integral formula, we obtain the imaginary part of the action as

$$ImR_{\pm} \equiv ImI_{\pm} = \pm\pi\omega M\sqrt{1+L}(1+2\beta m^2). \qquad (4.16)$$

Thus, the tunneling rate of the scalar particles becomes

$$\Gamma = \frac{P(emission)}{P(absorbtion)} = \frac{exp(-2ImI_+)}{exp(-2ImI_-)} = exp(-4ImI_+), \qquad (4.17)$$

which for SBHBGM reads

$$\Gamma = exp\left[-4\omega M\pi\sqrt{1+L}(1+2\beta m^2)\right]. \qquad (4.18)$$

Recalling the expression of the Boltzmann factor

$$\Gamma = exp\left(-\frac{\omega}{T}\right), \qquad (4.19)$$

one can read the modified Hawking temperature $\left(\tilde{T}_H\right)$ as follows

$$\tilde{T}_H = \frac{1}{8\pi M\sqrt{1+L}[1+2\beta m^2]} = \frac{T_H}{(1+2\beta m^2)}. \qquad (4.20)$$

As can be seen above, after terminating the GUP parameter i.e. $\beta = 0$, one can recover the standard Hawking temperature (3.16).

4.1.2 GUP-assisted HR of SBHBGM: fermions' tunneling

In this subsection, we aim to derive the modified Hawking temperature in the case of radiating fermions. To this end, we consider the Dirac equation, which is given by [134]

$$\{i\hbar\gamma^0\partial_0 + [m + i\hbar\gamma^\mu(\Omega_\mu + \hbar\beta\partial_\mu)](1 - \beta m^2 + \beta\hbar^2 g_{jk}\partial^j\partial^k)\}\psi = 0, \quad (4.21)$$

where ψ denotes the test spinor field. The γ^μ matrices for the metric (3.11) are given by

$$\gamma^t = \frac{1}{\sqrt{f(r)}}\begin{pmatrix} i & 0 \\ 0 & -i \end{pmatrix}, \qquad \gamma^r = \sqrt{\frac{f(r)}{1+L}}\begin{pmatrix} 0 & \sigma^3 \\ \sigma^3 & 0 \end{pmatrix},$$

$$\gamma^t = \frac{1}{r}\begin{pmatrix} 0 & \sigma^1 \\ \sigma^1 & 0 \end{pmatrix}, \qquad \gamma^\varphi = \frac{1}{rsin\theta}\begin{pmatrix} 0 & \sigma^2 \\ \sigma^2 & 0 \end{pmatrix}, \quad (4.22)$$

in which σ^i's represent the well-known Pauli matrices [135]. One can easily ignore the terms having β^2 since β is the effect of quantum gravity and it is a relatively very small quantity. For spin-up particles, the wave function can be expressed as [134]

$$\psi = \begin{pmatrix} 0 \\ X \\ 0 \\ Y \end{pmatrix} exp\left(\frac{i}{\hbar}I\right), \quad (4.23)$$

where X, Y, and I are functions of coordinates (t, r, θ, φ). I is the action of the emitted fermion. It is worth noting that here we only consider the spin-up case since it is physically same with the spin-down case; the only difference is the sign. Substitution of the wave function in the generalized Dirac equation (4.21) results in the following coupled equations

$$iX\frac{1}{\sqrt{f}}\partial_t I - Y(1-\beta m^2)\sqrt{\frac{f}{1+L}}\partial_r I - Xm\beta\left[\frac{f}{1+L}(\partial_r I)^2 + g^{\theta\theta}(\partial_\theta I)^2 + g^{\varphi\varphi}\left(\partial_\varphi I\right)^2\right] +$$

$$Y\beta\sqrt{\frac{f}{1+L}}\partial_r I\left[\frac{f}{1+L}(\partial_r I)^2 + g^{\theta\theta}(\partial_\theta I)^2 + g^{\varphi\varphi}\left(\partial_\varphi I\right)^2\right] + Xm(1-\beta m^2) = 0, \quad (4.24)$$

and

$$iY\frac{1}{\sqrt{f}}\partial_t I - X(1-\beta m^2)\sqrt{\frac{f}{1+L}}\partial_r I - Ym\beta\left[\frac{f}{1+L}(\partial_r I)^2 + g^{\theta\theta}(\partial_\theta I)^2 + g^{\varphi\varphi}\left(\partial_\varphi I\right)^2\right] +$$

$$X\beta\sqrt{\frac{f}{1+L}}\partial_r I\left[\frac{f}{1+L}(\partial_r I)^2 + g^{\theta\theta}(\partial_\theta I)^2 + g^{\varphi\varphi}\left(\partial_\varphi I\right)^2\right] + Ym(1-\beta m^2) = 0. \quad (4.25)$$

Then, one can get the following decoupled equations

$$X\left\{-(1-\beta m^2)\sqrt{g^{\theta\theta}}\partial_\theta I + \beta\sqrt{g^{\theta\theta}}\partial_\theta I\left[\frac{f}{1+L}(\partial_r I)^2 + g^{\theta\theta}(\partial_\theta I)^2 + g^{\varphi\varphi}\left(\partial_\varphi I\right)^2\right] -\right.$$

$$\left. i(1-\beta m^2)\sqrt{g^{\varphi\varphi}}\partial_\varphi I + i\beta\sqrt{g^{\varphi\varphi}}\partial_\varphi I\left[\frac{f}{1+L}(\partial_r I)^2 + g^{\theta\theta}(\partial_\theta I)^2 + g^{\varphi\varphi}\left(\partial_\varphi I\right)^2\right]\right\} = 0,$$

(4.26)

and

$$Y\left\{-(1-\beta m^2)\sqrt{g^{\theta\theta}}\partial_\theta I + \beta\sqrt{g^{\theta\theta}}\partial_\theta I\left[\frac{f}{1+L}(\partial_r I)^2 + g^{\theta\theta}(\partial_\theta I)^2 + g^{\varphi\varphi}\left(\partial_\varphi I\right)^2\right] -\right.$$

$$\left. i(1-\beta m^2)\sqrt{g^{\varphi\varphi}}\partial_\varphi I + i\beta\sqrt{g^{\varphi\varphi}}\partial_\varphi I\left[\frac{f}{1+L}(\partial_r I)^2 + g^{\theta\theta}(\partial_\theta I)^2 + g^{\varphi\varphi}\left(\partial_\varphi I\right)^2\right]\right\} = 0.$$

(4.27)

By using the fact that SBHBGM spacetime has a time-like Killing vector $\frac{\partial}{\partial r'}$, one can obtain the radial action by performing the separation of variables technique:

$$I = -\omega t + W(r) + \Theta(\theta,\varphi), \quad (4.28)$$

where ω is the fermion energy. Substituting Eq. (4.28) into Eqs. (4.24) -(4.27), we find out the identical equations for X and Y equations. Thus, we have

$$\beta\left[\frac{f}{1+L}(\partial_r W)^2 + g^{\theta\theta}(\partial_\theta\Theta)^2 + g^{\varphi\varphi}\left(\partial_\varphi\Theta\right)^2\left(\sqrt{g^{\theta\theta}}\partial_\theta\Theta + i\sqrt{g^{\varphi\varphi}}\partial_\varphi\Theta\right)\right] + (1 -$$

$$\beta m^2)\left(\sqrt{g^{\theta\theta}}\partial_\theta\Theta + \mathrm{i}\sqrt{g^{\varphi\varphi}}\partial_\varphi\Theta\right) = 0, \quad (4.29)$$

Or

$$\left(\sqrt{g^{\theta\theta}}\partial_\theta\Theta + \mathrm{i}\sqrt{g^{\varphi\varphi}}\partial_\varphi\Theta\right) \times\left[\beta\left(\frac{f}{1+L}(\partial_r W)^2 + g^{\theta\theta}(\partial_\theta\Theta)^2 + g^{\varphi\varphi}\left(\partial_\varphi\Theta\right)^2 + m^2\right) - 1\right] = 0. \tag{4.30}$$

It is obvious that the expression inside the square brackets cannot vanish; thus, one should have

$$\left(\sqrt{g^{\theta\theta}}\partial_\theta\Theta + i\sqrt{g^{\varphi\varphi}}\partial_\varphi\Theta\right) = 0, \tag{4.31}$$

and the solution of Θ, therefore, does not contribute to the tunneling rate. The above result helps us to simplify Eqs. (4.29) and (4.30) [with ansatz (4.28)] as follows

$$X\left\{\frac{i\omega}{\sqrt{f}} - m\beta\left[\frac{f}{1+L}(\partial_r W)^2\right] + m(1-\beta m^2)\right\} = Y\left\{(1-\beta m^2)\sqrt{\frac{f}{1+L}}\partial_r W - \beta\sqrt{\frac{f}{1+L}}\partial_r W\left[\frac{f}{1+L}(\partial_r W)^2\right]\right\}, \tag{4.32}$$

and

$$Y\left\{\frac{i\omega}{\sqrt{f}} - m\beta\left[\frac{f}{1+L}(\partial_r W)^2\right] + m(1-\beta m^2)\right\} = X\left\{(1-\beta m^2)\sqrt{\frac{f}{1+L}}\partial_r W - \beta\sqrt{\frac{f}{1+L}}\partial_r W\left[\frac{f}{1+L}(\partial_r W)^2\right]\right\}. \tag{4.33}$$

In the simple way, one can set

$$\begin{aligned} XA + YB &= 0, \\ YA + XB &= 0, \end{aligned} \tag{4.34}$$

where

$$A = \frac{i\omega}{\sqrt{f}} - m\left[\frac{f\beta}{1+L}(\partial_r W)^2 + 1 - \beta m^2\right], \tag{4.35}$$

and

$$B = -(1-\beta m^2)\sqrt{\frac{f}{1+L}}\,\partial_r W + \beta\sqrt{\frac{f}{1+L}}\,\partial_r W\left[\frac{f}{1+L}(\partial_r W)^2\right]. \tag{4.36}$$

After making some manipulations, we see that $A^2 - B^2 = 0$

$$\left(\frac{i\omega}{\sqrt{f}} - m\beta\left[\frac{f}{1+L}(\partial_r W)^2\right] + m(1-\beta m^2)\right)^2 = \left((1-\beta m^2)\sqrt{\frac{f}{1+L}}\,\partial_r W - \beta\sqrt{\frac{f}{1+L}}\,\partial_r W\left[\frac{f}{1+L}(\partial_r W)^2\right]\right)^2, \tag{4.37}$$

which yields

$$L_6(\partial_r W)^6 + L_4(\partial_r W)^4 + L_2(\partial_r W)^2 + L_0 = 0, \tag{4.38}$$

where

$$L_6 = \beta^2 f\left(\frac{f}{1+L}\right)^3, \tag{4.39}$$

$$L_4 = \beta\left(\frac{f}{1+L}\right)^2 f(m^2\beta - 2), \tag{4.40}$$

$$L_2 = \frac{f^2}{1+L}\left(\frac{2i\omega m}{\sqrt{f}} + (1-\beta m^2)(1+2m^2\beta)\right), \tag{4.41}$$

$$L_0 = \omega^2 - m^2 f(1-\beta m^2)^2 - 2i\omega m\sqrt{f}(1-\beta m^2), \tag{4.42}$$

ignoring O(β^2) terms, Eq. (4.38) reduces to

$$L_4(\partial_r W)^4 + L_2(\partial_r W)^2 + L_0 = 0. \tag{4.43}$$

Therefore, we have

$$W_\pm = \pm\int dr\,\frac{\sqrt{(1+L)(\omega^2+m^2 f)}}{f}\left[1+\beta\left(m^2+\frac{\omega^2}{f}\right)\right] \cong \pm i\pi\omega r_+(1+2\beta m^2) = \pm i2\pi M\omega\sqrt{1+L}(1+2\beta m^2), \tag{4.44}$$

in another form

$$ImW_\pm = 2\pi M\omega\sqrt{1+L}(1+2\beta m^2). \tag{4.45}$$

Recalling Eq. (4.18), we find the tunneling rate of fermions as follows

$$\Gamma \cong exp(-4ImW_{+}) = exp\left(8\pi M\omega\sqrt{1+L}(1+2\beta m^2)\right). \quad (4.46)$$

Thus, with the help of the Boltzmann factor (4.19), we get the GUP-consolidated temperature of the SBHBGM via the emission of the fermions:

$$T = \frac{1}{8\pi M\sqrt{1+L}(1+2\beta m^2)} = \frac{T_0}{(1+2\beta m^2)}, \quad (4.47)$$

in which T_0 represents the original Hawking temperature

$$T_0 = \frac{1}{8\pi M\sqrt{1+L}}. \quad (4.48)$$

The above result shows that GUP corrected temperature deviates from the standard Hawking temperature.

4.2 GUP Modified Hawking Radiation in Rotating Polytropic Black Hole

BHs are surrounded by different matter, such as accretion disks (accretion flew around a BH), galactic nuclei, strong magnetic fields, other stars and planets. Therefore, interactions happen with their surroundings and affect to the properties and stability of the BHs [138]. However, it is interesting to know that, a BH even interacts with the vacuum around it and creating pairs of particles and evaporating due to HR. Thus, a real BH can never be fully described by its basic parameters and is always in the perturbed state. Study about the coalescence of two identical neutron stars represented by polytropes was considered first time by Nakamura and Oohara in 1989 [139], and it is evaluated in many situations in the context of GR as well as in astrophysical problems [140-143]. Recently, BH solutions by considering the polytropic equations of state have been obtained [144] this equation of state which has been used in various astrophysical situation [145,146], defined as

$$P = K\rho^{1+\frac{1}{n}}, \quad (4.49)$$

where n is polytropic index and K is a positive constant. The rotating polytropic BH solution is obtained by applying the Newman-Janis algorithm without complexification [147] to its static version.

In this subsection, we consider the physical properties of rotating polytropic BH. As a starting point, the metric in the rotating coordinates is given by

$$ds^2 = \left(1 - \frac{2f}{\rho^2}\right)dt^2 - \frac{\rho^2}{\Delta}dr^2 + \frac{4af\sin^2\theta}{\rho^2}dtd\varphi - \rho^2 d\theta^2 - \frac{\Sigma \sin^2\theta}{\rho^2}d\varphi^2, \tag{4.50}$$

where

$$2f = r^2(1 - F),$$
$$\rho^2 = r^2 + a^2\cos^2\theta,$$
$$\Sigma = (r^2 + a^2)^2 - a^2\Delta\sin^2\theta, \tag{4.51}$$

in which

$$\Delta = a^2 + r^2F, \tag{4.52}$$

and

$$F = \frac{r^2}{L^2} - \frac{2M}{r}. \tag{4.53}$$

In Eq. (4.53), $L^2 = -\frac{3}{\Lambda}$, where Λ represents the cosmological constant. Throughout our study, we shall consider the negative cosmological constant, where empty space itself has negative energy density but positive pressure, like the anti-de Sitter space. The solution of $\Delta(r_\pm) = 0$ yields the horizons of the BH. Namely, we have

$$a^2 + r_\pm^2 F(r_\pm) = 0, \tag{4.54}$$

which yields

$$r_+ = \frac{\left[-\frac{2\sqrt[3]{6}a^2L^2}{d(a,M,L)} + \frac{6L^2M}{\sqrt{\frac{\sqrt[3]{6}a^2L^2}{d(a,M,L)} + \frac{1}{2}d(a,M,L)}} - d(a,M,L)\right]^{\frac{1}{2}} + \left[\frac{2\sqrt[3]{6}a^2L^2}{d(a,M,L)} + d(a,M,L)\right]^{\frac{1}{2}}}{2^{5/6}\sqrt[3]{3}},$$

(4.55)

where

$$d(a,M,L) = \sqrt[3]{\sqrt{3}\sqrt{27L^8M^4 - 16a^2L^2} + 9L^4M^2}. \quad (4.56)$$

One can easily observe from the above horizon condition that there exists a bound on the spin/mass-parameter, $\left(\frac{a}{M}\right)$ [147]. The allowed values for the spin/mass-parameter are constrained as follows [148]:

$$\frac{a}{M} < 3^{1/2}\left(\frac{L}{4M}\right)^{1/3}. \quad (4.57)$$

It is worth noting that above result differs from the Kerr case in which the constraint corresponds to $\frac{a}{M} < 1$. The Hawking temperature for the rotating polytropic black hole is given by [148]

$$T_H = \frac{1}{4\pi}\lim_{r\to r_+}\frac{\partial_r g_{tt}}{\sqrt{g_{tt}g_{rr}}} = \frac{-a^2(L^2(M+r_+) - 2r_+^3) + L^2Mr_+^2 + r_+^5}{2\pi L^2(a^2 + r_+^2)^2}. \quad (4.58)$$

Now, let discuss the line element in the dragging coordinate system, in this system, an inertial frame around a rotating black hole considered and a nonrotating observer is one who moves with coordinate angular velocity $\Omega = -\frac{g_{03}}{g^{33}}$ [149,150]. Performing the dragging coordinate transformation to the metric (4.50), we get

$$ds^2 = -\frac{\Delta\rho^2}{\Sigma}dt^2 + \frac{\rho^2}{\Delta}dr^2 + \rho^2 d\theta^2 = -Fdt^2 + \frac{1}{G}dr^2 + Kd\theta^2. \quad (4.59)$$

The generalized Klein-Gordon equation under GUP modification (4.4) can be used with a standard ansatz for ψ

$$\psi = exp\left[\frac{i}{\hbar} I(t,r,\theta)\right]. \tag{4.60}$$

Then we get

$$\left(\frac{1}{F}\right)(\partial_t I)^2 = \left[G(\partial_r I)^2 + \frac{1}{K}(\partial_\theta I)^2 + m^2\right] - 2\beta\left[G(\partial_r I)^2 + \frac{1}{K}(\partial_\theta I)^2 + m^2\right]^2. \tag{4.61}$$

To solve the above equation, we carry out the separation of variables as follows

$$I = -(\omega - j\Omega)t + R(r) + W(\theta) + K, \tag{4.62}$$

where ω and j are the energy of the particles and the angular momentum, respectively. K is a constant, which maybe can be complex. Substituting Eq. (4.62) into the Eq. (4.61) to obtain

$$a(\partial_r R)^4 + b(\partial_r R)^2 + c = 0, \tag{4.63}$$

where

$$a = -2\beta G^2, \tag{4.64}$$

$$b = G(1 - 4\beta m^2), \tag{4.65}$$

$$c = \frac{1}{K}(\partial_\theta W)^2 + m^2 - 2\beta m^4 - \frac{1}{F}(\omega - j\Omega)^2. \tag{4.66}$$

The solution of this quartic equation at the horizon is

$$R_\pm = \pm\int \frac{dr}{\sqrt{FG}}\sqrt{(\omega - j\Omega)^2 - F\left(\frac{1}{\rho^2(r_h)}(\partial_\theta W)^2 + m^2\right)} \times \left[1 + \beta\left(m^2 + \frac{1}{\rho^2(r_h)}(\partial_\theta W)^2\right) + \beta\frac{(\omega - j\Omega)^2}{F}\right], \tag{4.67}$$

where $+/-$ represent the outgoing and ingoing solutions. Here we have taken the near solution approximation, near the event horizon$(r = r_+)$,

$$\Delta(r) = \Delta(r_+) + (r - r_+)\Delta_{,r}(r_+) + O((r - r_+)^2) \cong (r - r_+)\Delta_{,r}(r_+). \tag{4.68}$$

Integrating Eq. (4.67) near the event horizon by using the residue theorem for semicircle, we acquire

$$R_{\pm} = \frac{i\pi(\omega - j\Omega_h)(r_h^2 + a^2)^2 L^2}{2(r_h^5 + Mr_h^2 L^2 + 2r^3 a^2 - ML^2 a^2 - r_h a^2 L^2)}[1 + \beta\Xi], \tag{4.69}$$

where

$$\Xi = \frac{1}{2}\left(m^2 + \frac{\left(\frac{d\omega}{d\theta}\right)^2}{r_h^2 + a^2 cos^2\theta} - \frac{(\omega - j\Omega_h)^2 \left(r_h^2 + a^2\right)^4}{3(r_h^2 + a^2 cos^2\theta)\left(r_h^5 + Mr_h^2 L^2 + 2r_h^3 a^2 - ML^2 a^2 - r_h a^2 L^2\right)^2}\right). \tag{4.70}$$

Based on the WKB approximation, the emission and absorption tunneling probabilities of the scalar particles passing the event horizon $r = r_+$ are defined as

$$\Gamma(emission) = exp[-2(ImR_+ + Im\xi)], \tag{4.71}$$

and

$$\Gamma(emission) = exp[-2(ImR_- + Im\xi)], \tag{4.72}$$

Thus, the tunneling rate for the scalar particles yields

$$\Gamma = exp[-4ImR_+], \tag{4.73}$$

where for the rotating polytropic BH is obtained

$$\Gamma = exp\left[\frac{-2\pi(\omega - j\Omega_h)(r_h^2 + a^2)^2 L^2}{(r_h^5 + Mr_h^2 L^2 + 2r^3 a^2 - ML^2 a^2 - r_h a^2 L^2)}(1 + \beta\Xi)\right]. \tag{4.74}$$

Hence, one can read the modified Hawking temperature T_H as follows

$$T_H = \frac{T_0}{1 + \beta\Xi}, \tag{4.75}$$

in which T_0 is the standard form of rotating polytropic BH's hawking temperature.

Chapter 5

SCALAR PERTURBATION

5.1 Scalar Perturbation and Effective Potential of SBHBGM

In this section, we shall first derive the effective potentials of the scalar perturbations in the geometry of the SBHBGM. Then, the effective potentials will be used for computing the GFs of the SBHBGM. The obtained results will be depicted with some plots and discussed. The massless Klein- Gordon equation is given by

$$\square\Psi = 0, \tag{5.1}$$

where the D'Alembert operator is denoted by the box symbol: $\square = \frac{1}{\sqrt{-g}}\partial_\mu\left(\sqrt{-g}g^{\mu\upsilon}\partial_\upsilon\right)$. For the SBHBGM metric,

$$ds^2 = -\left(1-\frac{2M}{r}\right)dt^2 + (1+L)\left(1-\frac{2M}{r}\right)^{-1}dr^2 + r^2(d\theta^2 + sin^2\theta d\varphi^2). \tag{5.2}$$

We have

$$\sqrt{-g} = r^2 sin\theta\sqrt{1+L}, \tag{5.3}$$

and therefore Eq. (5.1) reads

$$\square\Psi = \frac{1}{f}\partial_t^2 - \frac{1}{r^2(1+L)}(2rf\partial_r\Psi + r^2\partial_r f\partial_r\Psi + r^2 f\partial_r^2\Psi) + \frac{1}{r^2 sin\theta}\left(-cos\theta\partial_\theta\Psi - sin\theta\partial_\theta^2\Psi\right) - \frac{1}{r^2 sin^2\theta}\partial_\varphi^2\Psi. \tag{5.4}$$

We invoke the following ansatz for the scalar field in the above equation:

$$\Psi = P(r)A(\theta)e^{-i\omega t}e^{im\varphi}, \tag{5.5}$$

so that we have

$$\square\Psi = -\frac{\omega^2}{f} - \frac{1}{P(1+L)}\left[\frac{2f}{r}P' + f'P' + fP''\right] - \frac{1}{r^2 A sin\theta}\left[cos\theta A' + sin\theta A'' - \frac{m^2}{sin\theta}A\right] = 0, \quad (5.6)$$

when one changes the independent variable θ to $cos^{-1}z$, the angular equation is found to be

$$(1-z^2)A'' + 2zA' - \left[m^2 + \frac{\lambda_s}{1+L}(1-z^2)\right]A = 0, \quad (5.7)$$

where λ_s denotes the eigenvalue. The above equation is nothing but the Legendre differential equation when one sets

$$\lambda_s = -l(l+1)(1+L). \quad (5.8)$$

The radial equation then becomes

$$P'' + P'\left(\frac{f'}{f} + \frac{2}{r}\right) + \left[\frac{1+L}{f^2}\omega^2 + \frac{\lambda_s}{r^2 f}\right]P = 0. \quad (5.9)$$

Introducing a new variable $P = \frac{u}{r}$, we get a Schrödinger-like wave equation

$$\frac{du^2}{dr_*^2} + \left(\omega^2 - V_{eff}\right)u = 0, \quad (5.10)$$

Where r_* is the tortoise coordinate defined by

$$r_* = \sqrt{1+L}\int \frac{dr}{f}. \quad (5.11)$$

The effective potential felt by the scalar field then becomes

$$V_{eff} = f\left[\frac{f'}{(1+L)r} + \frac{l(l+1)}{r^2}\right]. \quad (5.12)$$

It is obvious from Fig. (5.1) that the effective potential vanishes both at the event horizon of the SBHBGT and at spatial infinity. This behavior will help us to analytically derive the GF of the scalar field emission from the SBHBGT.

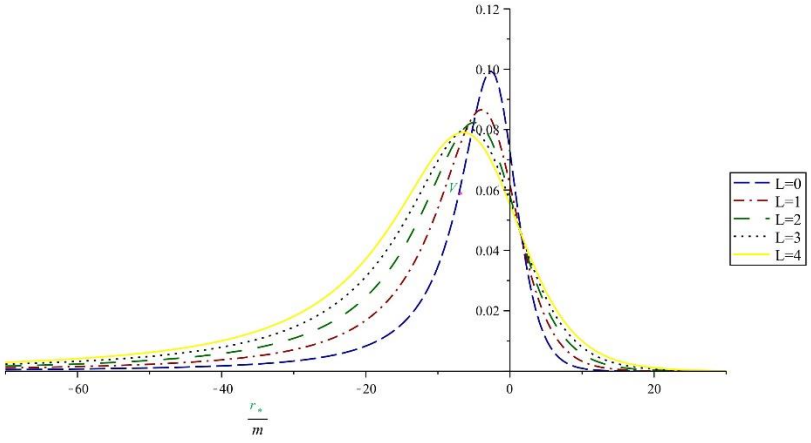

Figure 5.1: V_{eff} versus $\frac{r_*}{m}$ graph. The plots are governed by Eq. (5.12).

5.2 Scalar Perturbations for Charged de Rham-Gabadadz-Tolly Massive Gravity Black Holes in Nonlinear Electrodynamics

The purpose of this subsection is to study the scalar perturbation and defining the effective potential of the charged dRGT massive gravity BHs coupled with nonlinear electrodynamics.

Today, one of the best modification theories is the massive gravity, which consists of a massive graviton. Obviously, the perception of massive gravity theories is feasible with the help of gravitational wave astronomy. In 2010, a ghost-free non-linear extension of the FP action was proposed by de Rham–Gabadadze–Tolly (dRGT) [57-59]. According to this theory, the sixth Boulware and Deser (BD) [58] ghost mode is omitted by using a special type of potential to recover the Hamiltonian constraint, which is valid in any dimensions. In this new massive gravity, adding mass to the graviton does not change significantly the physics on a small scale from the GR, as it was expected. Here, we first introduce the 3 + 1-dimensional BH solutions in the dRGT massive gravity coupled with nonlinear electrodynamics [56]. The action of the dRGT

massive gravity without matter source and cosmological constant in 3 + 1-dimensions, which is given by

$$S = \frac{1}{2}\int d^4\chi\sqrt{-g}\left[R(g) + m_g^2(\mathcal{U}_2 + \alpha_3\mathcal{U}_3 + \alpha_4\mathcal{U}_4) + \mathcal{L}\right], \qquad (5.13)$$

in which

$$\mathcal{U}_2 = Tr(\mathcal{K})^2 - Tr(\mathcal{K}^2), \qquad (5.14)$$

$$\mathcal{U}_3 = Tr(\mathcal{K})^3 - 3Tr(\mathcal{K})Tr(\mathcal{K}^2) + 2Tr(\mathcal{K}^3), \qquad (5.15)$$

and

$$\mathcal{U}_4 = Tr(\mathcal{K})^4 - 6Tr(\mathcal{K}^2)Tr(\mathcal{K})^2 + 8Tr(\mathcal{K}^3)Tr(\mathcal{K}) + 3Tr(19\mathcal{K}^2)^2 - 6Tr(\mathcal{K}^4). \qquad (5.16)$$

Herein, m_g is the mass of the graviton, α_3 and α_4 are constants of the theory, and $\mathcal{K}$ represents a 4×4 matrix defined by

$$\mathcal{K}_\mu^\upsilon = \delta_\mu^\upsilon - \sqrt{g^{\alpha\gamma}f_{\gamma\beta}}. \qquad (5.17)$$

In latter equation, $g^{\alpha\gamma}$ is the inverse of the metric tensor and $f_{\gamma\beta}$ is a symmetric tensor, which is called reference (or fiducial) metric. The nonlinear electrodynamics Lagrangian $\mathcal{L}$ is defined by [151],

$$\mathcal{L} = \frac{-\mathcal{F}}{1 - \frac{b}{\sqrt{8}}\sqrt{-\mathcal{F}}}, \qquad (5.18)$$

where b is a positive parameter and $\mathcal{F} = F_{\alpha\beta}F^{\alpha\beta}$ is nothing but the Maxwell invariant with a pure electric field

$$\boldsymbol{F} = E(r)dt \wedge dr. \qquad (5.19)$$

Variation of the action with respect to electric potential admits the following Maxwell nonlinear equation

$$d\left(\widetilde{\boldsymbol{F}}\frac{d\mathcal{L}}{d\mathcal{F}}\right) = 0, \qquad (5.20)$$

where $\widetilde{\boldsymbol{F}}$ is the dual of $\boldsymbol{F}$. The variation of the metric with respect to the metric tensor yields the following field equations $G_{\mu}^{\upsilon} + m_g^2 \chi_{\mu}^{\upsilon} = T_{\mu}^{\upsilon}$, in which

$$\chi_{\mu\upsilon} = \mathcal{K}_{\mu\upsilon} - \mathcal{K} g_{\mu\upsilon} - \alpha\left(\mathcal{K}_{\mu\upsilon}^2 - \mathcal{K}\mathcal{K}_{\mu\upsilon} + \frac{\mathcal{U}_2}{2} g_{\mu\upsilon}\right) + 3\beta\left(\mathcal{K}_{\mu\upsilon}^3 - \mathcal{K}\mathcal{K}_{\mu\upsilon}^2 + \frac{\mathcal{U}_2}{2}\mathcal{K}_{\mu\upsilon} - \frac{\mathcal{U}_3}{6} g_{\mu\upsilon}\right), \quad (5.21)$$

with $\alpha = 1 + 3\alpha_3$ and $\beta = \alpha_3 + 4\alpha_4$. Furthermore, T_{μ}^{υ} denotes the nonlinear electrodynamics energy momentum tensor, which is given by

$$T_{\mu}^{\upsilon} = \frac{1}{2}\left(\mathcal{L}\delta_{\mu}^{\upsilon} - 4\mathcal{L}_F F_{\mu\lambda} F^{\upsilon\lambda}\right). \quad (5.22)$$

In spherically symmetric spacetime, we consider a line-element of the form

$$ds^2 = -n(r)dt^2 + \frac{dr^2}{f(r)} + L(r)^2(d\theta^2 + sin^2\theta d\varphi^2), \quad (5.23)$$

where $n(r), f\ (r)$, and $L(r)$ are to be obtained. The reference metric tensor can be chosen as

$$f_{\gamma\beta} = diag[0,0,h(r)^2, h(r)^2 sin^2\theta], \quad (5.24)$$

in which $h(r)^2$ is a coupling function. Having considered the actual metric (5.17) and the reference metric (5.18), one finds

$$\mathcal{K}_{\beta}^{\alpha} = diag\left[0,0,1 - \frac{h(r)}{L(r)}, 1 - \frac{h(r)}{L(r)}\right], \quad (5.25)$$

and consequently

$$X_t^t = X_r^r = -\frac{3L - 2h}{L} - \alpha\frac{(3L - h)(L - h)}{L^2} - \beta\frac{3(L - h)^2}{L^2}, \quad (5.26)$$

and

$$X_{\theta}^{\theta} = X_{\varphi}^{\varphi} = -\frac{3L - h}{L} - \alpha\frac{(3L - 2h)}{L} - \beta\frac{3(L - h)^2}{L}. \quad (5.27)$$

Also, the nonlinear Maxwell equation admits an electric field of the form [152,153]

$$E(r)=\frac{2}{b}\left(1-\frac{1}{\sqrt{1+\frac{qb}{r^2}}}\right), \tag{5.28}$$

and thus the energy momentum tensor components are explicitly found to be

$$T_t^t=T_r^r=\frac{-E}{\left(1-\frac{bE}{2}\right)^2}, \tag{5.29}$$

and

$$T_\theta^\theta=T_\varphi^\varphi=\frac{E^2}{1-\frac{bE}{2}}. \tag{5.30}$$

As $X_t^t=X_r^r$, one should impose $G_t^t=G_r^r$ which implies that

$$\frac{d}{dr}\left(\frac{n}{f}L'^2\right)=0, \tag{5.31}$$

where a prime denotes the derivative of a function with respect to its argument. One can easily check that for the case of $n(r)=f(r)$ and $L(r)=r$, Eq. (5.31) is satisfied. A substitution into the tt or rr components of the Einstein's equations yield

$$f(r)=1-\frac{2M}{r}+\frac{8r^2}{3b^2}\left(1+\frac{qb}{r^2}\right)^{\frac{3}{2}}-\frac{4q}{b}\left(1+\frac{2r^2}{3qb}\right)+\frac{m_g^2}{r}\int dr\left(3(1+\alpha+\beta)r^2-2(1+2\alpha+3\beta)hr+h^2(\alpha+3\beta)\right), \tag{5.32}$$

in which M is an integration constant. Finally, $\theta\theta$ or $\varphi\varphi$ components of the Einstein's equation admit a trivial solution for the function $h(r)=h_0$ where h_0 is a constant parameter. Setting $L(r)=r$ and using the rr component of the Einstein's equation, after some algebra, we obtain the following analytical metric function for the charged dGRT black hole in the nonlinear electrodynamics

$$f(r) = 1 - \frac{2M}{r} + \frac{8r^2}{3b^2}\left(1 + \frac{qb}{r^2}\right)^{\frac{3}{2}} - \frac{4q}{b}\left(1 + \frac{2r^2}{3qb}\right) + m_g^2\big((1 + \alpha + \beta)r^2 - 2(1 + 2\alpha + 3\beta)h_0 r + h_0^2(\alpha + 3\beta)\big), \quad (5.33)$$

in which M is an integration constant. On the other hand, it is also possible to obtain a second set of solutions by considering $h(r) = \frac{3\beta+2\alpha+1}{\alpha+3\beta}$. After making straightforward calculations, one gets the following BH solution

$$f(r) = 1 - \frac{2M}{r} - \left(m_g^2 \frac{(1 + \alpha^2 + \alpha - 3\beta)}{3(\alpha + 3\beta)} + \frac{8}{3b^2}\right)r^2 - \frac{4q}{b} + \frac{8r^2}{3b^2}\left(1 + \frac{qb}{r^2}\right)^{\frac{3}{2}}. \quad (5.34)$$

It is worth noting that the class of solutions obtained in this study is a special case of more general solution [154], which has an energy momentum tensor of cosmological constant type. The derivation of this generic solution [154] does not lean on the ansatz for the physical and reference metric or the Stückelberg field [155–157], apart from their isotropy. Namely, the solution is compatible with arbitrary matter component, including the nonlinear electrodynamics. Therefore, the massive gravity-induced fluid, which behaves like a cosmological constant, can coexist with the isotropically distributed matter, which could be an alternative to the dark energy. In the literature, there exist other remarkable studies which are based on the generic solution (see for example [158,159]).

Now, we shall study the thermal radiation of the charged dRGT massive gravity (coupled with nonlinear electrodynamics) BHs. To this end, we first consider the massless charged Klein–Gordon equation

$$\frac{1}{\sqrt{-g}} D_\mu\left[\sqrt{-g}\, g^{\mu\upsilon} D_\upsilon\right]\psi = 0, \quad (5.35)$$

where

$$D_\mu = \partial_\mu - iqA_\mu, \tag{5.36}$$

in which the electromagnetic potential is defined as

$$A_t = -\frac{2}{b}\left(r - \sqrt{r^2 + qb}\right), \qquad A_r = A_\theta = A_\varphi = 0. \tag{5.37}$$

Plugging the line-element (5.23) of the charged dRGT massive gravity black hole in the Klein–Gordon equation (5.35), we get

$$\left[-\frac{1}{f(r)}\partial_t^2\psi + \frac{1}{f(r)}q^2A_t^2\psi + \frac{2iqA_t}{f(r)}\partial_t\psi + \frac{2f}{r}\partial_r\psi + f'(r)\partial_r\psi \right.$$
$$\left. + f(r)\partial_r^2\psi + \frac{cos\theta}{r^2 sin\theta}\partial_\theta\psi + \frac{1}{r^2}\partial_\theta^2\psi + \frac{1}{r^2 sin^2\theta}\partial_\varphi^2\psi\right] = 0. \tag{5.38}$$

We use the following ansatz for the wave function

$$\psi(t, r, \Omega) = e^{i\omega t}\frac{\varphi(r)}{r}Y_{lm}(\Omega), \tag{5.39}$$

in which $e^{i\omega t}$ is the oscillating function and Y_{lm} (Ω) are spherical harmonics, which satisfy the following angular equation

$$\frac{1}{sin^2\theta}\frac{\partial^2 Y}{\partial\varphi^2} + \frac{1}{sin\theta}\left[\frac{\partial}{\partial\theta}\left(sin\theta\frac{\partial Y}{\partial\theta}\right)\right] = -\lambda Y, \tag{5.40}$$

where $\lambda = l\,(l + 1)$ is the eigenvalue having orbital quantum number l. Thus, the radial equation reads

$$\frac{f}{\varphi r}\frac{d}{dr}\left[r^2 f\frac{d}{dr}\left(\frac{\varphi}{r}\right)\right] + (\omega - qA_t)^2 - \frac{\lambda f}{r^2} = 0. \tag{5.41}$$

The tortoise coordinate is defined by $\frac{dr_*}{dr} = \frac{1}{f(r)}$, which helps us to permute the radial equation to the form of one-dimensional Schrödinger equation

$$\frac{d^2\varphi(r)}{dr_*^2} + \left[\omega^2 - V_{eff}\right]\varphi(r) = 0, \tag{5.42}$$

where the effective potential in general form for dRGT massive gravity BHs with nonlinear electrodynamics is defined as

$$V_{eff} = 2\omega q A_t - q^2 A_t^2 + \frac{\lambda f}{r^2} + \frac{f}{r} f', \tag{5.43}$$

in which $f' = \frac{df}{dr}$. Hereafter we split our calculations into the first and second solutions and clarify them by indexes 1 and 2. Let us rearrange Eq. (5.33) as

$$f_1(r) = 1 - \frac{2M}{r} + \frac{8r^2}{3b^2}\left(1 + \frac{qb}{r}\right)^{\frac{3}{2}} - \frac{4q}{b}\left(1 + \frac{2r^2}{3qb}\right) + (Ar^2 - Br + C), \tag{5.44}$$

where

$$A = m_g^2(1 + \alpha + \beta), B = m_g^2(1 + 2\alpha + 3\beta)h_0, C = m_g^2(\alpha + 3\beta)h_0^2. \tag{5.45}$$

By substituting Eqs. (5.37) and (5.44) into the general formula (5.43), then the effective potential for the first solution can be obtained as

$$V_{eff(1)} = 2\omega q\left(-\frac{2}{b}\left(r - \sqrt{r^2 + qb}\right)\right) - \left(-\frac{2q}{b}\left(r - \sqrt{r^2 + qb}\right)\right)^2 + \frac{\lambda}{r^2}\Bigg(1 - \frac{2M}{r} + \frac{8r^2}{3b^2}\left(1 + \frac{qb}{r}\right)^{\frac{3}{2}} - \frac{4q}{b}\left(1 + \frac{2r^2}{3qb}\right) + (Ar^2 - Br + C)\Bigg) + \frac{1}{r}\Bigg(1 - \frac{2M}{r} + \frac{8r^2}{3b^2}\left(1 + \frac{qb}{r}\right)^{\frac{3}{2}} - \frac{4q}{b}\left(1 + \frac{2r^2}{3qb}\right) + (Ar^2 - Br + C)\Bigg) \times \left(\frac{2M}{r^2} + \sqrt{1 + \frac{qb}{r}}\left(\frac{16r}{3b^2} + \frac{4q}{3b}\right) - \frac{16qr}{3qb^2} + 2Ar - B\right). \tag{5.46}$$

Following the approach of above to derive the effective potential of dRGT massive gravity with nonlinear electrodynamics for second solution. The metric function has been introduced by Eq. (5.34), which we can rewrite as

$$f_2(r) = 1 - \frac{2M}{r} - \left(D + \frac{8}{3b^2}\right)r^2 - \frac{4q}{b} + \frac{8r^2}{3b^2}\left(1 + \frac{qb}{r^2}\right)^{\frac{3}{2}}, \tag{5.47}$$

where $D = m_g^2 \frac{(1+\alpha^2+\alpha-3\beta)}{3(\alpha+3\beta)}$. The effective potential for the second solution is given by

$$V_{eff(2)} = 2\omega q\left(-\frac{2}{b}\left(r-\sqrt{r^2+qb}\right)\right)-\left(-\frac{2q}{b}\left(r-\sqrt{r^2+qb}\right)\right)^2+\frac{\lambda}{r^2}\Bigg(1-\frac{2M}{r}-$$

$$\left(D+\frac{8}{3b^2}\right)r^2-\frac{4q}{b}+\frac{8r^2}{3b^2}\left(1+\frac{qb}{r^2}\right)^{\frac{3}{2}}\Bigg)\times\left(\frac{2M}{r^2}-2r\left(D+\frac{8}{3b^2}\right)+\sqrt{1+\frac{qb}{r^2}}\left(\frac{16r}{3b^2}-\frac{8q}{3br}\right)\right).$$

(5.48)

The behaviors of dRGT effective potentials for both solutions, Eqs. (5.46) and (4.48), are depicted in Figs. 5.2.a and 5.2.b by varying the controlling parameter of ω which appeared in the effective potential by coupling of nonlinear electrodynamics. The parameters B and C are chosen to be zero and $A = -1$.

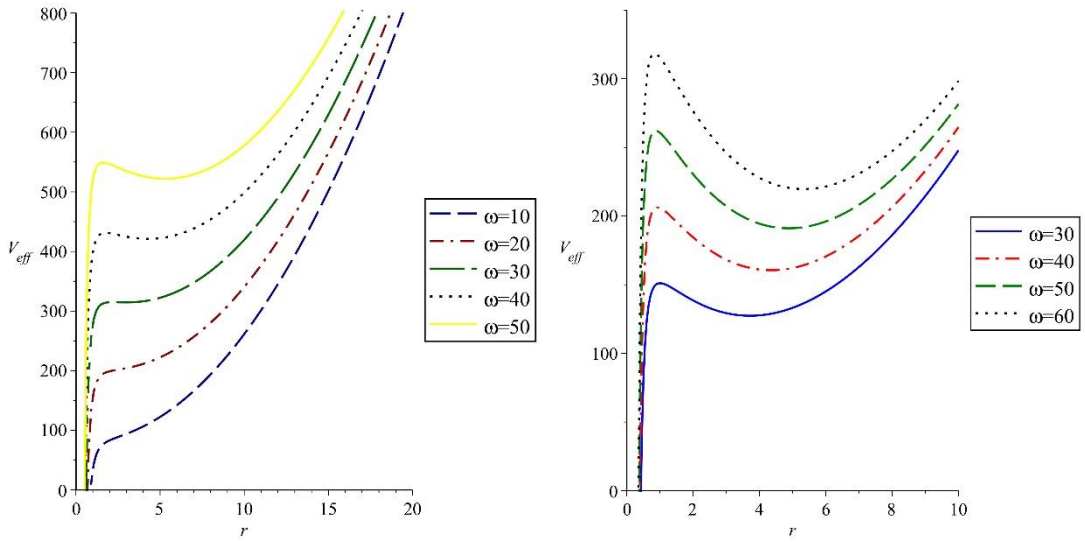

(a) (b)

Figure 5.2: Plots of V_{eff} versus r for a) the metric function (5.33). The plot is governed by Eq. (5.46). The physical parameters are chosen as; $M = 1, b = 50, q = 8$, and $\lambda = 0$. b) for the metric function (5.34). The plot is governed by Eq. (5.48). The physical parameters are chosen as; $M = 1, b = 10, q = 3$, and $\lambda = 0$.

It can be seen from both figures that V_{eff} which vanishes at the horizon, peaks right after the horizon and then quickly dampens toward the asymptotic region, this procedure happened for the second solution in a smaller amount rather than the first. Moreover, for both, by increasing the frequency the potential peak increases as well.

On the other hand, when the energy of the scalar waves increases, the peak value of the potential barrier near the event horizon also increases, which may lead to the caged of the waves. As being stated in Refs. [160-163], since the main contribution to the transmission amplitude comes from the $l = 0$ mode (i.e., s-wave case [164]), it is adequate to qualitatively analyze the potential (5.46) for s-waves. In a general comparison, we can see the behavior of the potential for second solution (5.48) is smoother in the same period than the first solution, in this case the role of constant parameter b is significant.

5.3 Scalar Perturbation of Kerr Like Spacetime in Bumblebee Gravity Model

In this subsection, we shall examine the scalar perturbations of the Kerr-like BH in BGM and derive the effective potential for scalar waves, which will be exposed in this geometry. To this end, we employ the massive Klein-Gordon equation:

$$\frac{1}{\sqrt{-g}}\partial_\mu\left(\sqrt{-g}g^{\mu\upsilon}\partial_\upsilon\right)\psi = \mu_0^2\psi, \tag{5.49}$$

where μ_0 is the mass of the scalar particle. Using the information in chapter 3, Eqs. (3.21) - (3.23) regarding to the metric (3.16) in Eq. (5.49), we get

$$-\frac{A}{\rho^2\Delta(1+L)}\partial_t^2\Psi - \frac{2Mra}{\Delta\rho^2\sqrt{1+L}}\partial_t\partial_\varphi\Psi + \frac{1}{\rho^2 sin\theta}\partial_\theta(sin\theta\partial_\theta)\Psi + \frac{1}{\rho^2}\partial_r(\Delta\partial_r)\Psi$$

$$-\frac{2Mra}{\rho^2\Delta\sqrt{1+L}}\partial_\varphi\partial_t\Psi + \frac{\rho^2 - 2Mr}{\Delta\rho^2(1+L)sin^2\theta}\partial_\varphi^2\Psi = \mu_0^2\Psi. \tag{5.50}$$

To apply the technique of separation of variables in Eq. (5.50), one can use the following ansatz:

$$\Psi(r,t) = R(r)S(\theta)e^{im\varphi}e^{-i\omega t}, \tag{5.51}$$

where m is azimuthal quantum number and ω represents the energy of the particles. Therefore, the radial equation becomes

$$\frac{1}{R(r)}\frac{d}{dr}\left(\Delta\frac{dR(r)}{dr}\right)+\frac{\omega^2(r^2+(1+L)a^2)^2}{\Delta(1+L)}+\frac{m^2a^2}{\Delta}-\frac{4Mram\omega}{\Delta\sqrt{1+L}}-\omega^2a^2(1+L)$$
$$-\mu_0^2r^2, \quad (5.52)$$

and the angular part reads

$$\frac{1}{S(\theta)sin\theta}\frac{d}{d\theta}\left(sin\theta\frac{dS(\theta)}{d\theta}\right)-\frac{m^2}{sin^2\theta}+c^2cos^2\theta. \quad (5.53)$$

As is known, angular and radial equations admit two same (in absolute) eigenvalues with opposite signs. Angular differential equation (5.53) has solutions in terms of the oblate spherical harmonic functions $S_{lm}(ic, cos\theta)$ having eigenvalue λ_{lm} [164] in which l, m are integers such that $|m| \leq l$ and $c^2 = a^2(1+L)(\omega^2-\mu_0^2)$ [165]. For simplicity, we consider the separation constant as $\lambda = \lambda_{lm}$. Thus, the radial differential equation becomes

$$\Delta\frac{d}{dr}\left(\Delta\frac{dR(r)}{dr}\right)+\left\{m^2a^2+\frac{\omega^2}{(1+L)}(r^2+(1+L)a^2)^2-\frac{4Mram\omega}{\sqrt{1+L}}-(\mu_0^2r^2+\right.$$
$$\left.\omega^2a^2(1+L)+\lambda)\Delta\right\}R(r)=0. \quad (5.54)$$

The radial solution is in general associated with a free oscillation mode of the propagating field. Stable modes have particular frequencies ω with complex negative imaginary values, so we have an exponentially subsidence in amplitude. Conversely, if the imaginary values of the frequencies are positive, then the amplitude of the oscillations exponentially increase and the modes consequently become unstable.

If we consider $M\omega \ll 1$ and $\mu M \ll 1$, which was first noticed by Starobinskii [165, 166], then Eq. (5.53) is amenable to analytic methods. If we assume the inequalities to hold then the angular part can be thought as spherical harmonics with $\lambda \cong l(l+1)$. For having one dimensional wave equation, we first use the following transformation

$$R(r) = \frac{U(r)}{\sqrt{r^2 + (1+L)a^2}}, \tag{5.55}$$

together with the tortoise coordinate:

$$\frac{dr_*}{dr} = \frac{r^2 + (1+L)a^2}{\sqrt{1+L}\Delta}. \tag{5.56}$$

Thus, Eq. (5.54) can be expressed as a one-dimensional Schrödinger equation

$$\frac{d^2U}{dr_*^2} + \left(\omega^2 - V_{eff}\right)U = 0, \tag{5.57}$$

where the effective potential reads

$$V_{eff} = \frac{(1+L)\Delta}{(r^2 + (1+L)a^2)^2}\left[\frac{\Delta' r + \Delta}{(r^2 + (1+L)a^2)} - \frac{3r^2\Delta}{(r^2 + (1+L)a^2)^2}\right.$$
$$\left. + \frac{4Mram\omega}{\Delta\sqrt{1+L}} - \frac{m^2a^2}{\Delta}(\mu_0^2 r^2 + \omega^2 a^2(1+L) + \lambda)\right]. \tag{5.58}$$

The prime symbol denotes the derivation with respect to r. The behavior of the effective potential under the effect of LSB parameter for scalar particles is illustrated in Fig. 5.3, which shows a significant deduction on the potential peak when the LSB parameter is increased.

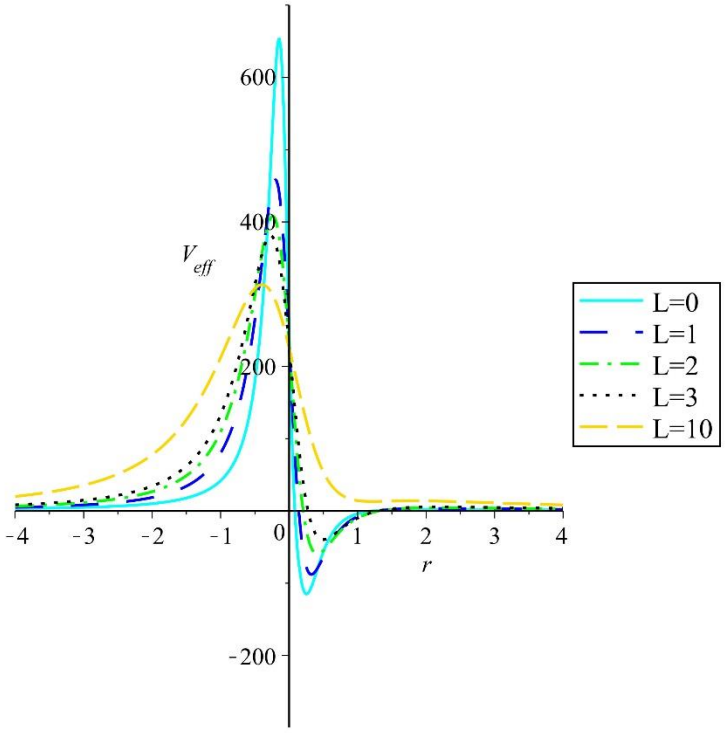

Figure 5.3: Plots of V_{eff} versus r for the spin-0 particles. The physical parameters are chosen as; $M = m = 1$, $\omega = 15$, $a = 0.3$, and $\lambda = 2$.

5.4 Scalar Perturbation of Kerr Polytropic Black Hole

In this section, we derive the effective potential of scalar particles for polytropic black hole in Kerr space time. To this aim, we shall consider the massive Klein-Gordon equation (5.49) for a propagating scalar field with mass μ_0 in the geometry of rotating polytropic BH (4.50). The determinant of the metric (4.50) tensor is given by the general Klein-Gordon

$$g \equiv det g_{\mu\upsilon} = -\rho^4 sin^2\theta. \tag{5.59}$$

After substituting Eq. (5.59) in Eq. (5.49), we get

$$\frac{\Sigma}{\rho^2\Delta}\partial_t^2\Psi + \frac{2af}{\rho^2\Delta}\partial_t\partial_\varphi\Psi - \frac{1}{\rho^2 sin\theta}\{cos\theta\partial_\theta + sin\theta\partial_\theta^2\}\Psi - \frac{1}{\rho^2}\partial_r(\Delta\partial_r)\Psi$$
$$+\frac{2af}{\rho^2\Delta}\partial_\varphi\partial_t\Psi - \frac{\Delta - a^2sin^2\theta}{\Delta\rho^2 sin^2\theta}\partial_\varphi^2\Psi = \mu_0^2\Psi. \tag{5.60}$$

We consider an ansatz of the scalar field

$$\Psi(t,r) = R(r)S(\theta)e^{im\varphi}e^{-i\omega t}, \tag{5.61}$$

where $e^{-i\omega t}$ implies the time evolution of the field and m is azimuthal quantum number. Therefore, by substituting Eq. (5.61) in Eq. (5.60), we obtain

$$\Delta\frac{d}{dr}\left(\Delta\frac{dR(r)}{dr}\right) + [m^2a^2 - 4afm\omega + \omega^2(r^2+a^2)^2 - (\omega^2a^2 + \mu_0^2r^2 + \lambda)\Delta]R(r) = 0, \tag{5.62}$$

where λ is the eigenvalue of the angular solution:

$$\frac{1}{S(\theta)}\frac{1}{sin\theta}\frac{d}{d\theta}\left(sin\theta\frac{dS(\theta)}{d\theta}\right) - \frac{m^2}{sin^2\theta} + c^2cos^2\theta = -\lambda_{lm}, \tag{5.63}$$

in which $c^2 = (\omega^2 - \mu_0^2)^2a^2$. Using the tortoise coordinate,

$$\frac{dr_*}{dr} = \frac{r^2+a^2}{\Delta}, \tag{5.64}$$

which maps the semi-infinity region from the horizon to infinity $(+\infty, -\infty)$ region. Using the following transformation

$$R = \frac{U}{\sqrt{r^2+a^2}}, \tag{5.65}$$

we acquire the Schrödinger-like wave equation for this stationary background,

$$\frac{dU}{dr_*^2} + \left(\omega^2 - V_{eff}\right)U = 0, \tag{5.66}$$

where

$$V_{eff} = \frac{\Delta}{(r^2+a^2)^2}\left[\frac{\Delta' r + \Delta}{r^2+a^2} - \frac{3r^2\Delta}{(r^2+a^2)^2} + \frac{4afm\omega - m^2a^2}{\Delta} + \omega^2a^2 + \mu_0^2r^2 + \lambda\right]. \tag{5.67}$$

To see this, we plot the expressions of the massless scalar effective potential function (Eq. (5.67)) versus radius r. One can see the typical behaviors of these effective potentials by varying the rotating parameter a in Fig. 5.4. The figure shows an increase for the potential barrier when rising the rotating parameter.

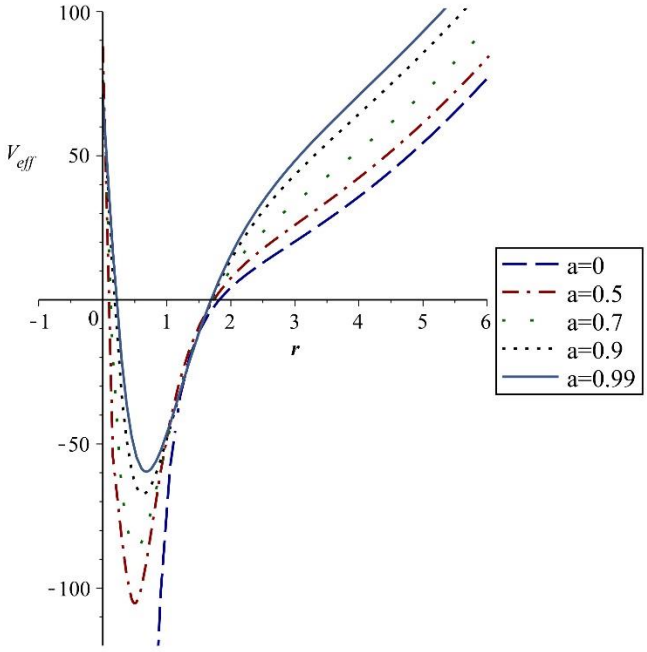

Figure 5.4: Plots of V_{eff} versus r for the spin-0 particles. The physical parameters are chosen as;$m = 1$;$M = \omega = 3$; $L = 1$; and $\lambda = 6$.

Chapter 6

DIRAC PERTURBATION

6.1 Fermionic Perturbation and Effective Potential in BGM

In this subsection, we shall employ the Newman-Penrose (NP) formalism [167] to find the effective potential of the fermion fields propagating in the geometry of the BGM. In a four-dimensional pseudo-Riemannian manifold, we make the choice of the following null tetrad basis 1-form $(l, n, m, \bar{m})$ of the NP formalism. One can introduce a tetrad of two real vectors denoted by l^{α} and n^{α} and two complex conjugate vectors m^{α} and $\bar{m}^{\alpha}$, where the null condition is satisfied as follows

$$l.l = n.n = m.m = \bar{m}.\bar{m} = 0, \tag{6.1}$$

$$l.m = l.\bar{m} = n.m = n.\bar{m} = 0, \tag{6.2}$$

$$l.n = -m.\bar{m} = 1, \tag{6.3}$$

where the co-vector is defined by $l_{\alpha} = \nabla_{\alpha} u$ so $l^{\alpha} = g^{\alpha\beta}\nabla_{\alpha} u$ is a null vector tangent to the generators of $u = const$. Therefore, the global metric can be represented in terms of null tetrad by

$$g_{\alpha\beta} = l_{\alpha} n_{\beta} + n_{\alpha} l_{\beta} - m_{\alpha}\bar{m}_{\beta} - \bar{m}_{\alpha} m_{\beta}, \tag{6.4}$$

or in condensed notation

$$g^{\alpha\beta} = \eta^{\mu\upsilon}\lambda^{\alpha}{}_{\mu}\lambda^{\beta}{}_{\upsilon}, \tag{6.5}$$

where $\mu = 1,2,3,4$ is the tetrad index, $\lambda^{\alpha}{}_{\mu} = (l^{\alpha}, n^{\alpha}, m^{\alpha}, \bar{m}^{\alpha})$ and

$$\eta^{\mu\nu} = \begin{pmatrix} 0 & 1 & 0 & 0 \\ 1 & 0 & 0 & 0 \\ 0 & 0 & 0 & -1 \\ 0 & 0 & -1 & 0 \end{pmatrix}. \tag{6.6}$$

Chandrasekar Dirac equations (CDEs) are given by [164,168]

$$(D + \varepsilon - \rho)F_1 + \left(\bar{\delta} + \pi - \alpha\right)F_2 = i\mu^* G_1, \tag{6.7}$$

$$(\delta + \beta - \tau)F_1 + (\Delta + \mu - \gamma)F_2 = i\mu^* G_1, \tag{6.8}$$

$$(D + \bar{\varepsilon} - \bar{\rho})G_2 - (\delta + \bar{\pi} - \bar{\alpha})G_1 = i\mu^* F_2, \tag{6.9}$$

$$(\Delta + \bar{\mu} - \bar{\gamma})G_1 - \left(\bar{\delta} + \bar{\beta} - \bar{\tau}\right)G_2 = i\mu^* F_1, \tag{6.10}$$

where F_1, F_2, G_1, and G_2 represent the components of the wave functions or the so-called Dirac spinors. D, Δ, δ, and $\bar{\delta}$ are the directional covariant derivative operators, which are given by

$$D = l^\mu \partial_\mu, \;\; \Delta = n^\mu \partial_\mu, \;\; \delta = m^\mu \partial_\mu, \;\; \bar{\delta} = \bar{m}^\mu \partial_\mu. \tag{6.11}$$

$\varepsilon, \rho, \pi, \alpha, \beta, \tau, \mu$, and γ are the spin coefficients, and a bar over a quantity denotes complex conjugation.

6.1.1 Bumblebee Black Hole in Non-Rotating Spacetime

In this part, we consider the NP formalism in non-rotating form of bumblebee BH Eq. (3.11). The non-zero spin coefficients are found to be

$$\varepsilon = \gamma = \frac{\sqrt{2}f'}{8\sqrt{f}\sqrt{1+L}}, \mu = \rho = \frac{\sqrt{2f}}{2r\sqrt{1+L}}, \beta = -\alpha = \frac{\sqrt{2}cot\theta}{4r}. \tag{6.12}$$

To have separable solutions for the CDEs (6.7) -(6.10), we introduce the following ansatzes

$$F_1 = f_1(z)A_1(\theta)exp[i(\omega t + m\varphi)], \tag{6.13}$$

$$G_1 = g_1(z)A_2(\theta)exp[(\omega t + m\varphi)], \tag{6.14}$$

$$F_2 = f_2(z)A_3(\theta)exp[i(\omega t + m\varphi)], \tag{6.15}$$

$$G_2 = g_2(z)A_4(\theta)exp[(\omega t + m\varphi)], \tag{6.16}$$

where m denotes the azimuthal number and ω is the frequency of the spinor fields. Since the directional derivatives are defined by $D = l^a\partial_a, \Delta = n^a\partial_a$ and $\delta = m^a\partial_a$, we have

$$D = \frac{1}{\sqrt{2f}}\partial_t + \sqrt{\frac{f}{2(1+L)}}\partial_r, \tag{6.17}$$

$$\Delta = \frac{1}{\sqrt{2f}}\partial_t - \sqrt{\frac{f}{2(1+L)}}\partial_r, \tag{6.18}$$

$$\delta = \frac{1}{r\sqrt{2}}\partial_\theta + \frac{i}{r\sqrt{2}sin\theta}\partial_\varphi, \tag{6.19}$$

$$\bar{\delta} = \frac{1}{r\sqrt{2}}\partial_\theta - \frac{i}{r\sqrt{2}sin\theta}\partial_\varphi. \tag{6.20}$$

After substituting Eqs. (6.12) and (6.17) -(6.20) into the CDEs, one can obtain the following set of equations:

$$\left[\frac{i\omega}{\sqrt{f}} + \frac{r\sqrt{f}}{\sqrt{1+L}}\partial_r + \frac{rf'}{4\sqrt{f(1+L)}} + \frac{\sqrt{f}}{\sqrt{1+L}}\right]\frac{f_1}{f_2} + \frac{\tilde{L}A_3}{A_1} - i\mu r\frac{g_1A_2}{f_2A_1} = 0, \tag{6.21}$$

$$\left[\frac{i\omega}{\sqrt{f}} - \frac{r\sqrt{f}}{\sqrt{1+L}}\partial_r - \frac{rf'}{4\sqrt{f(1+L)}} - \frac{\sqrt{f}}{\sqrt{1+L}}\right]\frac{f_2}{f_1} + \frac{\tilde{L}^\dagger A_1}{A_3} - i\mu r\frac{g_2A_4}{f_1A_3} = 0, \tag{6.22}$$

$$\left[\frac{i\omega}{\sqrt{f}} + \frac{r\sqrt{f}}{\sqrt{1+L}}\partial_r + \frac{rf'}{4\sqrt{f(1+L)}} + \frac{\sqrt{f}}{\sqrt{1+L}}\right]\frac{g_2}{g_1} - \frac{\tilde{L}^\dagger A_2}{A_4} - i\mu r\frac{f_2A_3}{g_1A_4} = 0, \tag{6.23}$$

$$\left[\frac{i\omega}{\sqrt{f}} - \frac{r\sqrt{f}}{\sqrt{1+L}}\partial_r - \frac{rf'}{4\sqrt{f(1+L)}} - \frac{\sqrt{f}}{\sqrt{1+L}}\right]\frac{g_1}{g_2} - \frac{\tilde{L}A_4}{A_2} - i\mu r\frac{f_1A_1}{g_2A_2} = 0, \tag{6.24}$$

where $\mu = \sqrt{2}\mu^*$, $\tilde{L}$, and $\tilde{L}^\dagger$ are the angular operators, which are known as the laddering operators:

$$\tilde{L} = \partial_\theta + \frac{m}{sin\theta} + \frac{cot\theta}{2}, \quad \tilde{L}^\dagger = \partial_\theta - \frac{m}{sin\theta} + \frac{cot\theta}{2}, \tag{6.25}$$

which lead to the spin-weighted spheroidal harmonics [169,170] with the following eigenvalue [171,172]:

$$\lambda_f = -\left(l + \frac{1}{2}\right). \tag{6.26}$$

By considering $g_1 = f_2$, $g_2 = f_1$, $A_2 = A_1$, and $A_4 = A_3$, then we reduce the CDEs (6.7) – (6.10) to two coupled differential equations:

$$\frac{r\sqrt{f}}{\sqrt{1+L}}\left(\frac{d}{dr} + \frac{i\omega\sqrt{1+L}}{f} + \frac{f'}{4f} + \frac{1}{r}\right) g_2 = \left(-\lambda_f + i\mu r\right) g_1, \tag{6.27}$$

$$\frac{r\sqrt{f}}{\sqrt{1+L}}\left(\frac{d}{dr} - \frac{i\omega\sqrt{1+L}}{f} + \frac{f'}{4f} + \frac{1}{r}\right) g_2 = \left(-\lambda_f - i\mu r\right) g_2. \tag{6.28}$$

Moreover, if one sets

$$g_1(r) = \frac{\psi_1}{r}, \qquad g_2(r) = \frac{\psi_2}{r}, \tag{6.29}$$

and substitute them into Eqs. (6.27) and (6.28), after some manipulations, we get:

$$\frac{r\sqrt{f}}{\sqrt{1+L}}\left(\frac{d}{dr} + \frac{i\omega\sqrt{1+L}}{f} + \frac{f'}{4f}\right) \psi_2 = \left(-\frac{\lambda_f}{r} + i\mu\right) \psi_1, \tag{6.30}$$

$$\frac{r\sqrt{f}}{\sqrt{1+L}}\left(\frac{d}{dr} - \frac{i\omega\sqrt{1+L}}{f} + \frac{f'}{4f}\right) \psi_1 = \left(-\frac{\lambda_f}{r} - i\mu\right) \psi_2. \tag{6.31}$$

By defining $\psi_1 = f^{-1/4} R_1(r)$ and $\psi_2 = f^{-1/4} R_2(r)$ and introducing the tortoise coordinate (r_*) as $\frac{f}{\sqrt{1+L}}\frac{d}{dr} = \frac{d}{dr_*}$, , we obtain

$$\left(\frac{d}{dr_*} + i\omega\right) R_2(r) = \sqrt{f}\left(-\frac{\lambda_f}{r} + i\mu\right) R_1, \tag{6.32}$$

$$\left(\frac{d}{dr_*} - i\omega\right) R_1(r) = \sqrt{f}\left(-\frac{\lambda_f}{r} - i\mu\right) R_2. \tag{6.33}$$

One can combine the above equations by letting

$$Z_+ = R_1 + R_2, \tag{6.34}$$

$$Z_- = R_2 - R_1. \tag{6.35}$$

Thus, we end up with the following pair of one dimensional Schrödinger-like wave equations:

$$\left(\frac{d^2}{dr_*^2}+\omega^2\right)Z_\pm = V_\pm Z_\pm, \tag{6.36}$$

where the effective potentials for the Dirac field read

$$V_\pm = f\left[\left(-\frac{\lambda_f}{r}\pm i\mu\right)^2 \pm \lambda_f \frac{1}{\sqrt{1+L}}\frac{d}{dr}\left(-\frac{\sqrt{f}}{r}\pm\frac{i\mu\sqrt{f}}{\lambda_f}\right)\right]$$

$$= f\left[\left(-\frac{2l+1}{2r}\pm i\mu\right)^2 \mp\left(l+\frac{1}{2}\right)\frac{1}{\sqrt{1+L}}\frac{d}{dr}\left(-\frac{\sqrt{f}}{r}\pm\frac{2i\mu\sqrt{f}}{2l+1}\right)\right], \tag{6.37}$$

Behaviors of $V_\pm$ (6.37) are depicted in Fig. 6.1

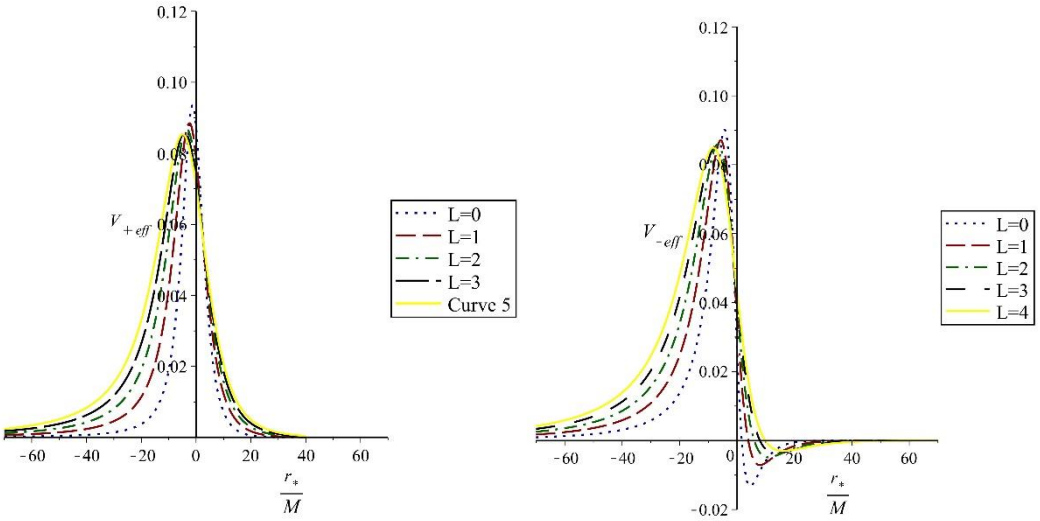

(a) (b)

Figure 6.1: Plots of $V_\pm$ versus $\frac{r_*}{M}$. The plots are governed by Eq. (6.37).

6.1.2 Bumblebee Black Hole in Rotating Spacetime

To proceed our analysis with the Dirac fields in the geometry of the Kerr-like black hole, we shall use the four-dimensional Dirac equation formulated in the Newman-Penrose (NP) formalism. By this way, we aim to derive the effective potentials for the fermionic fields propagating in this geometry. To achieve this goal, we use the orthogonal (dragging) coordinates [173, 174] for the metric (3.16) and get

$$ds^2 = -\frac{\Delta(1+L)}{\Sigma}d\tilde{\tau}^2 + \frac{\Sigma}{\Delta}dr^2 + \Sigma d\theta^2 + \frac{sin^2\theta}{\Sigma}d\tilde{\varphi}^2, \tag{6.38}$$

where $\Sigma = \rho^2$ and

$$d\tilde{\tau}^2 = \left(dt - a\sqrt{1+L}sin^2\theta d\varphi\right)^2, d\tilde{\varphi}^2 = \left((r^2 + (1+L)a^2)d\varphi - a\sqrt{1+L}dt\right)^2. \tag{6.39}$$

The NP tetrad of the Kerr-like BH geometry can be given by

$$l^\mu = \frac{1}{\Delta}\left[\frac{r^2 + a^2(1+L)}{\sqrt{1+L}}, \Delta, 0, a\right], \tag{6.40}$$

$$n^\mu = \frac{1}{2\Sigma}\left[\frac{r^2 + a^2(1+L)}{\sqrt{1+L}}, -\Delta, 0, a\right], \tag{6.41}$$

$$m^\mu = \frac{1}{\left(r + ia\sqrt{1+L}cos\theta\right)\sqrt{2}}\left[ia\sqrt{1+L}sin\theta, 0, 1, \frac{i}{sin\theta}\right], \tag{6.42}$$

$$\bar{m}^\mu = \frac{1}{\left(r - ia\sqrt{1+L}cos\theta\right)\sqrt{2}}\left[-ia\sqrt{1+L}sin\theta, 0, 1, \frac{-i}{sin\theta}\right]. \tag{6.43}$$

where, as mentioned before a bar over a quantity denotes complex conjugation. Thus, the dual co-tetrad of Eqs. (6.40) – (6.43) reads

$$l_\mu = \left[\sqrt{1+L}, -\frac{\Sigma}{\Delta}, 0, -a(1+L)sin^2\theta\right], \tag{6.44}$$

$$n_\mu = \frac{\Delta}{2\Sigma}\left[\sqrt{1+L}, \frac{\Sigma}{\Delta}, 0, -a(1+L)sin^2\theta\right], \tag{6.45}$$

$$m_\mu = \frac{1}{\left(r + ia\sqrt{1+L}cos\theta\right)\sqrt{2}}\left[ia\sqrt{1+L}sin\theta, 0, -\Sigma, -i(r^2 + a^2(1+L)sin\theta)\right], \tag{6.46}$$

$$\bar{m}_\mu = \frac{1}{\left(r - ia\sqrt{1+L}cos\theta\right)\sqrt{2}}\left[-ia\sqrt{1+L}sin\theta, 0, -\Sigma, i(r^2 + a^2(1+L)sin\theta)\right]. \tag{6.47}$$

Before deriving the non-zero spin coefficients, one can re-normalize the NP tetrad by using the spin boost Lorentz transformations:

$$l \longrightarrow \boldsymbol{l} = \zeta l, \;\; n \longrightarrow \boldsymbol{n} = \zeta^{-1} n, \;\; m \longrightarrow \boldsymbol{m} = e^{i\varphi} m, \;\; \bar{m} \longrightarrow \bar{\boldsymbol{m}} = e^{-i\varphi}\bar{m}, \tag{6.48}$$

where

$$\zeta = \sqrt{\frac{\Delta}{2\Sigma}}, \qquad e^{i\varphi} = \frac{\sqrt{\Sigma}}{r - ia\sqrt{1+L}cos\theta}. \tag{6.49}$$

Thus, we have

$$\boldsymbol{l}^{\mu} = \frac{1}{\sqrt{2\Delta\Sigma}}\left[\frac{r^2 + a^2(1+L)}{\sqrt{1+L}}, \Delta, 0, a\right], \tag{6.50}$$

$$\boldsymbol{n}^{\mu} = \frac{1}{\sqrt{2\Delta\Sigma}}\left[\frac{r^2 + a^2(1+L)}{\sqrt{1+L}}, -\Delta, 0, a\right], \tag{6.51}$$

$$\boldsymbol{m}^{\mu} = \frac{1}{\sqrt{2\Sigma}}\left[ia\sqrt{1+L}sin\theta, 0, 1, \frac{i}{sin\theta}\right], \tag{6.52}$$

$$\bar{\boldsymbol{m}}^{\mu} = \frac{1}{\sqrt{2\Sigma}}\left[-ia\sqrt{1+L}sin\theta, 0, 1, \frac{-i}{sin\theta}\right], \tag{6.53}$$

and

$$\boldsymbol{l}_{\mu} = \sqrt{\frac{\Delta}{2\Sigma}}\left[\sqrt{1+L}, -\frac{\Sigma}{\Delta}, 0, -a(1+L)sin^2\theta\right], \tag{6.54}$$

$$\boldsymbol{n}_{\mu} = \sqrt{\frac{\Delta}{2\Sigma}}\left[\sqrt{1+L}, \frac{\Sigma}{\Delta}, 0, -a(1+L)sin^2\theta\right], \tag{6.55}$$

$$\boldsymbol{m}_{\mu} = \frac{1}{\sqrt{2\Sigma}}\left[ia\sqrt{1+L}sin\theta, 0, -\Sigma, -i\left(r^2 + a^2(1+L)\right)sin\theta\right], \tag{6.56}$$

$$\bar{\boldsymbol{m}}_{\mu} = \frac{1}{\sqrt{2\Sigma}}\left[-ia\sqrt{1+L}sin\theta, 0, -\Sigma, i\left(r^2 + a^2(1+L)\right)sin\theta\right]. \tag{6.57}$$

The non-zero spin coefficients [164] can then be computed as

$$\pi = -\tau = \frac{\Sigma_{\theta}}{2\Sigma\sqrt{2\Sigma(1+L)}} + i\frac{asin\theta\Sigma_r}{2\Sigma\sqrt{2\Sigma}}, \tag{6.58}$$

$$\beta = -\alpha = -\frac{\Sigma_\theta}{4\Sigma\sqrt{2\Sigma(1+L)}} + \frac{cot\theta}{2\sqrt{2\Sigma(1+L)}} - \frac{iasin\theta\Sigma_r}{4\Sigma\sqrt{2\Sigma}}, \tag{6.59}$$

$$\rho = \mu = -\frac{\Sigma_r\sqrt{\Delta}}{2\Sigma\sqrt{2\Sigma}} - i\frac{a\sqrt{\Delta(1+L)}cos\theta}{\Sigma\sqrt{2\Sigma}}, \tag{6.60}$$

$$\varepsilon = \gamma = \frac{\Delta_r}{4\sqrt{2\Delta\Sigma}} - \frac{\Delta\Sigma_r}{4\Sigma\sqrt{2\Delta\Sigma}} - i\frac{a\sqrt{\Delta(1+L)}cos\theta}{2\Sigma\sqrt{2\Sigma}}. \tag{6.61}$$

After this step, we employ the CDEs Eq. (6.7) -(6.10) to find the equations governing the fermion fields. The form of the CDEs suggests that

$$F_i(t,r,\theta,\varphi) = \frac{1}{\sqrt{\left(r - ia\sqrt{1+L}cos\theta\right)}} e^{-i(\omega t + m\varphi)}\Psi_i(r,\theta), \tag{6.62}$$

$$G_i(t,r,\theta,\varphi) = \frac{1}{\sqrt{\left(r + ia\sqrt{1+L}cos\theta\right)}} e^{-i(\omega t + m\varphi)}\Phi_i(r,\theta). \tag{6.63}$$

Inserting Eqs. (6.60) – (6.63) into the CDEs, we obtain

$$\left\{\sqrt{\Delta}\partial_r - \frac{i\omega(r^2+(1+L)a^2)}{\sqrt{\Delta(1+L)}} + \frac{\Delta_r}{4\sqrt{\Delta}} - \frac{ima}{\sqrt{\Delta}}\right\}\Psi_1(r,\theta)$$
$$+\frac{1}{\sqrt{1+L}}\left\{\partial_\theta - \frac{m}{sin\theta} - a\omega\sqrt{1+L}sin\theta + \frac{cot\theta}{2}\right\}\Psi_2(r,\theta)$$
$$= i\mu\left(r - ia\sqrt{1+L}cos\theta\right)\Phi_1(r,\theta), \tag{6.64}$$

$$-\left\{\sqrt{\Delta}\partial_r + \frac{i\omega(r^2+(1+L)a^2)}{\sqrt{\Delta(1+L)}} + \frac{\Delta_r}{4\sqrt{\Delta}} + \frac{ima}{\sqrt{\Delta}}\right\}\Psi_2(r,\theta)$$
$$+\frac{1}{\sqrt{1+L}}\left\{\partial_\theta - \frac{m}{sin\theta} - a\omega\sqrt{1+L}sin\theta + \frac{cot\theta}{2}\right\}\Psi_1(r,\theta)$$
$$= i\mu\left(r - ia\sqrt{1+L}cos\theta\right)\Phi_2(r,\theta), \tag{6.65}$$

$$\left\{\sqrt{\Delta}\partial_r - \frac{i\omega(r^2+(1+L)a^2)}{\sqrt{\Delta(1+L)}} + \frac{\Delta_r}{4\sqrt{\Delta}} - \frac{ima}{\sqrt{\Delta}}\right\}\Phi_2(r,\theta)$$
$$-\frac{1}{\sqrt{1+L}}\left\{\partial_\theta + \frac{m}{sin\theta} + a\omega\sqrt{1+L}sin\theta + \frac{cot\theta}{2}\right\}\Phi_1(r,\theta)$$

$$= i\mu\left(r + ia\sqrt{1+L}cos\theta\right)\Psi_2(r,\theta), \quad (6.66)$$

$$-\left\{\sqrt{\Delta}\partial_r + \frac{i\omega(r^2+(1+L)a^2)}{\sqrt{\Delta(1+L)}} + \frac{\Delta_r}{4\sqrt{\Delta}} + \frac{ima}{\sqrt{\Delta}}\right\}\Phi_1(r,\theta)$$

$$-\frac{1}{\sqrt{1+L}}\left\{\partial_\theta - \frac{m}{sin\theta} - a\omega\sqrt{1+L}sin\theta + \frac{cot\theta}{2}\right\}\Phi_2(r,\theta)$$

$$= i\mu\left(r + ia\sqrt{1+L}cos\theta\right)\Psi_1(r,\theta). \quad (6.67)$$

Since the functions $\Psi_i(r,\theta)$ and $\Phi_i(r,\theta)$ depend on the radial and angular variables, one can separate them by introducing the following ansatzes

$$\Psi_1(r,\theta) = \Re_+(r)\aleph_+(\theta), \quad (6.68)$$

$$\Psi_2(r,\theta) = \Re_-(r)\aleph_-(\theta), \quad (6.69)$$

where $\Re_\pm(r) = \Delta^{-1/4}p(r)_{\pm 1/2}$. Using the tortoise coordinate (r_*) as $\frac{d}{dr_*} = \frac{\Delta\sqrt{1+L}}{r^2+a^2(1+L)}\frac{d}{dr}$, Eqs. (6.64) – (6.67) yield the following two one-dimensional Schrödinger-like radial equations:

$$\left\{\frac{d}{dr_*} - i\varpi\right\}p_{+1/2} = \frac{\lambda}{\sqrt{1+L}}\frac{\sqrt{\Delta}}{K}p_{-1/2}, \quad (6.70)$$

$$-\left\{\frac{d}{dr_*} + i\varpi\right\}p_{-1/2} = \frac{\lambda}{\sqrt{1+L}}\frac{\sqrt{\Delta}}{K}p_{+1/2}, \quad (6.71)$$

in which

$$K = \frac{r^2+(1+L)a^2}{\sqrt{1+L}}, \varpi = \omega + \frac{ma}{K}. \quad (6.72)$$

Setting the eigenvalue $\lambda = -\left(l + \frac{1}{2}\right)$ for the angular equations as

$$\frac{\mathcal{L}^\dagger\aleph_-(\theta)}{\aleph_+(\theta)} = -\lambda, \quad \frac{\mathcal{L}\aleph_+(\theta)}{\aleph_-(\theta)} = \lambda, \quad (6.73)$$

where $\mathcal{L}$ and $\mathcal{L}^\dagger$ are the angular operators

$$\mathcal{L} = \partial_\theta + \frac{m}{sin\theta} + \frac{cot\theta}{2} + a\omega\sqrt{1+L}sin\theta, \tag{6.74}$$

$$\mathcal{L}^\dagger = \partial_\theta - \frac{m}{sin\theta} + \frac{cot\theta}{2} - a\omega\sqrt{1+L}sin\theta, \tag{6.75}$$

one can have the spin-weighted spherical harmonics [175] for the angular equations. Moreover, if we let

$$Z_+ = p_{+1/2} + p_{-1/2}, \quad Z_- = p_{-1/2} - p_{+1/2}, \tag{6.76}$$

Eqs. (6.70) and (6.71) can be transformed to one-dimensional Schrödinger-like wave equations:

$$\left(\frac{d^2}{dr_*^2} + \varpi^2\right) Z_\pm = V_{eff}^+ Z_\pm. \tag{6.77}$$

From now on, for the sake of simplicity, we consider the massless ($\mu = 0$) fermions. In this case, the effective potentials for the propagating Dirac fields become

$$V_{eff}^\pm = \frac{\Delta}{K}\left\{\frac{\lambda^2}{K(1+L)} \pm \frac{d}{dr}\left(\frac{\lambda\sqrt{\Delta}}{K}\right)\right\}. \tag{6.78}$$

The behaviors of the effective potentials (6.78) are depicted in Figs. 6.2. a and 6.2.b, which stand for spin-up and spin-down particles, respectively.

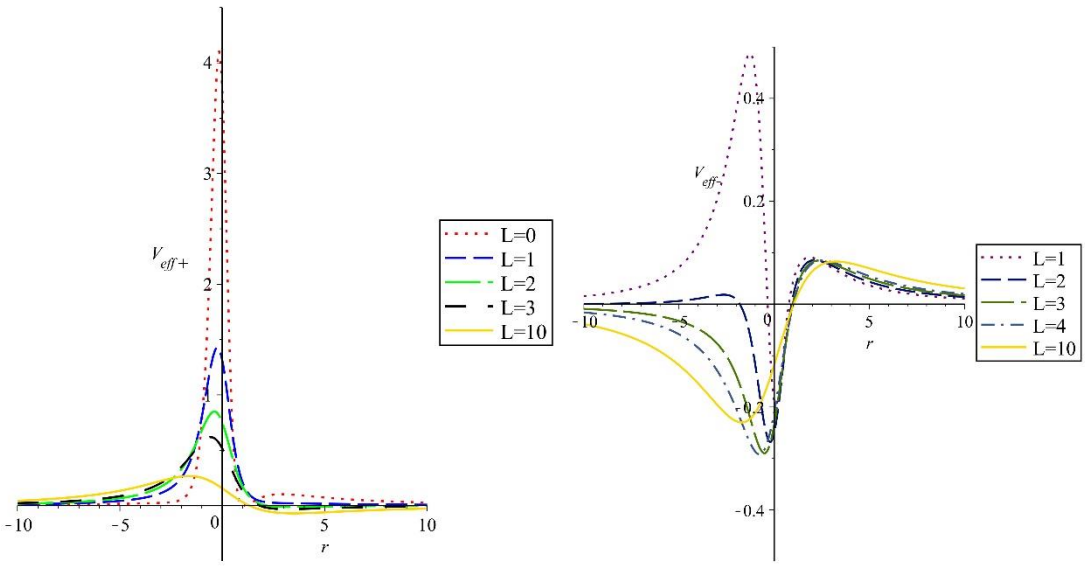

(a) (b)

Figure 6.2: a) Plots of V_{eff}^{+} versus r for the spin-$(+\,1/2)$ particles. b) Plots of V_{eff}^{-} versus r for fermions spin-$(-\,1/2)$ particles. The physical parameters are chosen as; $M = a = 1$, and $\lambda = -1.5$.

As shown in the Figs. 6.2, the pick of effective potential decrease by increasing the LSB parameter, also there is a significant gap between the zero and non-zero LSB parameter behavior (Fig. (6.2.a)). In order to have wide reach, this effect for spin down particles is depicted only for non-zero LSB parameter.

Chapter 7

GREYBODY FACTOR

In general relativity, the GF is one of the most important physical quantities related to the quantum nature of a BH. A high value of the GF indicates a high probability that HR can reach to spatial infinity. Among the different methods, here we explain some of them with considering the regarded investigation as an example.

7.1 Semi-analytic Method for Computing Greybody Factor

Here we employ the method of, which formulates the general semi-analytic bounds for GFs [176], this method is applied for bosonic and fermionic particles SBHBGM and Bardeen BH, and for the Kerr like BH in the BGM , for both 0-spin (bosons) and $\pm {}^{1}/_{2}$-spin (fermions) particles. This method is not appropriate in all cases, there are some limitations imposed by the borders of the integral in major semi-analytic equation

$$\sigma_l(\omega) \geq sech^2\left(\int_{-\infty}^{+\infty} \wp dr_*\right), \tag{7.1}$$

where $\sigma_l(\omega)$ are the dimensionless GFs that depend on the angular momentum quantum number l and frequency ω of the emitted particles, and

$$\wp = \frac{\sqrt{(h')^2 + \left(\omega^2 - V_{eff} - h^2\right)^2}}{2h}, \tag{7.2}$$

We have two conditions for the certain positive function h: 1) $h(r_*) > 0$ and 2) $h(-\infty) = h(+\infty) = \omega$ [176].

7.1.1 GFs of SBHBGM

Without loss of generality, we simply set $h = \omega$, which reduces the integration of Eq.(7.1) for SBHBGM (4.2) to

$$\sigma_l(\omega) \geq sech^2\left(\int_{-\infty}^{+\infty} \wp dr_*\right) = sech^2\left(\frac{\sqrt{1+L}}{2\omega}\int_{r_h}^{+\infty}\frac{V_{eff}}{f(r)}dr\right). \tag{7.3}$$

For a massless scalar field φ, considering the scalar effective potential of non-rotating bumblebee BH which is exhausted in chapter 4, given in Eq. (4.12), then Eq. (7.3) becomes

$$\sigma_l^s(\omega) \geq sech^2\left(\frac{\sqrt{1+L}}{2\omega}\int_{r_h}^{+\infty}\left[\frac{f'(r)}{(1+L)r}+\frac{l(l+1)}{r^2}\right]dr\right). \tag{7.4}$$

Taking cognizance of the integral part of Eq. (7.4):

$$\begin{aligned}\frac{1}{2\omega}\int_{-\infty}^{+\infty}&\left[\frac{l(l+1)}{r^2}f(r)dr_* + \frac{f'^{(r)}}{r(1+L)}f(r)dr_*\right]\\ &= \frac{\sqrt{1+L}}{2\omega}\left[l(l+1)\int_{r_h}^{+\infty}\frac{dr}{r^2}+\int_{r_h}^{+\infty}\frac{dr}{r(1+L)}\left(\frac{2M}{r^2}\right)\right]\\ &= \frac{\sqrt{1+L}}{2\omega r_h}\left[l(l+1)+\frac{1}{2(1+L)}\right],\end{aligned} \tag{7.5}$$

the GF of the SBHBGM due to scalar field radiation yields

$$\sigma_l^s(\omega) \geq sech^2\left\{\frac{\sqrt{1+L}}{2\omega r_h}\left[l(l+1)+\frac{1}{2(1+L)}\right]\right\}. \tag{7.6}$$

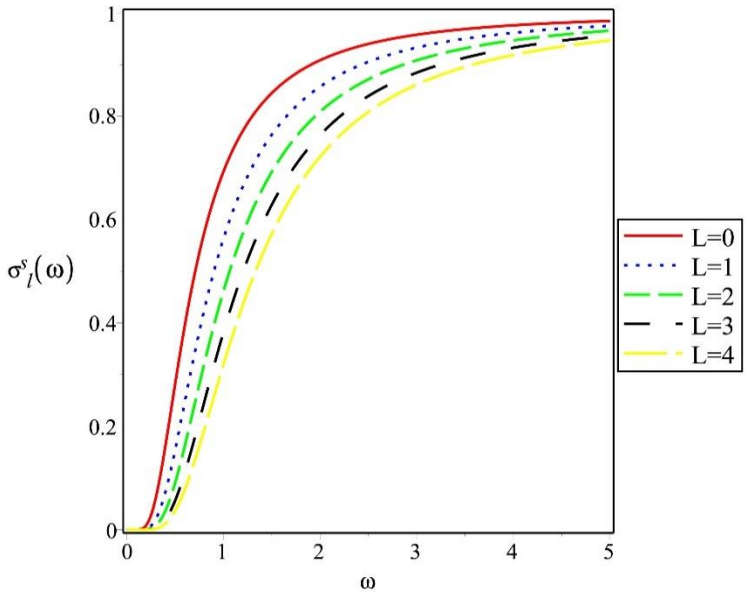

Figure 7.1: $\sigma_l^s(\omega)$ versus ω graph. The plots are governed by Eq. (7.6) with $M = 1$.

The behavior of the SBHBGM due to scalar field radiation under influence of LSB parameter is depicted in Fig. (7.1), which shows deduction by increasing the LSB parameter.

When one considers the effective potential (7.37) of the massless Dirac fields of the non-rotating bumblebee BH:

$$V_{\pm(\mu=0)} = f\left[\frac{\lambda_f^2}{r^2} \pm \lambda_f \frac{1}{\sqrt{1+L}} \frac{d}{dr}\left(-\frac{\sqrt{f}}{r}\right)\right], \tag{7.7}$$

the integral seen in Eq. (7.1) can be easily computed. Thus, we find the GF expression of the SBHBGM arising from the fermion radiation:

$$\sigma_l^f(\omega) \geq sech^2\left(\frac{1}{2\omega}\int_{-\infty}^{+\infty} f\left[\frac{\lambda_f^2}{r^2} \pm \lambda_f \frac{1}{\sqrt{1+L}} \frac{d}{dr}\left(-\frac{\sqrt{f}}{r}\right)\right] dr_*\right). \tag{7.8}$$

From now on, without loss of generality, we consider only V_+. After some manipulation, one can get

$$\sigma_l^f(\omega) \geq sech^2\left[\frac{\sqrt{1+L}}{2\omega}\left(\lambda_f^2 \int_{r_h}^{+\infty}\left(\frac{1}{r^2}\right)dr \pm \frac{\lambda_f}{\sqrt{1+L}}\int_{r_h}^{\infty}\left(1+\frac{M}{r}\right)\left(\frac{1}{r^2}-\frac{3M}{r^3}\right)dr\right)\right], \tag{7.9}$$

which recasts in

$$\sigma_l^f(\omega) \geq sech^2\left[\frac{\sqrt{1+L}}{2\omega}\left(\lambda_f^2\left(\frac{1}{r_h}\right) \pm \frac{\lambda_f}{\sqrt{1+L}}\left[\frac{1}{r_h} - \frac{M}{r_h^2} - \frac{M^2}{r_h^3}\right]\right)\right], \tag{7.10}$$

or in more compact form

$$\sigma_l^f(\omega) \geq sech^2\left[\frac{\left(l+\frac{1}{2}\right)\sqrt{1+L}}{4M\omega}\left(l+\frac{1}{2} \pm \frac{1}{4\sqrt{1+L}}\right)\right]. \tag{7.11}$$

We depict the greybody factors of the SBHBGM arising from the fermion (7.11) fields for V_+(spin up particles) and V_- (spin down particles) in Fig. 7.2.a and b, respectively.

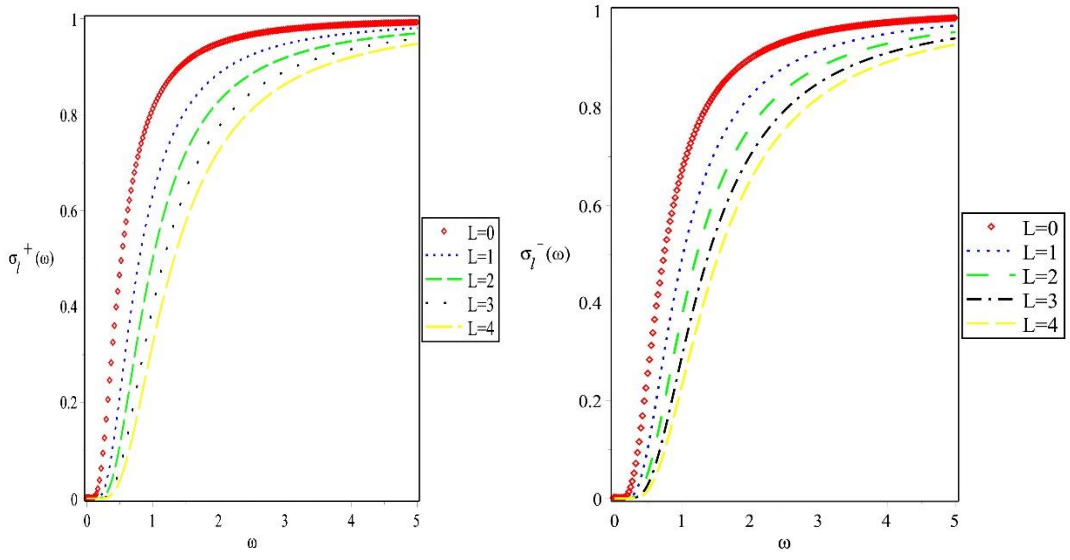

(a) (b)

Figure 7.2: Plots of $\sigma_l^f(\omega)$ versus ω. The plots are governed by Eq. (7.8). a) $\sigma_l^f(\omega)$ versus ω graph for V_+. b) $\sigma_l^f(\omega)$ versus ω graph for V_-.

As is well-known, the GF of the HR must be < 1 since a BH does not perform a complete black body radiation with a 100% absorption coefficient. Our findings, as shown in Figs. 7.2. a and b, are in good agreement with the latter remark. Also, it can be seen from these figures that the peak values of the GFs decreases with increasing LSB parameter L. In summary, LSB has reducing effect on the GF.

7.1.2 Bardeen Black Hole Surrounded by Quintessence (BBHSQ)

In another investigation, the GF of BBH with metric

$$ds^2 = -f(r)dt^2 + f^{-1}(r)dr^2 + r^2(d\theta^2 + sin^2\theta d\varphi^2), \tag{7.12}$$

where $f\ (r)$ has the following form

$$f(r) = 1 - \frac{2Mr^2}{(r^2+\beta^2)^{\frac{3}{2}}} - \frac{c}{r^{3\omega_q+1}}, \tag{7.13}$$

in which M is the mass of the BH and β can represent the monopole charge of a self-gravitating magnetic field described by a nonlinear electrodynamics source or an electric source with a field that does not behave as the Coulomb field [58]. In fact, c term is related to the density of quintessence:

$$\rho_q = \frac{-3c\omega_q}{2r^{3(\omega_q+1)}}, \tag{7.14}$$

where ω_q is the quintessence state parameter with range $-1 \leq \omega_q \leq -1/3$ and ρ_q is the density of the quintessence matter. To evaluate the GF of BBH, we use the semi-analytic method as explained. Here, by plugging the general form of scalar effective potential

$$V_{eff} = f\left[\frac{f'}{r} + \frac{\lambda}{r^2}\right], \tag{7.15}$$

into the semi-analytic greybody formula (7.1), also applying the tortoise coordinate as $dr_* = \frac{dr}{f(r)}$, we can obtain

$$\sigma_l(\omega) \geq sech^2\frac{1}{2\omega}\int_{r_h}^{+\infty}\left(\frac{\lambda}{r^2} + \frac{1}{r}\frac{df}{dr}\right)dr. \tag{7.16}$$

After making a straightforward calculation, one finds

$$\sigma_l(\omega) \geq sech^2\left(\frac{1}{2\omega}\left[\frac{l(l+1)}{r_h} + \frac{c(3\omega_q+1)}{(3\omega_q+2)r_h^{(3\omega_q+2)}} - \frac{2M}{\beta^2} + \frac{2M}{\beta^2\sqrt{1+\frac{\beta^2}{r_h^2}}} + \frac{2M}{r_h^2\left(1+\frac{\beta^2}{r_h^2}\right)^{\frac{3}{2}}}\right]\right), \tag{7.17}$$

where r_h represents the event horizon.

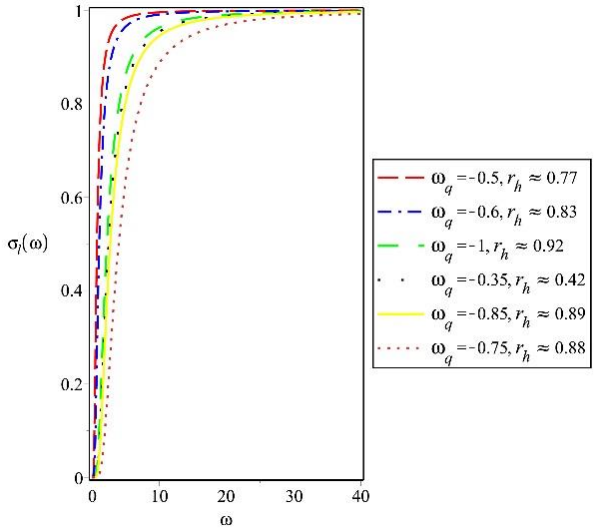

Figure 7.3: $\sigma_l(\omega)$ versus ω graph. The plots are governed by Eq. (7.13). For different ω_q values, the corresponding event horizons (i.e, $f(r_h) = 0$) are illustrated. The physical parameters for this plot are chosen as $M = l = c = 1$, and $\beta = 2$.

We depict the GFs of the BBHSQ in Fig. 7.3. As seen from Fig. 7.3, the values of $\omega_q$and event horizon (r_h) are linearly proportional to each other. It is obvious that greybody radiation strictly depends also on the state parameter ω_q. According to the information we obtained from the graph, a similar radiation emission occurs around critical ω_q values (-13 and -1).

However, while ω_q value moves away from those critical values, then the radiation may decrease or increase depending on ω_q.

We shall derive the fermionic GFs of the neutrinos emitted from BBHSQ. To this end, we consider the case of $\omega_q = -\frac{1}{3}$ in order to obtain analytical results from Eq. (7.1). In the case of $\omega_q = -\frac{1}{3}$ the potentials can be rewritten as [38]

$$V_{\pm} = \frac{\lambda}{r^2} f \pm \frac{\lambda(r-M)}{r^3}\sqrt{f} \mp \frac{2\lambda}{r^2} f^{\frac{3}{2}}, \tag{7.18}$$

in which

$$f = 1 - \frac{2Mr^2}{(r^2+\beta^2)^{\frac{3}{2}}} - c, \tag{7.19}$$

Following the procedure described in the previous section [see Eqs. (7.1) -(7.3)], one can get

$$\sigma_l^{\pm}(\omega) \geq sech^2\left(\frac{1}{2\omega}\int_{r_h}^{+\infty}\left[\frac{\lambda}{r^2} \pm \left(\frac{\lambda}{r^2} - \frac{\lambda M}{r^3}\right)\frac{1}{\sqrt{f}} \mp \frac{2\lambda}{r^2}\sqrt{f}\right] dr\right), \tag{7.20}$$

in which $\sigma_l^{+}(\omega)$ and $\sigma_l^{-}(\omega)$ stand for the GFs of the spin-up and spin-down fermions, respectively. After performing some tedious computations, the GFs of the fermions can be obtained as follows

$$\sigma_l^{\pm}(\omega) \geq sech^2\left\{\frac{\lambda}{2\omega}\left[\frac{1}{r} \pm \left(\frac{1}{r_h\sqrt{1-c}} + \frac{M\lambda}{2(1-c)^{\frac{3}{2}}r_h^2} + \frac{M^2}{2(1-c)^{\frac{5}{2}}r_h^3} + \frac{-3M\beta^2(1-c)^2+5M^3}{8r_h^4(1-c)^{\frac{7}{2}}} + \right.\right.\right.$$

$$\frac{-9M^2\beta^2(1-c)^2+\frac{35}{4}M^4}{10r_h^5(1-c)^{\frac{9}{2}}} - \frac{M}{2\sqrt{1-c}r_h^2} - \frac{M^2}{3(1-c)^{\frac{3}{2}}r_h^3} - \frac{3M^3}{8r_h^4(1-c)^{\frac{5}{2}}} - \frac{-3M^2\beta^2(1-c)^2+5M^4}{10r_h^5(1-c)^{\frac{7}{2}}} -$$

$$\left.\left.\left.\frac{-9M^3\beta^2(1-c)^2+\frac{35}{4}M^5}{12r_h^6(1-c)^{\frac{9}{2}}}\right) \mp \left(\frac{2\sqrt{1-c}}{r_h} - \frac{M}{\sqrt{1-c}r_h^2} - \frac{M^2}{3(1-c)^{\frac{3}{2}}r_h^2} + \frac{\sqrt{1-c}\left(3M\beta^2(1-c)^2-M^3\right)}{4r_h^4(1-c)^3} + \right.\right.\right.$$

$$\left.\left.\left.\frac{\sqrt{1-c}\left(12M^2\beta^2(1-c)^2-5M^4\right)}{20r_h^5(1-c)^4}\right)\right]\right\} \quad (for\ 0 \leq c < 1). \tag{7.21}$$

In order to observe the impression of quintessence on greybody radiation Eq. (7.21) , the Figs. 7.4 and 7.5 are illustrated bases on variating the density parameter of quintessence c. The graphs are sketched for zero (and almost zero) and non-zero density parameter, which increasing in parameter c and decreasing in r_h, reduce the GFs in both cases for spin up particles.

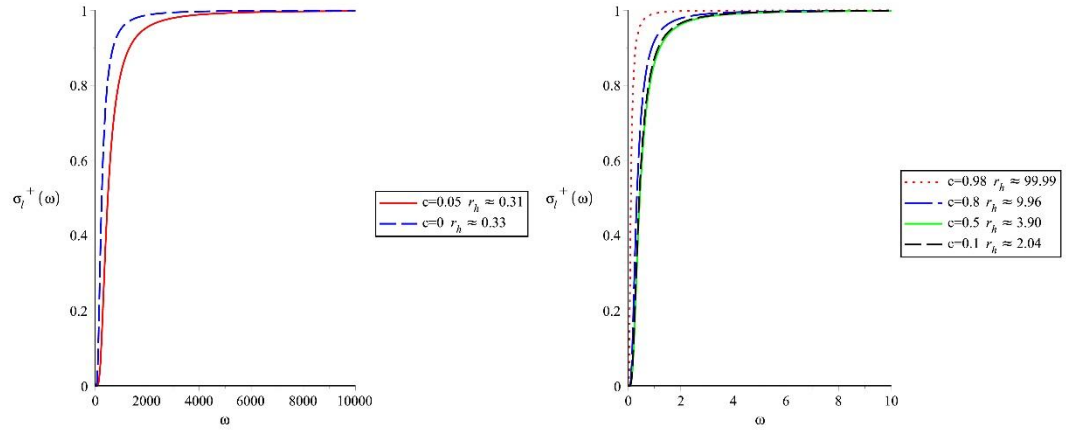

(a) (b)

Figure 7.4: $\sigma_l^+(\omega)$ versus ω graph for the case of $\omega_q = -1/3$. The plots are governed by Eq. (7.18). For different c values, the corresponding event horizons (i.e, $f(r_h) = 0$) are illustrated. The physical parameters for these plots are chosen as $M = l = 1$, and $\beta = 0.5$. a) for $c \approx 0$ values, b) for $c > 0$ values.

As can be seen from Figs. 7.5. a and b, the GFs of spin-down fermions exhibit almost the same behaviors as spin-up particles as c changes.

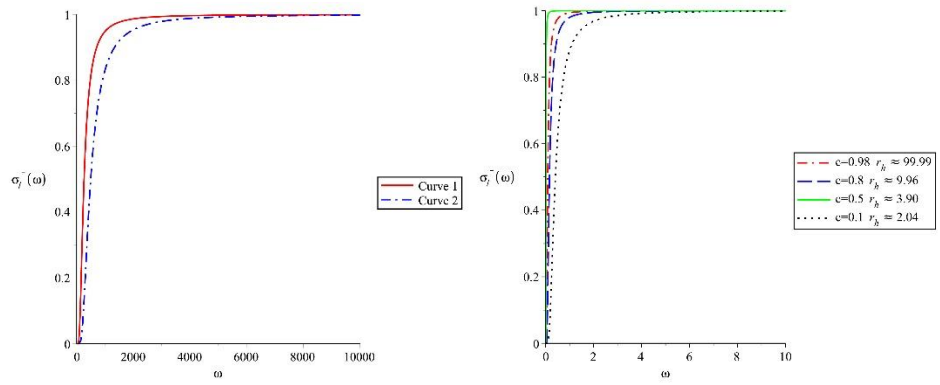

(a) (b)

Figure 7.5: $\sigma_l^-(\omega)$ versus ω graph for the case of $\omega_q = -1/3$. The plots are governed by Eq. (65). For different c values, the corresponding event horizons (i.e, $f(r_h) = 0$) are illustrated. The physical parameters for these plots are chosen as $M = l = 1$, and $\beta = 0.5$. a) for $c \approx 0$ values, b) for $c > 0$ values.

7.1.3 For Kerr-like Bumblebee Black Hole

We also applied the semi-analytic method for defining the GF of bumblebee gravity model in the Kerr spacetime. Derivation of the GF can be conducted as previous parts by using Eq. (7.1).

To have an immaculately integration, let us consider the massless form of the bosonic effective potential (5.58). Since the tortoise coordinate (5.56) varies from $-\infty$ (the event horizon r_h: lower boundary of the integral) and to $+\infty$ (spatial infinity: upper boundary of the integral) in Eq. (7.1) by considering the regarded conditions, we get $\sigma_l \geq sech^2$,

$$\left(\left(\frac{1}{2\omega}\int_{r_h}^{+\infty}\frac{\sqrt{1+L}}{(r^2+(1+L)a^2)}\left[\frac{\Delta' r+\Delta}{(r^2+(1+L)a^2)}-\frac{3r^2\Delta}{(r^2+(1+L)a^2)^2}\right.\right.\right.$$

$$\left.\left.\left.+\frac{4Mram\omega}{\Delta\sqrt{1+L}}-\frac{m^2a^2}{\Delta}+(\omega^2a^2(1+L)+\lambda)\right]dr\right)\right), \qquad (7.22)$$

After using the series and evaluating the integral, the GF can be obtained as follows

$$\sigma_l \geq sech^2\left(\frac{\sqrt{1+L}}{2\omega}\right)\left\{\left(-\frac{8a^2}{3r_h^3}+\frac{M}{r_h^2(1+L)}-\frac{2a^4(1+L)}{5r_h^5}+\frac{2Ma^2}{r_h^4}\right)-m^2a^2(1+L)\left(\frac{1}{3r_h^3}+\right.\right.$$

$$\left.\frac{M}{2r_h^4}+\frac{4M^2-2a^2(1+L)}{5r_h^5}-\frac{3Ma^2(1+L)-4M^3}{3r_h^6}\right)+(\omega^2a^2(1+L)+\lambda)\left[\frac{1}{r_h}-\frac{(1+L)a^2}{3r_h^3}+\right.$$

$$\left.\left.\frac{(1+L)^2a^4}{5r_h^5}\right]+4Mam\omega\sqrt{1+L}\left(\frac{1}{2r_h^2}+\frac{2M}{3r_h^3}-\frac{(1+L)a^2-2M^2}{2r_h^4}-\frac{6Ma^2(1+L)-8M^3}{5r_h^5}\right)\right\}. \qquad (7.23)$$

In Fig. 7.6, the behaviors of the obtained bosonic GF of the Kerr-like black hole are demonstrated. Thus, the effect of LSB on the bosonic GF is visualized.

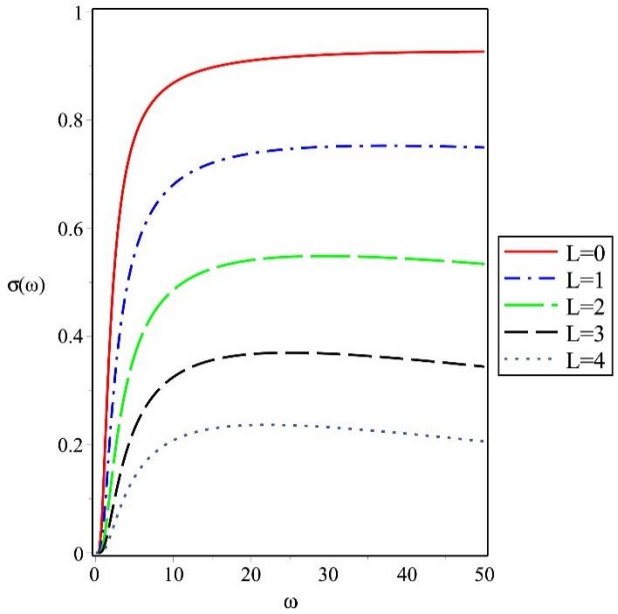

Figure 7.6: Plots of $\sigma_l(\omega)$ versus ω for the spin-0 particles. The physical parameters are chosen as; $M = r = 1, a = 0.03$ and $\lambda = 2$.

As can be seen from the plots, σ_l clearly decreases with the increasing LSB parameter. Namely, LSB plays a kind of dimmer role for the GF of spin-0 particles.

Now, we shall concentrate on the GF of the fermions to elicit the effect of the LSB on their emission from the Kerr-like BH in the BGM. For this purpose, we use the effective potentials (6.78) in Eq. (7.1):

$$\sigma_l^{(\pm)}(\omega) \geq sech^2\left(\int_{r_h}^{+\infty} \frac{dr}{2\omega}\left\{\frac{\lambda^2 dr}{\left(r^2+a^2(1+L)\right)\sqrt{1+L}} \pm \lambda \frac{d}{dr}\left(\frac{\sqrt{\Delta(1+L)}}{r^2+a^2(1+L)}\right)\right\}\right). \tag{7.24}$$

We then employ the classical term-by-term integration technique used for obtaining asymptotic expansions of integral, which requires the integrand to have an uniform asymptotic expansion in the integration variable. Thus, the evaluation of the integral (7.21) yields

$$\sigma_l^{(\pm)}(\omega) \geq sech^2$$

$$\left(\frac{\lambda}{2\omega}\left\{\frac{\lambda}{\sqrt{1+L}r_h}\left(1-\frac{a^2(1+L)}{3r_h^2}\right)\pm\left(\frac{M^2-a^2(1+L)}{2r_h^3}\right)\right.\right.$$

$$\left.\left.\mp\left[M\left(\frac{M}{3r_h^3}+\frac{3}{8}\frac{M^2-a^2(1+L)}{r_h^4}\right)+\frac{1}{r_h}-\frac{M}{r_h^2}\right]\right\}\right). \qquad (7.25)$$

The behaviors of both spin-$(+1/2)$ and spin-$(-1/2)$ under the influence of LSB effect are depicted in Figs. 7.7.a and b, respectively. As it shown, the GF grows by rising the LSB parameter which is contrary to the effect of LSB parameter for SBHBGM in the almost same level

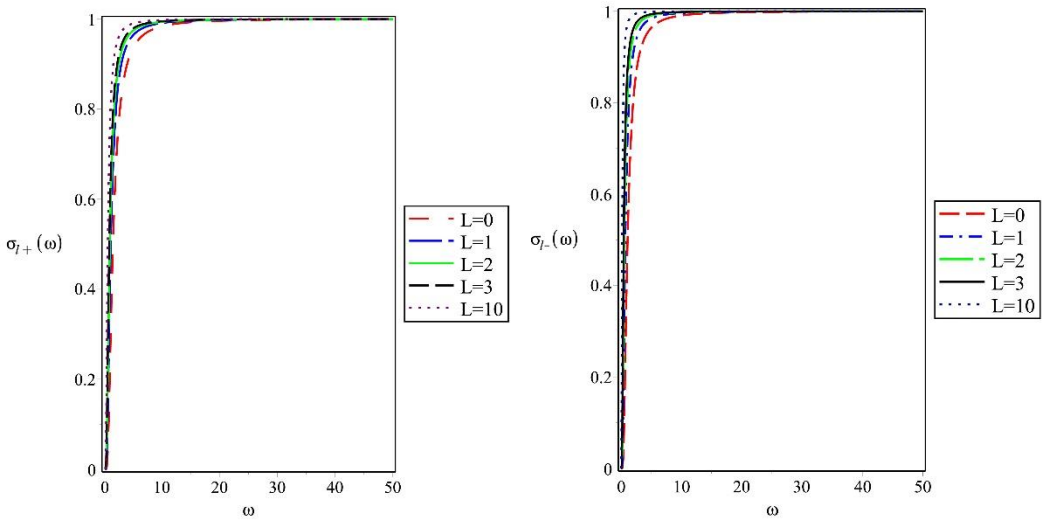

(a) (b)

Figure 7.7: Plots of $\sigma_{l+}(\omega)$ versus ω for fermions with spin-$(+\,^1/_2)$ (a) and plots of $\sigma_{l-}(\omega)$versus ω for the spin-$(-\,^1/_2)$ particles (b). The physical parameters are chosen as; $M = r = 1, a = 0{:}\,03$ and $\lambda = -1.5$.

7.2 Miller-Good Transformation for Bardeen Black Hole

In this section, we shall focus on the Miller–Good transformation method [177] to derive the GF of the Schwarzschild BH surrounded by quintessence (SBHSQ). The Miller–Good transformation generates a general bound on quantum transmission

probabilities. In this method, a particular transformation is applied to the Schrödinger equation

$$\frac{d^2S(r)}{dr_*^2} + \left(\omega^2 - V_{eff}\right)S(r) = 0, \tag{7.26}$$

in such a way that the effective potential (7.12) is modified in order to yield a better transmission probability for the Hawking quanta [178].

Defining the new radial function $S(r) = \frac{\psi(r)}{\sqrt{f}}$ in one-dimensional Schrödinger equation where the effective radial potential in the Schrödinger-like wave equation (7.23) reads

$$V_{eff} = \frac{f}{r}\left(f' + \frac{\lambda}{r}\right). \tag{7.27}$$

Eq. (7.23) can be rewritten in the following compact form:

$$\frac{d^2\psi(r)}{dr^2} + k^2(r)\psi(r) = 0, \tag{7.28}$$

where

$$k^2(r) = \left\{\frac{\omega^2}{f^2} - \frac{f'}{rf} - \frac{\lambda}{r^2 f} - \frac{f''}{2f} + \frac{f'^2}{4f^2}\right\}. \tag{7.29}$$

Considering the Miller–Good transformation method, we first apply the following special transformation:

$$\psi(r) = \frac{1}{\sqrt{R'(R)}}\Psi[R(r)]. \tag{7.30}$$

in which R is the new position variable such that $R\ (r)$ is an invertible function, which implies that $\frac{dR(r)}{dr} \neq 0$. Without loss of generality, one can assert $\frac{dR(r)}{dr} > 0$, whence also $\frac{dr}{dR(r)} > 0$. Thus, the derivatives of the new function (7.27) yield

$$\psi'(r) = \sqrt{R'(r)}\Psi_R\big(R(r)\big) - \frac{1}{2}\frac{R''(r)}{R'(r)\sqrt{R'(r)}}\Psi\big(R(r)\big), \tag{7.31}$$

$$\psi''(r) = R'(r)\sqrt{R'(r)}\Psi_{RR}\big(R(r)\big) - \frac{1}{2}\frac{R'''(r)}{R'(r)\sqrt{R'(r)}}\Psi\big(R(r)\big)$$

$$+\frac{3}{4}\frac{R''^2(r)}{R'^2(r)\sqrt{R'^2(r)}}\Psi\big(R(r)\big). \qquad (7.32)$$

where Ψ_R indicates $\frac{d\Psi}{dR}$. Thus, Eq. (7.27) recasts in

$$\Psi_{RR}\big(R(r)\big) + \left\{\frac{k^2}{R'^2(r)} + \frac{3}{4}\frac{R''^2(r)}{R'^4(r)} - \frac{1}{2}\frac{R'''(r)}{R'^3(r)}\right\}\Psi\big(R(r)\big) = 0. \qquad (7.33)$$

Letting

$$K^2 = \frac{1}{R'^2(r)}\left\{\frac{\omega^2}{f^2} - \frac{f'}{rf} - \frac{\lambda}{r^2 f} - \frac{f''}{2f} + \frac{f'^2}{4f^2} - \frac{1}{2}\frac{R'''(r)}{R'(r)} + \frac{3}{4}\frac{R''^2(r)}{R'^2(r)}\right\}, \qquad (7.34)$$

one can rewrite Eq. (7.30) as a new Schrödinger-like wave equation:

$$\Psi_{RR} + K^2\Psi = 0. \qquad (7.35)$$

Namely, Schrödinger equation (7.27) expressed in terms of $\psi(r)$ and $K(r)$ has been transformed into a new Schrödinger equation in terms of $\Psi\big(R(r)\big)$ and $K\ (R\ (r))$. Meanwhile, the following combination

$$\sqrt{R'}\left(\frac{1}{\sqrt{R'(r)}}\right)'' = -\frac{1}{2}\frac{R'''(r)}{R'(r)} + \frac{3}{4}\frac{R''^2(r)}{R'^4(r)}, \qquad (7.36)$$

is named as the "Schwarzian derivative" [180]. Thus, K can be simplified as

$$K^2 = \frac{1}{R'^2(r)}\left\{\frac{\omega^2}{f^2} - \frac{f'}{rf} - \frac{\lambda}{r^2 f} - \frac{f''}{2f} + \frac{f'^2}{4f^2} + \sqrt{R'}\left(\frac{1}{\sqrt{R'(r)}}\right)''\right\}. \qquad (7.37)$$

As we have mentioned above, the parameter $R'(r)$ must be positive. To this end, we choose another parameter as

$$j(r) \equiv R'(r), \qquad (7.38)$$

with $j\ (r)\ >\ 0$, we can then write

$$K^2 = \frac{1}{j^2(r)}\left\{\frac{\omega^2}{f^2} - \frac{f'}{rf} - \frac{\lambda}{r^2 f} - \frac{f''}{2f} + \frac{f'^2}{4f^2} - \frac{1}{2}\frac{j''(r)}{j(r)} + \frac{3}{4}\frac{j'^2(r)}{j^2(r)}\right\}. \tag{7.39}$$

Furthermore, setting

$$j(r) = \frac{1}{J^2(r)}, \tag{7.40}$$

with $J\,(r) > 0$, we get

$$j'(r) = -\frac{2J'(r)}{J^3(r)}, \;\; j''(r) = \frac{6J'^2(r)}{J^4(r)} - \frac{2J''(r)}{J^3(r)}, \tag{7.41}$$

and

$$K^2 = J^4(r)\left\{\frac{\omega^2}{f^2} - \frac{f'}{rf} - \frac{\lambda}{r^2 f} - \frac{f''}{2f} + \frac{f'^2}{4f^2} + \frac{J''(r)}{J(r)}\right\}. \tag{7.42}$$

In the case of $J = 1$, one can immediately observe that $K^2(R) = k^2(r)$; therefore, both potentials [$K^2(R)$ and $k^2(r)$] have the same transmission amplitudes and consequently the same transmission probability. The second probability is to find the relation between two parameters J and f such that we will have different potentials and whence different transmission probabilities. For the latter case, one can get the transmission probability from the following definition [177]:

$$\mathcal{T} \geq sech^2\left\{\int_{-\infty}^{+\infty} \wp\, dr\right\}, \tag{7.43}$$

in which $\wp$ is given by

$$\wp = \frac{\sqrt{(h')^2 + [k^2 - h^2]^2}}{2h}, \tag{7.44}$$

with $h\,(r) > 0$. Let us redefine function $\wp$ as $\widetilde{\wp}$ in order to show the difference between $k\,(r)$ and $K\,(R)$. Then, we have

$$\mathcal{T} \geq sech^2\left\{\int_{-\infty}^{+\infty} \widetilde{\wp}\, dR\right\}, \tag{7.45}$$

where $\widetilde{\wp}$ is the function with respect to new transformation parameters and

$$dR = R'dr = jdr, \tag{7.46}$$

so that Eq. (7.45) is given by

$$\mathcal{T} \geq sech^2\left\{\int_{-\infty}^{+\infty} \frac{\sqrt{(h_R)^2 + [K^2 - h^2]^2}}{2h}\, dR\right\}. \tag{7.47}$$

After substituting Eqs. (7.39) and (7.46) into Eq. (7.47) and further using $h_R = \frac{dh}{dr}\frac{dr}{dR}$, one can obtain

$$\mathcal{T} \geq sech^2\left\{\int_{-\infty}^{+\infty} \frac{1}{2h}\sqrt{\left(\frac{h'}{R'}\right)^2 + \left[\frac{1}{j^2}\left\{\frac{\omega^2}{f^2} - \frac{f'}{rf} - \frac{\lambda}{r^2 f} - \frac{f''}{2f} + \frac{f'^2}{4f^2} - \frac{1}{2}\frac{j''(r)}{j(r)} + \frac{3}{4}\frac{j'^2(r)}{j^2(r)}\right\} - h^2\right]^2} j dr\right\}. \tag{7.48}$$

As we have mentioned before $R' = j$, Eq. (7.48) recasts in

$$\mathcal{T} \geq sech^2\left\{\int_{-\infty}^{+\infty} \frac{1}{2h}\sqrt{(h')^2 + \left[\frac{1}{j}\left\{\frac{\omega^2}{f^2} - \frac{f'}{rf} - \frac{\lambda}{r^2 f} - \frac{f''}{2f} + \frac{f'^2}{4f^2} - \frac{1}{2}\frac{j''(r)}{j(r)} + \frac{3}{4}\frac{j'^2(r)}{j^2(r)}\right\} - jh^2\right]^2} dr\right\}. \tag{7.49}$$

which gives us the first form of the improved bound with the condition of $h(r) > 0$; then, $j(r) > 0$, too. One can further improve the bound by transforming j to J as follows

$$dR = R'dr = J^{-2}dr. \tag{7.50}$$

Therefore, the second form of the improved bound for the transmission probability is given by

$$\mathcal{T} \geq sech^2\left\{\int_{-\infty}^{+\infty} \frac{1}{2h}\sqrt{(h')^2 + \left[J^2\left\{\frac{\omega^2}{f^2} - \frac{f'}{rf} - \frac{\lambda}{r^2 f} - \frac{f''}{2f} + \frac{f'^2}{4f^2} + \frac{J''}{J}\right\} - \frac{h^2}{J^2}\right]^2} dr\right\}. \tag{7.51}$$

Here, we consider $J_{\pm\infty} \neq 1$ with the help of $h(+\infty) = h(-\infty) = \omega$ and then $h' = 0$. So, one can write Eq. (7.48) as

$$\mathcal{T} \geq sech^2\left\{\frac{1}{2\omega}\int_{-\infty}^{+\infty}\left[J^2\left\{\frac{\omega^2}{f^2}-\frac{f'}{rf}-\frac{\lambda}{r^2 f}-\frac{f'}{2f}+\frac{f'^2}{4f^2}+\frac{J''}{J}\right\}-\frac{\omega^2}{J^2}\right]dr\right\}. \quad (7.52)$$

Moreover, we assume that the first and second terms of the integral are equal to make Eq. (7.52) more expressive. To this end, we set $J^2 = f$ so then

$$f' = 2JJ', \quad f'' = 2J'^2 + 2JJ''. \quad (7.53)$$

We finally compute the transmission probability of the SBHSQ as follows:

$$\mathcal{T} \geq sech^2\left\{-\frac{1}{2\omega}\int_{-\infty}^{+\infty}\left(\frac{2JJ'}{r}+\frac{\lambda}{r^2}\right)dr\right\}. \quad (7.54)$$

Now, we shall focus on the GF of Schwarzschild BH surrounded by quintessence, namely the SBHSQ. Within a semi-classical approximation, GFs can be investigated by using the Schrödinger-like one-dimensional wave equation to study the field scattering by the BH background. Actually, with the help of this method, we will be able to define the transmission and reflection coefficients of the BH. Here, we concentrate on Eqs. (7.27) and (7.39) to define two kinds of GFs and compare the obtained results over their graphs. The formula of the general semi-analytic bounds for the GFs is Eq. (7.45). After substituting the general form of the effective potential (7.27) and the derivative of the metric function into

$$\sigma_l(\omega) \geq sech^2\left(\frac{1}{2\omega}\int_{r_h}^{+\infty} V_{eff}\frac{dr}{f(r)}\right), \quad (7.55)$$

we obtain

$$\sigma_l(\omega) \geq sech^2\left(\frac{1}{2\omega}\int_{r_h}^{+\infty}\left(\frac{2M}{r^3}-\frac{c}{r}+\frac{\lambda}{r^2}\right)dr\right). \quad (7.56)$$

But the result of Eq. (7.56) has a natural logarithm (ln) term, which means that the GF of SBHSQ is measureless. Namely, the method that we have followed is failed. To overcome this difficulty, we shall consider the Miller– Good transformation. To this end, let us rewrite Eq. (7.54) in the form of

$$\mathcal{T} \geq sech^2\left\{-\frac{1}{2\omega}\int_{r_h}^{+\infty}\left(\frac{2M-cr^2+\lambda r}{r^3}\right)\frac{rdr}{r-2M-cr^2}\right\}, \tag{7.57}$$

which can be rewritten as

$$\mathcal{T} \geq sech^2\left\{\frac{1}{2\omega}\int_{r_h}^{+\infty}(2M-cr^2+\lambda r)\left(\frac{1}{r^4}\right)\frac{dr}{c+\frac{2M}{r^2}-\frac{1}{r}}\right\}. \tag{7.58}$$

By considering the following asymptotic expansion

$$\frac{1}{\frac{dr}{c+\frac{2M}{r^2}-\frac{1}{r}}} \cong \frac{1}{c}+\frac{1}{c^2r}+\frac{-\frac{2M}{c}+\frac{1}{c^2}}{cr^2}\ldots \tag{7.59}$$

we find (for the similar procedure, the reader is refereed to [180])

$\sigma_l(\omega) \equiv \mathcal{T} \geq sech^2$

$$\left\{\frac{1}{2\omega}\left[\frac{2M}{3cr_h^3}+\frac{2M}{4c^2r_h^4}+\frac{2M\left(\frac{1}{c^2}-\frac{2M}{c}\right)}{5cr_h^5}-\frac{1}{r_h}-\frac{1}{2cr_h^2}-\frac{-\frac{2M}{c}+\frac{1}{c^2}}{3r_h^3}\right.\right.$$
$$\left.\left.+\frac{\lambda}{2cr_h^2}+\frac{\lambda}{3c^2r_h^3}+\frac{\lambda\left(-\frac{2M}{c}+\frac{1}{c^2}\right)}{4cr_h^4}\right]\right\}. \tag{7.60}$$

The above result represents the GF of SBHSQ, which is obtained by the Miller–Good transformation. It is obvious that the specific form of the GF depends on some parameters which are related to the potential barrier. This is indeed the case that gives the greybody factor in terms of the transmission coefficient corresponding to the potential barrier. The result obtained in Eq. (7.60) is depicted in Fig. 7.8.

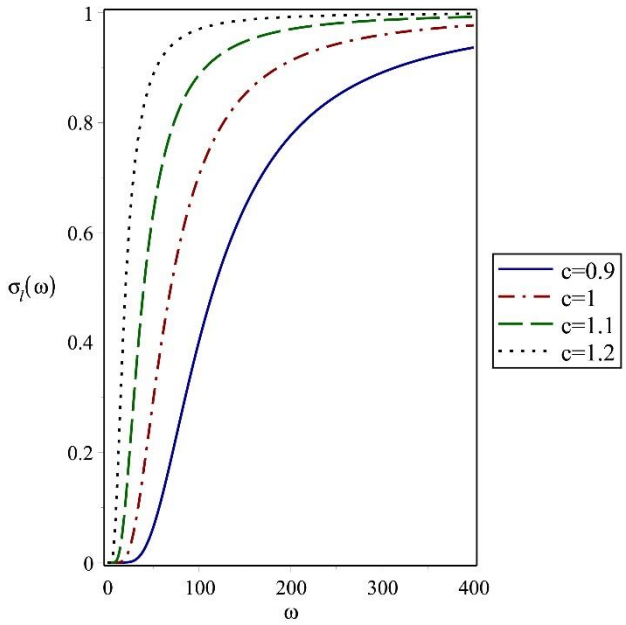

Figure 7.8: $\sigma_l(\omega)$ versus ω graph. The plots are governed by Eq. (7.60). For different c values, the corresponding GFs are illustrated. The physical parameters for this plot are chosen as $M = l = 1$

7.3 Rigorous Bound on Greybody Factor in dRGT Massive Gravity

In this section, we shall apply the rigorous bounds [181] on the GF to the $3 + 1$-dimensional black hole in dRGT massive gravity coupled with nonlinear electrodynamics. To this end, we first recall the formulation of the GF (T) (7.1) and (7.2) with the same condition to simplifies Eq. (7.2) to: [182,183]

$$T \geq sech^2\left(\frac{1}{2\omega}\int_{-\infty}^{+\infty} V\, dr_*\right). \tag{7.61}$$

In the part 5.2, the scalar perturbations for charged dRGT massive gravity coupled with nonlinear electrodynamics were obtained for first and second solution. Here, the greybody radiation is considered for two different effective potentials came by part 5.2 regarded to first and second solution.

First solution

By using the tortoise coordinate and the effective potential of first solution (Eq. (5.46)), then the GF equation (7.61) can be written as

$$T \geq sech^2 \frac{1}{2\omega}$$

$$\left\{\int_{r_h}^{R_h}\left(\frac{\lambda}{r^2}+\frac{2M}{r^3}-\frac{2q^2}{r^4}+2A-\frac{B}{r}\right)dr\right.$$

$$+\int_{r_h}^{R_h}\frac{2\omega q^2 r-q^4}{Ar^4-Br^3+(1+c)r^2-2Mr+q^2}\,dr$$

$$\left.-\int_{r_h}^{R_h}\frac{\omega q^3 b}{2(Ar^5-Br^4+(1+c)r^3-2Mr^2+q^2r)}\,dr\right\}, \tag{7.62}$$

the result is an awkward formula from the point of view of integration. To prevail over this issue we use the Taylor expansion, which accomplishes the GF as

$$T_1 \geq sech^2 \frac{1}{2\omega}\left\{-\frac{\lambda}{R_h-r_h}-\frac{M}{R_h^2-r_h^2}+\frac{2q^2}{3\left(R_h^3-r_h^3\right)}-\left(B+\frac{1}{2}\omega q b\right)ln(R_h-r_h)+W_1(R_h-\right.$$

$$\left.r_h)+X_1(R_h^2-r_h^2)+Y_1(R_h^3-r_h^3)+Z_1(R_h^4-r_h^4)-P_1\left(R_h^5-r_h^5\right)\right\}, \tag{7.63}$$

where

$$W_1 = 2A-\frac{\omega b A}{q}-q^2, \tag{7.64}$$

$$X_1 = \left(\omega+\frac{\omega b}{4q^2}\left(q(1+c)-\frac{4M^2}{q}\right)-M\right), \tag{7.65}$$

$$Y_1 = -\frac{\omega b}{6q^2}\left(qB-\frac{4M(q^2(1+c)-2M^2)}{q^3}\right)+\frac{q^2(1+c)-4M^2+4\omega M}{3q^2}, \tag{7.66}$$

$$Z_1 = \frac{\omega}{2q^2}\left(-(1+c)+\frac{4M^2}{q^2}\right)$$

$$-\frac{1}{8q^2}\left(-\omega q b A+\frac{\omega b(1+c)^2}{q}+\frac{4\omega b M(Bq^4-3Mq^2(1+c)+4M^3)}{q^5}\right)$$

$$-\frac{1}{4q^2}\left(q^2B+\frac{4M(-q^2(1+c)+2M^2)}{q^2}\right), \quad (7.67)$$

and

$$P_1=\frac{\omega b}{5q^2}\left((-q^2(1+c)+6M^2)B-2MAq^2\right)$$
$$-\frac{2\omega bM(1+c)}{5q^7}(-q^2(1+c)+2M^2)$$
$$-\frac{\omega bM}{5q^9}(-q^4(1+c^2)+12M^2q^2(1+c)-2cq^4-16M^4)$$
$$+\frac{1}{5q^2}\left(-q^2A+4BM+(1+c)^2-\frac{4M^2(3q^2(1+c)-4M^2)}{q^4}\right)$$
$$-\frac{2}{2q^2}\left(\omega B+\frac{4\omega M(-q^2(1+c)+2M^2)}{q^4}\right), \quad (7.68)$$

Two parameters R_h and r_h, are upper and lower rigorous bounds respectively, which can obtained by [184]

$$R_h=\frac{2}{(-2A)^{\frac{1}{3}}}\left[\sqrt{\frac{2\sqrt{3}}{\beta}+4}cos\left(\frac{1}{3}sec^{-1}\left(\frac{\sqrt{\frac{\sqrt{3}}{\beta}+2}\left(2\sqrt{2}\beta+\sqrt{6}\right)}{5\beta+3\sqrt{3}}\right)\right)-1\right], \quad (7.69)$$

and the lower one reads

$$r_h=\frac{-2}{(-2A)^{\frac{1}{3}}}\left[\sqrt{\frac{2\sqrt{3}}{\beta}+4}cos\left(\frac{1}{3}sec^{-1}\left(\frac{\sqrt{\frac{\sqrt{3}}{\beta}+2}\left(2\sqrt{2}\beta+\sqrt{6}\right)}{5\beta+3\sqrt{3}}\right)+\frac{\pi}{3}\right)+1\right]. \quad (7.70)$$

We demystify our results obtained, by illustrating the GFs for different charge values, in this case to approach in ideal form of figure we got a significantly smaller amount of b (around 0.1) than its value ($b = 50$) in effective potential case. The remarkable point in Fig. 6.9 is that GF for $h_0 = 0$ behaves as in the case of the AdS/dS black string [184,185]. The Fig. (7.9) is shown the changes of the GF by varying the charge parameter q, this changes are not stable since it grows by rising charge parameter up to $q = 4.5$ and the start to decrease for $q = 5$ and $q = 5.5$. In another word, from Fig.

(7.9), one can see that the GF increases by only increasing a small range of charge but afterwards it has an inverse behavior.

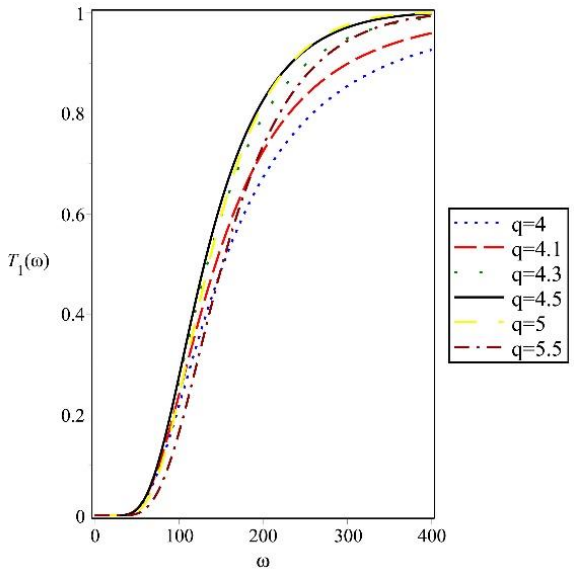

Figure 7.9: Plots of T versus ω for the metric functionf_1. The plot is governed by Eq. (7.63). The physical parameters are chosen as; $M = 1, b = 0.1, \lambda = 0, A = -1,$ and $B = C = 0$.

Second solution

Based on previous part, let us substitute the effective potential of second solution Eq. (5.48) into Eq. (7.61) to get,

$$T_2 \geq sech^2 \frac{1}{2\omega}$$

$$\left\{\int_{r_h}^{R_h}\left(\frac{\lambda}{r^2}+\frac{2M}{r^3}-\frac{2q^2}{r^4}-2D\right)dr + \int_{r_h}^{R_h}\frac{2\omega q^2 r - q^4}{-Dr^4+r^2-2Mr+q^2}dr - \int_{r_h}^{R_h}\frac{\omega q^3 b}{2(-Dr^5+r^3-2Mr^2+q^2r)}dr\right\}, \quad (7.71)$$

then after integration and using the Taylor expansion, the greybody equation is defined as

$$T_2 \geq sech^2 \frac{1}{2\omega},$$

$$\left\{-\frac{\lambda}{R_h - r_h} - \frac{M}{R_h^2 - r_h^2} + \frac{2q^2}{3(R_h^3 - r_h^3)} - \frac{1}{2}\omega q b ln(R_h - r_h)\right.$$
$$- W_2(R_h - r_h) + X_2(R_h^2 - r_h^2) + Y_2(R_h^3 - r_h^3)$$
$$\left. + Z_2(R_h^4 - r_h^4) + P_2\left(R_h^5 - r_h^5\right)\right\}, \tag{7.72}$$

where

$$W_2 = 2D + q^2 + \frac{\omega b M}{q}, \tag{7.73}$$

$$X_2 = \omega - \left(\frac{-\omega b}{4q} + \frac{\omega b M^2}{q^3}\right) - M, \tag{7.74}$$

$$Y_2 = \frac{q^2 - 4M^2 + 4\omega M}{3q^2} + \frac{2\omega b M(q^2 - 2M^2)}{3q^5}, \tag{7.75}$$

$$Z_2 = \frac{\omega}{2q^2}\left(\frac{4M^2}{q^2} - 1\right) - \frac{\omega b}{8q^2}\left(-qD + \frac{(q^2 - 12M^2)}{q^3} + \frac{16M^4}{q^5}\right), \tag{7.76}$$

and

$$P_2 = -\frac{1}{10q^3}\left(2\omega b M\left(2D + \frac{3}{q^2} - \frac{16M^2}{q^4} + \frac{16M^4}{q^6}\right)\right)$$
$$-\frac{1}{5q^2}\left(1 - q^2 D + \frac{4M}{q^4}\left(M(4M^2 - 3q^2) + 2\omega(-q^2 + 2M^2)\right)\right). \tag{7.77}$$

From Eq. (7.72), one can see the rigorous bounds on the GFs for the second solution of dRGT massive gravity coupled with nonlinear electrodynamics and its plotted as shown in Fig. 7.10, the constant parameter b is chosen to be small in comparison with the potential case, for both solutions of GF.

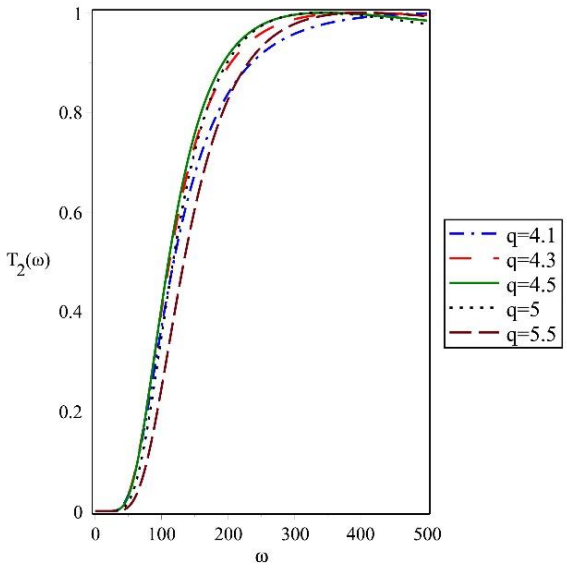

Figure 7.10: Plots of T versus ω for the metric function f_2. The plot is governed by Eq. (7.72). The physical parameters are chosen as; $M = 1, b = 0.1, \lambda = 0$, and $D = 0.8$.

We can see that by increasing the charge parameter gradually, the GF approaches its maximum value then it starts to dwindle, this alteration happens after $q = 4.5$ for both solutions. Therefore, we can conclude that, having a monotonous behavior in existence of charge for GF is far from expectation.

7.4 Reflection and Transmission Coefficients of Rotating Polytropic Black Hole

In this section, we investigate the computation of reflection and transmission coefficients via the WKB method. It is well known that the GFs in the Hawking radiation are related to the transmission through the BH perturbation potentials. To obtain those, one has to solve the classical scattering problem of incoming radiation being transmitted or reflected at the potential barrier. Let us consider a wave reaches the BH from the cosmological horizon $r_* \longrightarrow \infty\ (r \longrightarrow r_c)$; due to the gravitational potential some of it will be transmitted and some will be reflected. The scattering boundary conditions have the following form [186]

$$\Psi = T(\omega)e^{-i\omega r_*} \qquad r_* \longrightarrow -\infty, \tag{7.78}$$

$$\Psi = e^{-i\omega r_*} + R(\omega)e^{i\omega r_*} \qquad r_* \longrightarrow -\infty, \tag{7.79}$$

where $T(\omega)$ and $R(\omega)$ are transmission and reflection coefficients, respectively. Now to determine the square of the wave function's amplitude, we can use the fact that the total probability of finding a wave must obey the normalization condition given

$$|T|^2 + |R|^2 = 1, \tag{7.80}$$

Therefore, the GF can be defined as

$$\gamma_l(\omega) = |T(\omega)|^2. \tag{7.81}$$

For accurate evaluation of the transmission and reflection coefficients, one can use the sixth order WKB formula [230], the reflection coefficient is given by

$$R = \frac{1}{\sqrt{1 + exp(-2\pi i\mathfrak{H})}}, \tag{7.82}$$

and transmission coefficient

$$T = \frac{1}{\sqrt{1 + exp(2\pi i\mathfrak{H})}}, \tag{7.83}$$

where

$$\mathfrak{H} = i\,\frac{\omega_n^2 - V(r_0)}{\sqrt{-2V''(r_0)}} - \Lambda_2 - \Lambda_3, \tag{7.84}$$

in which Λ_2 and Λ_3 represent the second and third order WKB formula correction:

$$\Lambda_2 = \frac{1}{\sqrt{-2V_0''}}\left[\frac{1}{8}\left(\frac{V_0^{(4)}}{V_0''}\right)\left(\frac{1}{4} + \alpha^2\right) - \frac{1}{288}\left(\frac{V_0^{(3)}}{V_0''}\right)^2 (7 + 60\alpha^2)\right], \tag{7.85}$$

and

$$\Lambda_3 = \frac{1}{\sqrt{-2V_0^{''}}}\left[\frac{5}{6912}\left(\frac{V_0^{(3)}}{V_0^{''}}\right)^4 (77+188\alpha^2) - \frac{1}{384}\left(\frac{V_0^{'''(2)}V_0^{(4)}}{V_0^{''(3)}}\right)(51+100\alpha^2) + \right.$$

$$\left.\frac{1}{2304}\left(\frac{V_0^{(4)}}{V_0^{''}}\right)^2 (67+68\alpha^2) - \frac{1}{288}\left(\frac{V_0^{'''}V_0^{(5)}}{V_0^{''(2)}}\right)(19+28\alpha^2) - \frac{1}{288}\left(\frac{V_0^{(6)}}{V_0^{''}}\right)(5+4\alpha^2)\right].$$

(7.86)

Prime and the superscript (n) denote differentiation with respect to r_*. Recall that, potential formula was given in Eq. 5.67.

The performance of the reflection and transmission coefficients for rotating parameter $a = 0.011$ and $a = 0.5$ are depicted in Fig. 7.11 and Fig. 7.12, respectively. In order to develop a broader perspective, Fig. (7.13) is depicted, which represents more detachments.

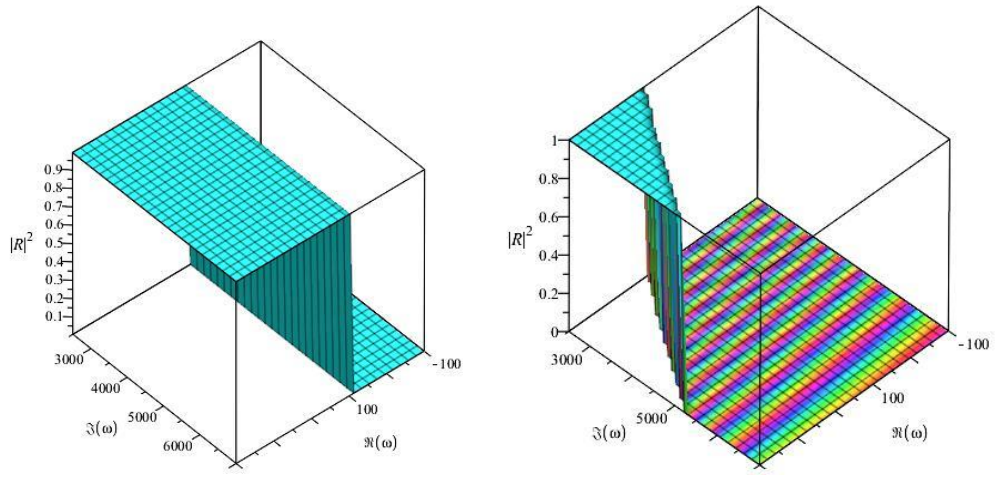

(a) (b)

Figure 7.11: Plots of reflection probability for $a = 0.011\ (a)$ and $a = 0.50\ (b)$. The physical parameters are chosen as; $M = 3; m = 1;\ L = 1$, and $\lambda = 6$.

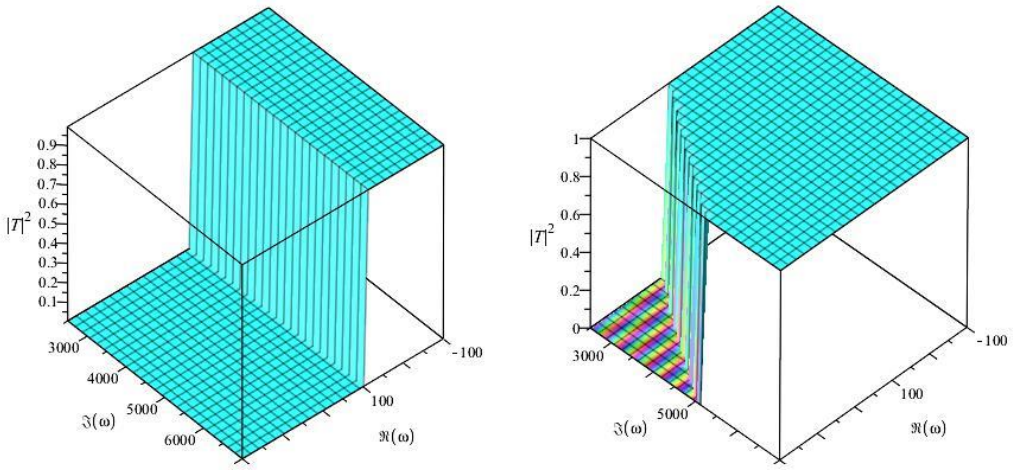

(a) (b)

Figure 7.12: Plots of transmission probability for $a = 0.011$ (a) and $a = 0.50$ (b). The physical parameters are chosen as; $M = 3; m = 1;\ L = 1$, and $\lambda = 6$.

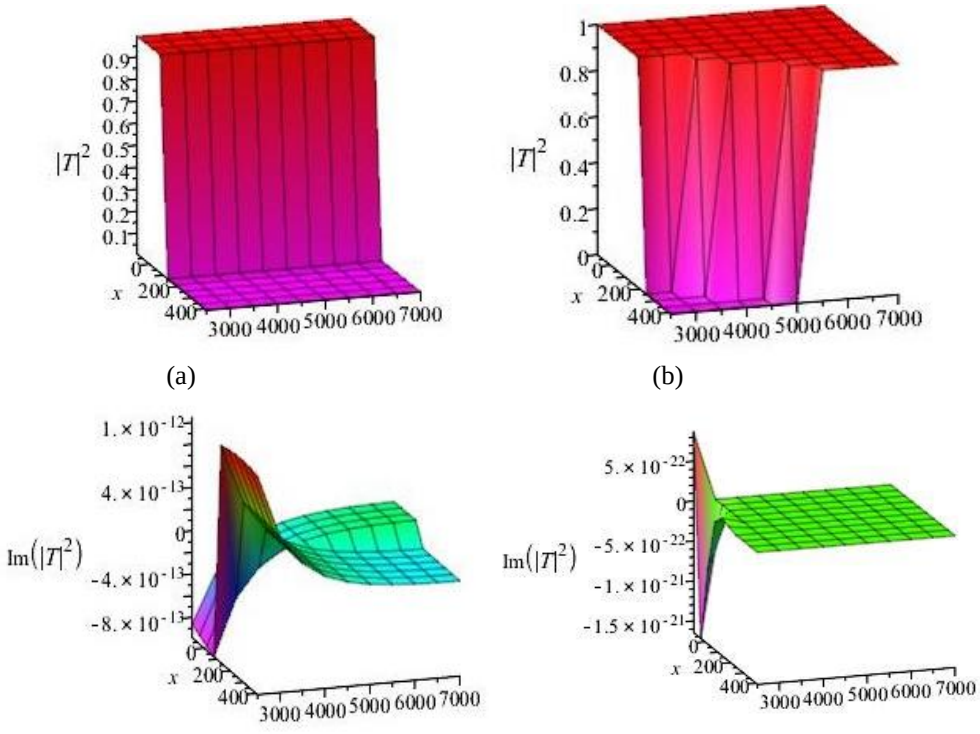

(a) (b)

(c) (d)

Figure 7.13: comparison between the imaginary and real part of the transmission probability in Fig. 7.12

Namely, in the Fig. (7.13), under the change of a, the real and imaginary parts can be compared. It is seen that the imaginary part undergoes more changes than the real part with the variation of a parameter.

Chapter 8

QUASINORMAL MODES

Non-trivial information about thermalisation in quantum field theory are obtained by studying small perturbations of a BH away from the equilibrium. Such perturbations are described by QNMs [188, 189]. These special oscillations are similar to normal modes of a closed system. However, since the perturbation can fall into the BH or radiate to infinity, the corresponding frequencies are complex [190]. The oscillation frequency is defined by the real part and the rate of specific damping mode as a result of a radiation is determined by imaginary part. Thus, by getting the QNMs in the BGM, the comparison of theoretical predictions with the experimental data supplied by "future" LIGO and VIRGO type experiments would help us to numerically constrain the LSB parameter. Thus, in general, it is important to accumulate data on QNMs of BHs in various theories of gravity [191].

8.1 Scalar and Dirac Quasinormal Modes of Kerr like BH in BGM

In this section, for both scalar and Dirac perturbations, we follow the WKB approximation method [192, 193] to derive the frequencies of the QNMs of the Kerr-like BH in the BGM. To this end, we shall simply transform the obtained one-dimensional Schrödinger-like equation [see Eqs. (7.23)] to the following Zerilli [164] type differential equation:

$$\frac{d^2Z}{dr_*^2} + V_{Geff}Z = 0, \tag{8.1}$$

where Z function is assumed to have a time-dependence $e^{i\omega t}$, V_{Geff} is the generic effective potential, and r_* is the tortoise coordinate as being stated above.

Comparing with the numerical results, the WKB approach is known to be a good prediction for obtaining the QNMs. In this method, V_{Geff} is written by using the tortoise coordinate so as to be constant at $r_* \longrightarrow 0$ (event horizon) and at $r_* \longrightarrow +\infty$ (spatial infinity). The maximum value of V_{Geff}, which we symbolize it as V_0 from now on, is achieved at r_*^0. Three regions are defined as follows: region-I from $-\infty$ to r_1, which is the first turning point where the potential becomes zero, region-II from r_1 to r_2, namely the second turning point, and region-III from r_2 to $+\infty$. In region-II, the Taylor expansion is made over r_*^0. In Regions-I and -III, the solution can be approximated by an exponential function:

$$Z \sim exp\left[\frac{1}{\zeta}\sum_{n=0}^{\infty}\zeta^n \Xi_n(x)\right], \quad \zeta \longrightarrow 0. \tag{8.2}$$

This expression can be substituted in Eq. (8.1) to get Ξ_n as a function of the potential and its derivative. We then impose the boundary conditions of the QNMs

$$Z \sim e^{-i\omega r_*} \quad r_* \longrightarrow -\infty, \tag{8.3}$$

$$Z \sim e^{i\omega r_*} \quad r_* \longrightarrow -\infty, \tag{8.4}$$

and match the solutions of regions-I and -III with the solution of region-II at the turning points, r_1 and r_2, respectively. The WKB approximation can be extended from the third to sixth order. This allows us to obtain the complex frequencies of the QNMs from the following expression

$$\omega^2 = \left[V_0 + \sqrt{2V_0^{''}}\Lambda(n) - i\left(n+\frac{1}{2}\right)\sqrt{-2V_0^{''}}\left(1+\Omega(n)\right)\right], \tag{8.5}$$

where Λ(n) and Ω(n) are defined in Eqs. (7.85) and (7.86). With the help of the effective potential (5.58), one can easily get V_{Geff}. After making straightforward calculations and numerical analysis, we have obtained the bosonic QNMs, which are tabulated in Table 8.1 for the angular momentum $l = 2$. In Table 8.1, the case of $m = 0$ for the first (fundamental) overtone $n = 0$ is considered (higher tones also show similar results that are parallel to the behaviors of the n = 0 mode). The revealed knowledge from Table 8.1 is that the oscillations decrease when the LSB parameter increases. But for the damping rate, there is no ostensive information about the LSB effect. At the beginning, we have a decrease in the imaginary part of the QNM frequencies but then this linear relationship between them disappears and shows an irregular behavior. Those bizarre behaviors can be understandable from Fig. 5.3 which shows the potential barriers that scalar QNMs are affected: the potential can take negative and positive values.

In the next step, we shall apply the methodology applied for QNM bosons in the previous section to the fermions. To this end, we consider the potentials obtained in Eq. (6.78) and use them in Eqs. (8.5)–(8.7). Table 8.2 constitutes the main results of this part: the numerically computed QNM frequencies for varying values of the LSB parameter for the fix rotating parameter $a = 0.4$ are displayed in the table. It is obvious from Table 8.2 that both oscillatory and damping parts of the fermionic QNMs tend to decrease with the increasing LSB parameter. On the contrary, they increase with increasing l and n values: hence, the characteristic fermionic QNMs are different from the bosonic ones.

Table 8.1: QNMs of scalar waves in the Kerr-like BH Spacetime in the BGM.

L	ω_{bosons}
0	$0.374411 - 0.089694i$
1	$0.372640 - 0.045766i$
1.1	$0.372553 - 0.044986i$
1.2	$0.372473 - 0.044784i$
1.3	$0.372399 - 0.045302i$
1.4	$0.372332 - 0.046902i$
1.5	$0.372269 - 0.050064i$
1.6	$0.372210 - 0.056650i$
1.7	$0.372155 - 0.073158i$
1.8	$0.372104 - 0.244808i$
1.9	$0.372063 - 0.099344i$
2	$0.372025 - 0.071826i$
2.1	$0.371990 - 0.058375i$
2.2	$0.371956 - 0.050093i$

Table 8.2: QNMs of Dirac waves in the Kerr-like BH Spacetime in the BGM.

l	n	L	$\omega_{fermions}$
1	0	1	$0.228468 - 0.065297i$
		2	$0.191896 - 0.052521i$
		3	$0.170421 - 0.044723i$
1	1	1	$0.265474 - 0.169833i$
		2	$0.221535 - 0.137485i$
		3	$0.195343 - 0.117735i$
2	0	1	$0.360666 - 0.065766i$
		2	$0.300382 - 0.052794i$
		3	$0.265097 - 0.044763i$
	1	1	$0.389890 - 0.182970i$
		2	$0.323537 - 0.147340i$
		3	$0.284319 - 0.125374i$
	2	1	$0.427069 - 0.279806i$
		2	$0.353472 - 0.225666i$
		3	$0.309573 - 0.192416i$

Chapter 9

CONCLUSION

After giving general information about HR, GF and QNM in the introduction (chapter 2) of this thesis, chapter 3 has been devoted to the BHs of the BGM, which are SBHBGM and Kerr like BH in the BGM. In the sequel, in chapter 4, we have moved on to the GUP modified theory which is one of the simplest theory in confirmation of the existence of minimal observable length. In section 4.1, we have obtained the modified Hawking temperatures of the SBHBGM, within the framework of GUP: the bosons' GUP modified HR has been given in subsection 4.1.1 whereas fermions' modified HR has been studied in subsection 4.1.2. The results seen in Eqs. (4.20) and (4.47) have shown us how HR is affected by the GUP and LSB parameter scalar and fermionic perturbations, respectively. In particular, we have revealed that, being independent of the spin of the emitted particle, GUP causes a change in the Hawking temperature of the BH. In addition, the effect of LSB parameter is noticeable.

For the GUP modified HR, we have also studied the rotating Polytropic BH in the Kerr spacetime. To this end, the dragging coordinate system has been applied to the rotating polytropic BH metric to diagonalize the metric (4.50) as in Eq. (4.56). The evaluation is considered in boson's tunneling and the GUP modified Klein Gordon equation is employed for that dragging line-element (4.56).

For computing the GF or transmission probability, first the effective potential should be handled, which is derived from the one-dimensional Schrödinger like wave equation. In line with this purpose, the scalar and Dirac perturbations are considered, in chapters 5 and 6. In the fifth chapter, where we have considered both massless (5.1) and massive (5.49) Klein-Gordon equations for the bosonic perturbations, we have first derived the effective potential (5.67) of the SBHBGM. The behaviors of these effective potentials by are depicted in Fig. 5.1 according to the change in L parameter. In other words, we have shown that LSB has a potential barrier-reducing property.

Furthermore, the same process for the scalar perturbation of the charged dRGT massive gravity BHs in nonlinear electrodynamics has been considered in section 5.2. However, we have used the charged Klein-Gordon equations [Eqqs. (5.35) and (5.36] for this purpose. The Schrödinger equation and effective potential are derived for both solutions of charged dRGT massive gravity BH, see Eqs. (5.46) and (5.48). Finally, the impression of the controlling parameter of ω which appeared in the effective potential by coupling of nonlinear electrodynamics for both solutions is evaluated in Figures 5.2.a and 5.2.b which for both, by increasing the frequency the potential peak increases as well.

In sections 5.3 and 5.4, we have studied the scalar perturbations in Kerr space time for bumblebee and polytropic BHs. The massive Klein-Gordon equation (5.49) has been employed to determine the effective potential in Eq. (5.58). The process was not as straightforward as non-rotating spacetime since there were physical parameters that simultaneously depended on r and θ. Fig. 5.3 shows the effect of LSB parameter on the effective potential of the Kerr like BH in the BGM it was seen that, the presence or absence of LSB makes a significant difference in the effective potential. The same

procedure was repeated in section 5.2, for the rotating polytropic BH. Fig. (5.4) which is about effective potential of the rotating polytropic BH (5.67), reveals a that there is a deduction in the potential barrier in the case of increasing L^2 parameter. Since L^2 parameter is inversely proportional to the cosmological constant, we can say that the height of the effective potentials (i.e, barrier) increases with the cosmological constant. Chapter 6 has been allocated to the Dirac perturbation in which, we employed the NP formalism to find the effective potential of the fermion fields propagating in the BH geometry of the BGM. To this end, we used the Chandrasekar Dirac equations (6.7) - (6.10) which comprise with the components of the wave functions, spin coefficients, and directional covariant derivative operators for the SBHBGM in section 6.1.1 and for Kerr BGM in section 6.1.2. Since the Dirac perturbation belongs to the spinor particles, the results are dual one for spin-up and one for spin-down which are separated by $(+/-)$ signs, respectively. The obtained effective potentials (6.37) are illustrated in Fig. 6.1 for spin-(+1/2) and spin-(-1/2) in order to exhibit the reaction of the both effective potentials under influence of the LSB parameter. To avoid the complicated calculations for the Kerr like (rotating)BH in the BGM, the Kerr geometry, in section 6.1.2, the dragging coordinate transformation has been applied, see Eq. (6.38). Then the NP tetrad and the dual co-tetrad of the Kerr-like BH geometry have been defined in Eqs. (6-50)- (6-57). After normalizing them by spin boost Lorentz transformation (6.48) and solving the CDEs, by substituting the non-zero spin coefficients, we have obtained the massless fermionic effective potentials in Eq. (6.78), which have been shown in the Figs. 6.2.a and 6.2.b.

In Chapter 7, we have studied various methods of greybody radiation which mostly are analyzed by major semi-analytic equation (7.1) having the effective potential as

the basic parameter. Computation of the GFs under alterations of physical parameters showed us that GFs are mainly under the control of the effective potential. The method followed in this thesis has been represented in section 7.1 for both bosonic and fermionic particles by regarding the following two conditions: 1) $h(r_*) > 0$ and 2) $h(-\infty) = h(+\infty) = \omega$, to simplify Eq. (7.2). Moreover, the integration determined in tortoise coordinate (r_*). Making use of the semi-analytic method directly is not an appropriate way in all geometries, since it is included only the lowers bound.

In order to refine the semi-analytic method, we have applied the Miller-Good transformation in section 7.2 for the SBHSQ. The Miller-Good transformation generates a general bound on quantum transmission probabilities. In this approach, a particular transformation is applied to the Schrödinger equation in such a way that the effective potential (7.12) is modified to yield a better transmission probability for the Hawking quanta. The results given in Eq. (7.57) and Fig. (7.8) has represented the behavior of the GF of the SBHSQ, which are all obtained by the Miller–Good transformation. It is obvious that the specific form of the GF depends on some parameters that are related to the potential barrier.

The rigorous bound method in the content of massive gravity is a proper method to calculate the GF which has been addressed in section 7.3 for the solutions of charged dRGT massive gravity coupled with nonlinear electrodynamics. In this approach, the existence of the boundaries, see Eqs. (7.67) and (7.68), are facilitated to determine the GFs. Fig. 7.9 has revealed that the charge parameter is a constructive factor in the GF for the first solution. But for the second solution which has been depicted by Fig (7.10) the behavior of the GF is not monotonous under varying the charge parameter q.

The greybody radiation is also determined by the transmission coefficient, we have considered the WKB method to get the reflection and transmission coefficients in section 7.4, for the rotating polytropic BH. From Figs. (7.11) and (7.12), it has been seen that both reflection and transmission coefficients increase with the growing rotating parameter, where the latter remark is in accordance with the behavior of the relevant effective potentials. In the Fig. (7.13) the comparison between the imaginary and real parts for a) $a = 0.011$ and b) $a = 0.05$ which has been made, It can be seen from the related Fig. (7.13), while the real part is rising by increasing the rotating parameter the imaginary part decrease significantly. On the other hand, we have found that the change in the rotation parameter a does not radically change the transmission and reflection coefficients.

In chapter 8, the QNMs of the Kerr like BH in the BGM has been studied. In subsection 8.1, for both scalar and Dirac perturbations, we followed the six order WKB approximation method to derive the frequencies of the QNMs of the Kerr-like BH in the BGM. To this end, we have obtained the corresponding one-dimensional Schrödinger-like equations. Those obtained numerical results which are from the complex frequencies seen in Eq. (8.5) have been tabulated for different quantum parameters with the LSB parameter in Tables 8.1 and 8.2. The fixed physical parameters seen in Table 8.1 are as follows; angular momentum $l = 2$ and $m = 0$ (for the first (fundamental) overtone $n = 0$). Thus we have evaluated the effect of LSB parameter on the bosonic QNMs, which shows a regular behavior in the real part (oscillation frequency) rather than imaginary part. The fermionic QNM results have been served in Table 8.2, it was seen that for both oscillatory and damping parts, QNM values tend to decrease with the increasing LSB parameter.

Throughout this thesis studies, five scientific articles are published [56,38,39,93,94]. In addition, an article regarding to the GUP modified Hawking radiation for the rotating polytropic BH is currently under review by a scientific journal at the time of publication of this thesis. I will continue to use the knowledge and experience that I have gained with this dissertation to reveal the physical properties of other black holes, wormholes, and even the black strings. Those will be my near future goals.

REFERENCES

[1] Abbott, B. P., Abbott, R., Abbott, T. D., Abernathy, M. R., Acernese, F., Ackley, K., ... & Cavalieri, R. (2016). Observation of gravitational waves from a binary black hole merger. *Physical review letters*, *116*(6), 061102.

[2] Abbott, B. P., Abbott, R., Abbott, T. D., Abernathy, M. R., Acernese, F., Ackley, K., ... & Chamberlin, S. J. (2016). GW151226: observation of gravitational waves from a 22-solar-mass binary black hole coalescence. *Physical review letters*, *116*(24), 241103.

[3] Akiyama, K., Alberdi, A., Alef, W., Asada, K., Azulay, R., Baczko, A. K., ... & Rao, R. (2019). First M87 event horizon telescope results. V. Physical origin of the asymmetric ring. *The Astrophysical Journal Letters*, *875*(1), L5.

[4] Gibson-Even, A., & Collaboration, A. T. L. A. S. (2012). A Particle Consistent with the Higgs Boson Observed with the ATLAS Detector at the Large Hadron Collider.

[5] Hawking, S. W. (1974). Black hole explosions? *Nature*, *248*(5443), 30-31.

[6] Yu, H., & Zhang, J. (2008). Understanding Hawking radiation in the framework of open quantum systems. *Physical Review D*, *77*(2), 024031.

[7] Miyamoto, U., & Murata, K. (2008). Hawking radiation from black rings. *Physical Review D*, *77*(2), 024020.

[8] Ali, M. H. (2007). Hawking radiation via tunneling from hot NUT–Kerr–Newman–Kasuya spacetime. *Classical and Quantum Gravity*, *24*(23), 5849.

[9] Morsink, S. M., & Mann, R. B. (1991). Black hole radiation of Dirac particles in 1+ 1 dimensions. *Classical and Quantum Gravity*, *8*(12), 2257.

[10] Punsly, B. (1992). Evaporation of rotating black holes and the equivalence principle. *Physical Review D*, *46*(4), 1312.

[11] Chardin, G., & Rax, J. M. (1992). CP violation. A matter of (anti) gravity?. *Physics Letters B*, *282*(1-2), 256-262.

[12] Nouicer, K. (2010). Hawking radiation and thermodynamics of dynamical black holes in a phantom-dominated universe. *Classical and Quantum Gravity*, *28*(1), 015005.

[13] Jiang, Q. Q., & Wu, S. Q. (2006). Hawking radiation of charged particles as tunneling from Reissner–Nordström–de Sitter black holes with a global monopole. *Physics Letters B*, *635*(2-3), 151-155.

[14] Liu, W. (2006). New coordinates for BTZ black hole and Hawking radiation via tunnelling. *Physics Letters B*, *634*(5-6), 541-544

[15] Brustein, R., & Medved, A. J. M. (2015). How black holes burn: Entanglement entropy evolution for an evaporating black hole. *Physical Review D*, *91*(8), 084062.

[16] Page, D. N. (1976). Particle emission rates from a black hole. II. Massless particles from an uncharged, nonrotating hole. *Physical Review D, 13*(12), 198.

[17] Page, D. N. (1976). Particle emission rates from a black hole. II. Massless particles from a rotating hole. *Physical Review D, 14*(12), 3260.

[18] Cvetič, M., & Larsen, F. (1997). Greybody factors for rotating black holes in four dimensions. *Nuclear Physics B, 506*(1-2), 107-120.

[19] Parikh, M. K., & Wilczek, F. (2000). Hawking radiation as tunneling. *Physical review letters, 85*(24), 5042.

[20] Ngampitipan, T., & Boonserm, P. (2013). Bounding the greybody factors for non-rotating black holes. *International Journal of Modern Physics D*, *22*(09), 1350058.

[21] Fernando, S. (2005). Greybody factors of charged dilaton black holes in 2+ 1 dimensions. *General Relativity and Gravitation*, *37*(3), 461-481.

[22] Lange, P. (2007). *Calculation of Hawking radiation as quantum mechanical tunneling* (Doctoral dissertation, Thesis, Uppsala Universitet).

[23] Kim, W., & Oh, J. J. (2007). Greybody factor and Hawking radiation of charged dilatonic black holes. *arXiv preprint arXiv:0709.1754*.

[24] Escobedo, J. (2008). *Greybody factors: Hawking radiation in disguise* (Doctoral dissertation, Masters Thesis, University of Amsterdam).

[25] Harmark, T., Natario, J., & Schiappa, R. (2010). Greybody factors for d-dimensional black holes. *Advances in Theoretical and Mathematical Physics*, *14*(3), 727-794.

[26] Abedi, J., & Arfaei, H. (2014). Fermionic greybody factors in dilaton black holes. *Classical and Quantum Gravity*, *31*(19), 195005.

[27] Ahmed, J., & Saifullah, K. (2017). Greybody factor of scalar fields from black strings. *The European Physical Journal C*, *77*(12), 1-7.

[28] Cvetič, M., & Larsen, F. (2009). Greybody factors and charges in Kerr/CFT. *Journal of High Energy Physics*, *2009*(09), 088.

[29] Sharif, M., & Ama-Tul-Mughani, Q. (2020). Greybody factor for quintessential Kerr–Newman black hole. *Physics of the Dark Universe*, *27*, 100436.

[30] Chen, S., & Jing, J. (2010). Greybody factor for a scalar field coupling to Einstein's tensor. *Physics Letters B*, *691*(5), 254-260.

[31] Sakalli, I. (2016). Analytical solutions in rotating linear dilaton black holes: resonant frequencies, quantization, greybody factor, and Hawking radiation. *Physical Review D*, *94*(8), 084040.

[32] Chen, S., & Jing, J. (2010). Greybody factor for a scalar field coupling to Einstein's tensor. *Physics Letters B*, *691*(5), 254-260.

[33] Hassan, S. F., & Rosen, R. A. (2012). Bimetric gravity from ghost-free massive gravity. *Journal of High Energy Physics*, *2012*(2), 1-12.

[34] Koyama, K., Niz, G., & Tasinato, G. (2011). Analytic solutions in nonlinear massive gravity. *Physical review letters*, *107*(13), 131101.

[35] Nieuwenhuizen, T. M. (2011). Exact Schwarzschild-de Sitter black holes in a family of massive gravity models. *Physical Review D*, *84*(2), 024038.

[36] Al-Badawi, A., Sakallı, İ., & Kanzi, S. (2020). Solution of Dirac equation and greybody radiation around a regular Bardeen black hole surrounded by quintessence. *Annals of Physics*, *412*, 168026.

[37] Al-Badawi, A., Kanzi, S., & Sakallı, İ. (2020). Effect of quintessence on geodesics and Hawking radiation of Schwarzschild black hole. *The European Physical Journal Plus*, *135*(2), 1-21.

[38] Casadio, R., & Scardigli, F. (2020). Generalized uncertainty principle, classical mechanics, and general relativity. *Physics Letters B*, *807*, 135558.

[39] Vaníček, J. (2004). Dephasing representation: Employing the shadowing theorem to calculate quantum correlation functions. *Physical Review E*, *70*(5), 055201.

[40] Jacobson, T., & Myers, R. C. (1993). Black hole entropy and higher curvature interactions. *Physical review letters*, *70*(24), 3684.

[41] Rovelli, C. (1994). Class. Quantum Grav. 10, 1549 and 1567 (1993). A. Connes and C. Rovelli. *Class. Quantum Grav*, *11*, 2899.

[42] Reznik, B. (1992). Thermodynamics of event horizons in (2+ 1)-dimensional gravity. *Physical Review D*, *45*(6), 2151.

[43] Zaslavskii, O. B. (1992). The first law of thermodynamics for black holes with Skyrme hair. *Physics Letters A*, *168*(3), 191-193.

[44] Czinner, V. G., & Iguchi, H. (2017). Thermodynamics, stability and Hawking–Page transition of Kerr black holes from Rényi statistics. *The European Physical Journal C*, *77*(12), 1-18.

[45] Schiffer, M. (1991). Does thermodynamics rule out the existence of cosmological singularities? *International journal of theoretical physics*, *30*(4), 419-436.

[46] Morita, T. (2009). Modification of gravitational anomaly method in Hawking radiation. *Physics Letters B*, *677*(1-2), 88-92.

[47] Kanzi, S., & Sakallı, İ. (2021). GUP modified Hawking Radiation and Transmission/Reflection Coefficients of Rotating Polytropic Black Hole. *arXiv preprint arXiv:2107.11776*.

[48] Jiang, Q. Q., Wu, S. Q., & Cai, X. (2007). Hawking radiation from dilatonic black holes via anomalies. *Physical Review D*, *75*(6), 064029.

[49] Setare, M. R. (2007). Gauge and gravitational anomalies and Hawking radiation of rotating BTZ black holes. *The European Physical Journal C*, *49*(3), 865-868.

[50] Lin, K., & Yang, S. (2009). Fermions tunneling from higher-dimensional Reissner-Nordström black hole. *arXiv preprint arXiv:0903.1983*.

[51] Saida, H. (2006). The generalized second law and the black hole evaporation in an empty space as a nonequilibrium process. *Classical and Quantum Gravity*, *23*(22), 6227.

[52] Barcelo, C., Liberati, S., Sonego, S., & Visser, M. (2011). Minimal conditions for the existence of a Hawking-like flux. *Physical Review D*, *83*(4), 041501.

[53] Shankaranarayanan, S. (2003). Temperature and entropy of Schwarzschild–de Sitter space-time. *Physical Review D*, *67*(8), 084026.

[54] Audretsch, J., & Müller, R. (1992). Amplification of the black-hole Hawking radiation by stimulated emission. *Physical Review D*, *45*(2), 513.

[55] Harris, C. M., & Kanti, P. (2003). Hawking radiation from a (4+ n)-dimensional black hole: Exact results for the Schwarzschild phase. *Journal of High Energy Physics*, *2003*(10), 014.

[56] Kanzi, S., Mazharimousavi, S. H., & Sakallı, İ. (2020). Greybody factors of black holes in dRGT massive gravity coupled with nonlinear electrodynamics. *Annals of Physics*, *422*, 168301.

[57] De Rham, C., & Gabadadze, G. (2010). Generalization of the Fierz-Pauli action. *Physical Review D*, *82*(4), 044020.

[58] De Rham, C., Gabadadze, G., & Tolley, A. J. (2011). Resummation of massive gravity. *Physical Review Letters*, *106*(23), 231101.

[59] Boulware, D. G., & Deser, S. (1972). Can gravitation have a finite range? *Physical Review D*, *6*(12), 3368.

[60] Ding, C., Liu, C., Casana, R., & Cavalcante, A. (2020). Exact Kerr-like solution and its shadow in a gravity model with spontaneous Lorentz symmetry breaking. *The European Physical Journal C*, *80*(3), 1-7.

[61] Hawking, S. W. (1975). Particle creation by black holes. In *Euclidean quantum gravity* (pp. 167-188).

[62] Hajicek, P. (1987). Origin of Hawking radiation. *Physical Review D*, *36*(4), 1065.

[63] Bardeen, J. M., Carter, B., & Hawking, S. W. (1973). The four laws of black hole mechanics. *Communications in mathematical physics*, *31*(2), 161-170.

[64] Bekenstain, J. D. (1973). Black Holes and Entropy. *Physical Review D*, *7*(4), 2333.

[65] Hawking, S. W. (1974). Black hole explosions?. *Nature*, *248*(5443), 30-31.

[66] Brout, R., Massar, S., Parentani, R., & Spindel, P. (1995). A primer for black hole quantum physics. *Physics Reports*, *260*(6), 329-446.

[67] Steinhauer, J. (2014). Observation of self-amplifying Hawking radiation in an analogue black-hole laser. *Nature Physics*, *10*(11), 864-869.

[68] Saida, H., & Sakagami, M. A. (2000). Black hole radiation with high frequency dispersion. *Physical Review D*, *61*(8), 084023.

[69] Mannarrelli, M., Grasso, D., Trabucco, S., & Chiofalo, M. L. (2021). Hawking temperature and phonon emission in acoustic holes. *Physical Review D*, *103*(7), 076001.

[70] Kolobov, V. I., Golubkov, K., de Nova, J. R. M., & Steinhauer, J. (2021). Observation of stationary spontaneous Hawking radiation and the time evolution of an analogue black hole. *Nature Physics*, *17*(3), 362-367.

[71] Unruh, W. G. (1981). Experimental black-hole evaporation? *Physical Review Letters*, *46*(21), 1351.

[72] Weinfurtner, S., Tedford, E. W., Penrice, M. C., Unruh, W. G., & Lawrence, G. A. (2011). Measurement of stimulated Hawking emission in an analogue system. *Physical review letters*, *106*(2), 021302.

[73] Barceló, C. (2019). Analogue black-hole horizons. *Nature Physics*, *15*(3), 210-213.

[74] Barceló, C., Liberati, S., & Visser, M. (2011). Analogue gravity. *Living reviews in relativity*, *14*(1), 1-159.

[75] Amati, D., Ciafaloni, M., & Veneziano, G. (1989). Can spacetime be probed below the string size?. *Physics Letters B*, *216*(1-2), 41-47.

[76] Konishi, K., Paffuti, G., & Provero, P. (1990). Minimum physical length and the generalized uncertainty principle in string theory. *Physics Letters B*, *234*(3), 276-284.

[77] Maggiore, M. (1993). A generalized uncertainty principle in quantum gravity. *Physics Letters B*, *304*(1-2), 65-69.

[78] Gross, D. J., & Mende, P. F. (1987). The high-energy behavior of string scattering amplitudes. *Physics Letters B*, *197*(1-2), 129-134.

[79] Hossenfelder, S. (2013). Minimal length scale scenarios for quantum gravity. *Living Reviews in Relativity*, *16*(1), 1-90.

[80] Konishi, K., Paffuti, G., & Provero, P. (1990). Minimum physical length and the generalized uncertainty principle in string theory. *Physics Letters B*, *234*(3), 276-284.

[81] Garay, L. J. (1995). Quantum gravity and minimum length. *International Journal of Modern Physics A*, *10*(02), 145-165.

[82] Magueijo, J., & Smolin, L. (2005). String theories with deformed energy-momentum relations, and a possible nontachyonic bosonic string. *Physical Review D*, *71*(2), 026010.

[83] Amelino-Camelia, G., Procaccini, A., & Arzano, M. (2004). A glimpse at the flat-spacetime limit of quantum gravity using the Bekenstein argument in reverse. *International Journal of Modern Physics D*, *13*(10), 2337-2343.

[84] Maggiore, M. (1993). The algebraic structure of the generalized uncertainty principle. *Physics Letters B*, *319*(1-3), 83-86.

[85] Basilakos, S., Das, S., & Vagenas, E. C. (2010). Quantum gravity corrections and entropy at the planck time. *Journal of Cosmology and Astroparticle Physics*, *2010*(09), 027.

[86] Das, S., & Mann, R. B. (2011). Planck scale effects on some low energy quantum phenomena. *Physics Letters B*, *704*(5), 596-599.

[87] Nozari, K., & Karami, M. (2005). Minimal length and generalized Dirac equation. *Modern Physics Letters A*, *20*(40), 3095-3103.

[88] Anacleto, M. A., Brito, F. A., Luna, G. C., Passos, E., & Spinelly, J. (2015). Quantum-corrected finite entropy of noncommutative acoustic black holes. *Annals of Physics*, *362*, 436-448.

[89] Dutta, A., & Gangopadhyay, S. (2014). Remnant mass and entropy of black holes and modified uncertainty principle. *General Relativity and Gravitation*, *46*(6), 1-10.

[90] Feng, Z. W., Li, H. L., Zu, X. T., & Yang, S. Z. (2016). Quantum corrections to the thermodynamics of Schwarzschild–Tangherlini black hole and the generalized uncertainty principle. *The European Physical Journal C*, *76*(4), 1-9.

[91] Isi, M., Mureika, J., & Nicolini, P. (2013). Self-completeness and the generalized uncertainty principle. *Journal of High Energy Physics*, *2013*(11), 1-18.

[92] Gangopadhyay, S. (2016). Minimal length effects in black hole thermodynamics from tunneling formalism. *International Journal of Theoretical Physics*, *55*(1), 617-624.

[93] Kanzi, S., & Sakallı, I. (2019). GUP modified Hawking radiation in bumblebee gravity. *Nuclear Physics B*, *946*, 114703.

[94] Kanzi, S., & Sakallı, İ. (2021). Greybody radiation and quasinormal modes of Kerr-like black hole in Bumblebee gravity model. *The European Physical Journal C*, *81*(6), 1-11.

[95] Colladay, D., & Kostelecký, V. A. (1997). CPT violation and the standard model. *Physical Review D*, *55*(11), 6760.

[96] Colladay, D., & Kostelecký, V. A. (1998). Lorentz-violating extension of the standard model. *Physical Review D*, *58*(11), 116002.

[97] Coleman, S., & Glashow, S. L. (1999). High-energy tests of Lorentz invariance. *Physical Review D*, *59*(11), 116008.

[98] Kostelecký, V. A., & Samuel, S. (1989). Phenomenological gravitational constraints on strings and higher-dimensional theories. *Physical Review Letters*, *63*(3), 224.

[99] Kostelecký, V. A., & Samuel, S. (1989). Gravitational phenomenology in higher-dimensional theories and strings. *Physical Review D*, *40*(6), 1886.

[100] Kostelecký, V. A., & Lehnert, R. (2001). Stability, causality, and Lorentz and CPT violation. *Physical Review D*, *63*(6), 065008.

[101] Bailey, Q. G., & Kostelecký, V. A. (2006). Signals for Lorentz violation in post-Newtonian gravity. *Physical Review D*, *74*(4), 045001.

[102] Bluhm, R. (2007). Nambu–Goldstone modes in gravitational theories with spontaneous Lorentz breaking. *International Journal of Modern Physics D*, *16*(12b), 2357-2363.

[103] Lehnert, R. (2009). CPT and Lorentz-invariance violation. *Hyperfine Interactions*, *193*(1), 275-281.

[104] Jacobson, T., & Mattingly, D. (2001). Gravity with a dynamical preferred frame. *Physical Review D*, *64*(2), 024028.

[105] Jacobson, T. (2007). PoS QG-PH, 020.

[106] Kostelecký, V. A. (2004). Gravity, Lorentz violation, and the standard model. *Physical Review D*, *69*(10), 105009.

[107] Bertolami, O., & Paramos, J. (2005). Vacuum solutions of a gravity model with vector-induced spontaneous Lorentz symmetry breaking. *Physical Review D*, *72*(4), 044001.

[108] Casana, R., Cavalcante, A., Poulis, F. P., & Santos, E. B. (2018). Exact Schwarzschild-like solution in a bumblebee gravity model. *Physical Review D*, *97*(10), 104001.

[109] Övgün, A., Jusufi, K., & Sakallı, İ. (2019). Exact traversable wormhole solution in bumblebee gravity. *Physical Review D*, *99*(2), 024042.

[110] Bluhm, R. (2007). Effects of spontaneous Lorentz violation in gravity. *arXiv preprint arXiv:0801.0141*.

[111] Seifert, M. D. (2010). Generalized bumblebee models and Lorentz-violating electrodynamics. *Physical Review D*, *81*(6), 065010.

[112] Kostelecký, V. A., & Tasson, J. D. (2011). Matter-gravity couplings and Lorentz violation. *Physical Review D*, *83*(1), 016013.

[113] Guiomar, G., & Páramos, J. (2014). Astrophysical constraints on the bumblebee model. *Physical Review D*, *90*(8), 082002.

[114] Hernaski, C. A. (2014). Quantization and stability of bumblebee electrodynamics. *Physical Review D*, *90*(12), 124036.

[115] Maluf, R. V., Silva, J. E. G., & Almeida, C. A. S. (2015). Radiative corrections in bumblebee electrodynamics. *Physics Letters B*, *749*, 304-308.

[116] Santos, A. F., Jesus, W. D. R., Nascimento, J. R., & Petrov, A. Y. (2015). Gödel solution in the bumblebee gravity. *Modern Physics Letters A*, *30*(02), 1550011.

[117] Bardeen, J. M., Carter, B., & Hawking, S. W. (1973). The four laws of black hole mechanics. *Communications in mathematical physics*, *31*(2), 161-170.

[118] Hawking, S. W. (1976). Commun. 240 Math. *Phys*, *46*, 206.

[119] 冨松彰. (1986). RM Wald: General Relativity, University of Chicago Press, Chicago and London, 1984, xiii+ 492 ページ, 24× 17cm, 15,730 円. *日本物理学会誌*, *41*(4), 363-364.

[120] Wald, R. M. (2001). The thermodynamics of black holes. *Living reviews in relativity*, *4*(1), 1-44.

[121] Parikh, M. K., & Wilczek, F. (2000). Hawking radiation as tunneling. *Physical review letters*, *85*(24), 5042.

[122] Kanti, P. (2004). Black holes in theories with large extra dimensions: A Review. *International journal of modern physics A*, *19*(29), 4899-4951.

[123] Barceló, C., Liberati, S., & Visser, M. (2011). Analogue gravity. *Living reviews in relativity*, *14*(1), 1-159.

[124] Pasaoglu, H., & Sakalli, I. (2009). Hawking radiation of linear dilaton black holes in various theories. *International Journal of Theoretical Physics*, *48*(12), 3517-3525.

[125] Cai, R. G., Cao, L. M., & Hu, Y. P. (2009). Hawking radiation of an apparent horizon in a FRW universe. *Classical and Quantum Gravity*, *26*(15), 155018.

[126] Mazharimousavi, S. H., Sakalli, I., & Halilsoy, M. (2009). Effect of the Born–Infeld parameter in higher dimensional Hawking radiation. *Physics Letters B*, *672*(2), 177-181.

[127] Sakallı, İ., Jusufi, K., & Övgün, A. (2018). Analytical solutions in a cosmic string Born–Infeld-dilaton black hole geometry: quasinormal modes and quantization. *General Relativity and Gravitation*, *50*(10), 1-24.

[128] Vanzo, L., Acquaviva, G., & Di Criscienzo, R. (2011). Tunnelling methods and Hawking's radiation: achievements and prospects. *Classical and Quantum Gravity*, *28*(18), 183001.

[129] Akhmedov, E. T., Akhmedova, V., & Singleton, D. (2006). Hawking temperature in the tunneling picture. *Physics Letters B*, *642*(1-2), 124-128.

[130] Srinivasan, K., & Padmanabhan, T. (1999). Particle production and complex path analysis. *Physical Review D*, *60*(2), 024007.

[131] Hemming, S., & Keski-Vakkuri, E. (2001). Hawking radiation from AdS black holes. *Physical Review D*, *64*(4), 044006.

[132] Amelino-Camelia, G., Arzano, M., Ling, Y., & Mandanici, G. (2006). Black-hole thermodynamics with modified dispersion relations and generalized uncertainty principles. *Classical and Quantum Gravity*, *23*(7), 2585.

[133] Wang, P., Yang, H., & Ying, S. (2016). Quantum gravity corrections to the tunneling radiation of scalar particles. *International Journal of Theoretical Physics*, *55*(5), 2633-2642.

[134] Rahman, M. A., & Hossain, M. I. (2012). Hawking radiation of Schwarzschild–de Sitter black hole by Hamilton–Jacobi method. *Physics Letters B*, *712*(1-2), 1-5.

[135] Hossenfelder, S. (2013). Minimal length scale scenarios for quantum gravity. *Living Reviews in Relativity*, *16*(1), 1-90.

[136] Maluf, R. V., Almeida, C. A. S., Casana, R., & Ferreira Jr, M. M. (2014). Einstein-Hilbert graviton modes modified by the Lorentz-violating bumblebee Field. *Physical Review D*, *90*(2), 025007.

[137] Bluhm, R., & Kostelecký, V. A. (2005). Spontaneous Lorentz violation, Nambu-Goldstone modes, and gravity. *Physical Review D*, *71*(6), 065008.

[138] Cao, X. I. N. W. U., & Zhang, J. I. A. L. Ü. (1994). Stability of a polytropic accretion disk around a black hole. *Astronomy and Astrophysics*, *285*, 1047-1051.

[139] Stergioulas, N. (2003). Rotating stars in relativity. *Living Reviews in Relativity*, *6*(1), 1-109.

[140] Herrera, L., & Barreto, W. (2004). Evolution of Relativistic Polytropes in the Post–Quasi–Static Regime. *General Relativity and Gravitation*, *36*(1), 127-150.

[141] Contreras, E., Rincón, Á., Koch, B., & Bargueño, P. (2018). Scale-dependent polytropic black hole. *The European Physical Journal C*, *78*(3), 1-8.

[142] Contreras, E., & Bargueño, P. (2018). Minimal geometric deformation in asymptotically (A-) dS space-times and the isotropic sector for a polytropic black hole. *The European Physical Journal C*, *78*(12), 1-5.

[143] Setare, M. R., & Adami, H. (2015). Polytropic black hole as a heat engine. *General Relativity and Gravitation*, *47*(11), 1-5.

[144] Setare, M. R., & Adami, H. (2015). Polytropic black hole. *Physical Review D*, *91*(8), 084014.

[145] Tiwari, R. N., Rao, J. R., & Kanakamedala, R. R. (1986). Electromagnetic mass models in general relativity: Lane-Emden–type models. *Physical Review D*, *34*(4), 1205.

[146] Ray, S. (2002). Static spherically symmetric electromagnetic mass models with charged dust sources in Einstein-Cartan theory: Lane-Emden models. *Astrophysics and space science*, *280*(4), 345-355.

[147] Contreras, E., Ramirez–Velasquez, J. M., Rincón, Á., Panotopoulos, G., & Bargueño, P. (2019). Black hole shadow of a rotating polytropic black hole by the Newman–Janis algorithm without complexification. *The European Physical Journal C*, *79*(9), 1-10.

[148] Ma, Z. Z. (2008). Hawking temperature of Kerr–Newman–AdS black hole from tunneling. *Physics letters B*, *666*(4), 376-381.

[149] Bardeen, J. M. (1970). Press, WH & Teukolsky, SA 1972. *ApJ*, *178*, 347.

[150] Tredcr, I. J. (1975). Cw misner, ks thorne, ja wheeler: Gravitation. wh freeman and company limited, reading (england) 1973—xxvi+ 1279 seiten, preis£ 19.20 (clothbound);£ 8.60 (paperbound).

[151] Mazharimousavi, S. H., & Halilsoy, M. (2019). Electric Black Holes in a Model of Nonlinear Electrodynamics. *Annalen der Physik*, *531*(12), 1900236.

[152] Kruglov, S. I. (2019). Dyonic and magnetic black holes with nonlinear arcsin-electrodynamics. *Annals of Physics*, *409*, 167937.

[153] Mazharimousavi, S. H., & Halilsoy, M. (2019). Electric Black Holes in a Model of Nonlinear Electrodynamics. *Annalen der Physik*, *531*(12), 1900236.

[154] Motohashi, H., & Suyama, T. (2012). Self-accelerating solutions in massive gravity on an isotropic reference metric. *Physical Review D*, *86*(8), 081502.

[155] Hassan, S. F., Schmidt-May, A., & von Strauss, M. (2012). Proof of consistency of nonlinear massive gravity in the Stückelberg formulation. *Physics Letters B*, *715*(4-5), 335-339.

[156] Klusoň, J. (2012). Comments about Hamiltonian formulation of non-linear massive gravity with Stückelberg fields. *Journal of High Energy Physics*, *2012*(6), 1-17.

[157] Klusoň, J. (2012). Comments about Hamiltonian formulation of non-linear massive gravity with Stückelberg fields. *Journal of High Energy Physics*, *2012*(6), 1-17.

[158] Gratia, P., Hu, W., & Wyman, M. (2012). Self-accelerating Massive Gravity: Exact solutions for any isotropic matter distribution. *Physical Review D*, *86*(6), 061504.

[159] Motloch, P., Hu, W., & Motohashi, H. (2016). Self-accelerating massive gravity: hidden constraints and characteristics. *Physical Review D*, *93*(10), 104026.

[160] Boonserm, P., Ngampitipan, T., & Wongjun, P. (2019). Greybody factor for black string in dRGT massive gravity. *The European Physical Journal C*, *79*(4), 1-9.

[161] Bamba, K., Makarenko, A. N., Myagky, A. N., Nojiri, S. I., & Odintsov, S. D. (2014). Bounce cosmology from F (R) gravity and F (R) bigravity. *Journal of Cosmology and Astroparticle Physics*, *2014*(01), 008.

[162] Ngampitipan, T., Boonserm, P., Chatrabhuti, A., & Visser, M. (2016, June). The rigorous bound on the transmission probability for massless scalar field of non-negative-angular-momentum mode emitted from a Myers-Perry black hole. In *AIP Conference Proceedings* (Vol. 1739, No. 1, p. 020020). AIP Publishing LLC.

[163] T. Ngampitipan, P. Boonserm, J. Phys. Conf. Ser. **435**, 012027 (2013). arXiv:1301.7527 [math-ph].

[164] Chandrasekhar, S., & Chandrasekhar, S. (1998). *The mathematical theory of black holes* (Vol. 69). Oxford university press.

[165] Abramowitz, M., & Stegun, I. A. (1970). Handbook of mathematical functions with Formulas, Graphs, and Mathematical Tables" edited by Dover Publications. *Inc., New York, Ninth Printing*.

[166] Detweiler, S. (1980). Klein-Gordon equation and rotating black holes. *Physical Review D*, *22*(10), 2323.

[167] Jogia, S., & Griffiths, J. B. (1980). A Newman-Penrose-type formalism for space-times with torsion. *General Relativity and Gravitation*, *12*(8), 597-617.

[168] Krishnan, B. (2012). The spacetime in the neighborhood of a general isolated black hole. *Classical and quantum gravity*, *29*(20), 205006.

[169] Newman, E. T., & Penrose, R. (1966). Note on the bondi-metzner-sachs group. *Journal of Mathematical Physics*, *7*(5), 863-870.

[170] Goldberg, J. N., MacFarlane, A. J., Newman, E. T., Rohrlich, F., & Sudarshan, E. G. (1967). Spin-s Spherical Harmonics and ð. *Journal of Mathematical Physics*, *8*(11), 2155-2161.

[171] Teukolsky, S. A. (1973). Perturbations of a rotating black hole. I. Fundamental equations for gravitational, electromagnetic, and neutrino-field perturbations. *The Astrophysical Journal*, *185*, 635-648.

[172] Lee, C. H. (1976). Coupled gravitational and electromagnetic perturbations around a charged black hole. *Journal of Mathematical Physics*, *17*(7), 1226-1235.

[173] Chen, B., & Stein, L. C. (2017). Separating metric perturbations in near-horizon extremal Kerr spacetimes. *Physical Review D*, *96*(6), 064017.

[174] Nikolić, B. D., & Pantić, M. R. (2012). A possible intuitive derivation of the Kerr metric in orthogonal form based on ellipsoidal metric ansatz. *arXiv preprint arXiv:1210.5922*.

[175] del Castillo, G. F. T. (2003). *3-D spinors, spin-weighted functions and their applications* (Vol. 32). Springer Science & Business Media.

[176] Miao, Y. G., & Xu, Z. M. (2017). Hawking radiation of five-dimensional charged black holes with scalar fields. *Physics Letters B*, *772*, 542-546.

[177] Boonserm, P., & Visser, M. (2008). Transmission probabilities and the Miller–Good transformation. *Journal of Physics A: Mathematical and Theoretical*, *42*(4), 045301.

[178] Kiselev, V. V. (2003). Quintessence and black holes. *Classical and Quantum Gravity*, *20*(6), 1187.

[179] Weiss, J. (1983). The Painlevé property for partial differential equations. II: Bäcklund transformation, Lax pairs, and the Schwarzian derivative. *Journal of Mathematical Physics*, *24*(6), 1405-1413.

[180] Faure, F., & Weich, T. (2015). Asymptotic spectral gap for open partially expanding maps. *arXiv preprint arXiv:1504.06728*.

[181] Ahmed, J., & Saifullah, K. (2017). Greybody factor of scalar fields from black strings. *The European Physical Journal C*, *77*(12), 1-7.

[182] Boonserm, P., Ngampitipan, T., & Visser, M. (2013). Regge-Wheeler equation, linear stability, and greybody factors for dirty black holes. *Physical Review D*, *88*(4), 041502.

[183] Ngampitipan, T., & Boonserm, P. (2013, April). Bounding the greybody factors for the Reissner-Nordström black holes. In *Journal of Physics: Conference Series* (Vol. 435, No. 1, p. 012027). IOP Publishing.

[184] Boonserm, P., Ngampitipan, T., & Wongjun, P. (2018). Greybody factor for black holes in dRGT massive gravity. *The European Physical Journal C*, *78*(6), 1-12.

[185] Gabadadze, G., Hinterbichler, K., Pirtskhalava, D., & Shang, Y. (2013). Potential for general relativity and its geometry. *Physical Review D*, *88*(8), 084003.

[186] Völkel, S. H., Konoplya, R., & Kokkotas, K. D. (2019). Inverse problem for Hawking radiation. *Physical Review D*, *99*(10), 104025.

[187] Konoplya, R. A. (2003). Quasinormal behavior of the D-dimensional Schwarzschild black hole and the higher order WKB approach. *Physical Review D*, *68*(2), 024018.

[188] Schutz, B. F., & Will, C. M. (1985). Black hole normal modes: a semianalytic approach. *The Astrophysical Journal*, *291*, L33-L36.

[189] Seidel, E., & Iyer, S. (1990). Black-hole normal modes: A WKB approach. IV. Kerr black holes. *Physical Review D*, *41*(2), 374.

[190] Carlson, W. A., Cornell, A. S., & Jordan, B. (2012). Fermion Quasi-normal modes of the Kerr Black-Hole. *arXiv preprint arXiv:1201.3267*.

[191] Zinhailo, A. F. (2018). Quasinormal modes of the four-dimensional black hole in Einstein–Weyl gravity. *The European Physical Journal C*, *78*(12), 1-7.

[192] Iyer, S. (1987). Black-hole normal modes: A WKB approach. II. Schwarzschild black holes. *Physical Review D*, *35*(12), 3632.

[193] Iyer, S., & Will, C. M. (1987). Black-hole normal modes: A WKB approach. I. Foundations and application of a higher-order WKB analysis of potential-barrier